

UNIVERSITY OF MINNESOTA  
**ST. ANTHONY FALLS LABORATORY**  
Engineering, Environmental and Geophysical Fluid Dynamics

**Project Report No. 477**

# **Quasi-2D Model for Runoff Temperature from a Paved Surface**

by

Ben Janke, William Herb, Omid Mohseni, and Heinz Stefan



Prepared for

**Minnesota Pollution Control Agency**  
St. Paul, Minnesota

August 2006  
**Minneapolis, Minnesota**

The University of Minnesota is committed to the policy that all persons shall have equal access to its programs, facilities, and employment without regard to race, religion, color, sex, national origin, handicap, age or veteran status.

## Abstract

Thermal pollution from urban runoff is considered to be a significant contributor to the degradation of coldwater ecosystems. Impervious surfaces (streets, parking lots and buildings) are characteristic of urban watersheds. A model for predicting rainfall runoff temperatures and runoff rates from an impervious surface (parking lot) is described in this report. The model has been developed from basic principles. It is a portion of a larger project to develop a modeling tool to assess the impact of urban development on the temperature of coldwater streams. Heat transfer and runoff processes on an impervious surface were investigated for both dry and wet weather periods. The principal goal of the effort was to describe and quantify the heat transfer between a paved surface and storm water runoff during a rainfall event. A kinematic wave scheme was used to predict runoff flow rates as a function of distance and time on a paved surface, and a numerical approximation of the 1-D unsteady heat diffusion equation was used to calculate temperature distributions in the sub-surface. Equations to predict the magnitude of the radiative, convective, conductive and evaporative heat fluxes at a dry or wet surface, using standard climate data as input, were developed. The model can simulate surface runoff (flow) and temperature continuously throughout a specified time period (e.g. a month) or for a single rainfall event. It also predicts the 'total heat export' for an event, which is defined as the heat contained in the runoff above a reference temperature. A sensitivity study was performed to investigate the extent to which heat export is affected by antecedent pavement temperature, characteristics of the rainfall event, and physical parameters of the paved surface. In general, it was found that heat export was more sensitive to rainfall intensity, rainfall duration, and antecedent pavement temperature conditions than the physical properties of the paved surface (slope, roughness, length). It was also found that lower-intensity events extracted more heat from the pavement per depth of rainfall than higher-intensity events, and an increase in rainfall duration increased the total event heat export, especially for higher-intensity events. Finally, atmospheric forcing was determined to have a significant influence on runoff temperature and heat export, leading to a reduction in heat export that was a function of rainfall intensity.

## TABLE OF CONTENTS

NOTATIONS AND UNITS .....	5
1. INTRODUCTION .....	8
2. PREVIOUS STUDIES AND MODELS .....	9
3. MODEL FORMULATION .....	11
3.1. Model 1 for standing water without outlet .....	11
3.2. Model 2 for spatially-averaged runoff .....	13
3.3. Model 3 for spatial and temporal variation in runoff .....	16
4. HEAT TRANSFER BETWEEN RUNOFF WATER AND PAVEMENT .....	20
4.1. Convective heat transfer from pavement surface to water .....	20
4.2. Conductive heat transfer from ground to pavement surface .....	22
4.3. Pavement surface temperature and runoff temperature .....	23
5. METHODS USED TO SOLVE HEAT AND MASS BALANCE EQUATIONS .....	24
5.1. Numerical solution of the kinematic wave equation .....	24
5.2. Numerical solution of the runoff energy balance equation .....	25
5.3. Numerical solution of the unsteady soil heat conduction equation .....	28
5.4. Computational sequence .....	29
6. MODEL INPUT AND IMPLEMENTATION .....	30
7. MODEL RESULTS/ SENSITIVITY STUDY .....	33
7.1. Objectives of the sensitivity study .....	33
7.2. Results of the sensitivity study: Horizontal distributions of water (runoff) depth and temperature .....	36
7.3. Results of the sensitivity study: Hydrographs, thermographs and heat export rates .....	41
7.4. Results of the sensitivity study: Heat export including the effect of atmospheric heat transfer .....	54
7.5. Summary of sensitivity study .....	57
8. VALIDATION OF SURFACE RUNOFF MODEL .....	59
9. CONCLUSIONS .....	61
10. IMPLICATIONS .....	62
ACKNOWLEDGMENTS .....	63
REFERENCES .....	64
APPENDIX A. COMPONENTS OF THE WATER BALANCE .....	67
Infiltration .....	67
Evaporation .....	69
APPENDIX B. HEAT FLUXES ACROSS THE WATER SURFACE .....	70
Net radiative heat flux .....	70
Evaporative heat flux .....	71
Convective heat flux from air to water .....	72
APPENDIX C. ADVECTIVE HEAT FLUXES .....	74
Precipitation heat flux .....	74
Infiltration heat flux .....	74
Runoff (net lateral advection) heat flux .....	74
APPENDIX D. DRY WEATHER HEAT BUDGET OF PAVEMENT AND SOIL: GROUND TEMPERATURE PROFILE BEFORE A RAINFALL EVENT .....	75
Estimation of an initial sub-surface temperature profile for sensitivity study .....	76
APPENDIX E. THERMAL PROPERTIES OF SOILS AND PAVEMENT .....	77

## NOTATIONS AND UNITS

$\alpha$ :	parameter used in kinematic wave equation [dimensionless], also used for generic thermal diffusivity [ $\text{m}^2/\text{s}$ ]
$\alpha_i$ :	reflectivity of a surface with respect to longwave radiation [dimensionless]
$\alpha_p$ :	thermal diffusivity of pavement/soil [ $\text{m}^2/\text{s}$ ]
$\alpha_s$ :	reflectivity of a surface with respect to solar radiation [dimensionless]
$\alpha_0$ :	thermal diffusivity of top soil layer [ $\text{m}^2/\text{s}$ ]
$\beta$ :	parameter used in kinematic wave equation [dimensionless]
$\Delta x$ :	width of runoff cell [m]
$\Delta z$ :	thickness of soil layer [m]
$\Delta z_0$ :	thickness of top soil layer [m]
$\varepsilon$ :	surface emissivity [dimensionless]
$\mu$ :	dynamic viscosity of water [ $\text{N}\cdot\text{s}/\text{m}^2$ ]
$\kappa$ :	von Karman constant [dimensionless]
$\eta$ :	soil porosity [dimensionless]
$\theta$ :	soil moisture content [dimensionless]
$\theta_v$ :	virtual air temperature [ $^{\circ}\text{C}$ ]
$\rho$ :	density [ $\text{kg}/\text{m}^3$ ]
$\rho_s$ :	density of soil [ $\text{kg}/\text{m}^3$ ]
$\rho_w$ :	density of water [ $\text{kg}/\text{m}^3$ ]
$\sigma$ :	Stefan-Boltzmann constant [ $\text{kJ K}^{-4} \text{m}^{-2} \text{day}^{-1}$ ]
$\Psi_f$ :	suction pressure (head) at wetting front [cm]
$a$ :	flow parameter in kinematic wave equation [dimensionless]
$a_i$ :	time-dependent coefficient used in TDMA method [dimensionless]
$A$ :	cross-sectional area in a vertical section of runoff [ $\text{m}^2$ ]
$A_s$ :	surface area of paved surface [ $\text{m}^2$ ]
$b_i$ :	time-dependent coefficient used in TDMA method [dimensionless]
$ci$ :	time-dependent coefficient used in TDMA method [dimensionless]
$C_{fc}$ :	free convection bulk transfer coefficient [dimensionless]
$C_{H0}$ :	bare soil bulk transfer coefficient [dimensionless]
$C_{Hg}$ :	ground-canopy bulk transfer coefficient [dimensionless]
$C_p$ :	specific heat [ $\text{J}/\text{kg}\cdot\text{K}$ ]
$C_{p,s}$ :	specific heat of soil [ $\text{J}/\text{kg}\cdot\text{K}$ ]
$C_{p,w}$ :	specific heat of water [ $\text{J}/\text{kg}\cdot\text{K}$ ]
$C_l$ :	shape factor for sub-surface temperature profile [dimensionless]
$d$ :	displacement height [cm]
$d_i$ :	time-dependent coefficient used in TDMA method [dimensionless]
$D_s$ :	soil water diffusivity [ $\text{cm}^2/\text{h}$ ]
$e$ :	evaporation rate [cm/h]
$e_a$ :	actual vapor pressure of air [kPa]
$e_s$ :	saturation vapor pressure of air, evaluated at runoff temperature [kPa]
$e_{sa}$ :	saturation vapor pressure of air, evaluated at air temperature [kPa]
$f$ :	infiltration rate [cm/h]
$g$ :	acceleration due to gravity [ $9.8 \text{ m}/\text{s}^2$ ]

$F$ :	cumulative infiltration depth [cm]
$F_c$ :	cloudiness factor [dimensionless]
$F_p$ :	cumulative infiltration depth at ponding time [cm]
$h_l$ :	net incoming longwave radiation [ $W/m^2$ ]
$h_s$ :	net incoming solar radiation [ $W/m^2$ ]
$h_{cond,g}$ :	conduction between ground and atmosphere [ $W/m^2$ ]
$h_{cond,pv}$ :	conduction between pavement and runoff water [ $W/m^2$ ]
$h_{conv,atm}$ :	convection between runoff and atmosphere [ $W/m^2$ ]
$h_{conv,pv}$ :	convection between pavement and runoff [ $W/m^2$ ]
$h_{evap}$ :	heat transfer by evaporation [ $W/m^2$ ]
$h_{exp}$ :	instantaneous heat export rate, per unit area of lot [ $W/m^2$ ]
$h_f$ :	heat transfer by infiltration [ $W/m^2$ ]
$h_{net}$ :	net (total) heat transfer at surface [ $W/m^2$ ]
$h_{outflow}$ :	heat transfer via outflow in Model 2 [ $W/m^2$ ]
$h_{rad}$ :	net shortwave and longwave radiation [ $W/m^2$ ]
$h_{rain}$ :	heat transfer by rainfall [ $W/m^2$ ]
$h_{total}$ :	total (net) heat transfer at surface [ $W/m^2$ ]
$H_{exp}$ :	total event heat export, per unit area of lot [ $kJ/m^2$ ]
$i$ :	superscript used to denote time step [dimensionless], also used to denote rainfall intensity [cm/h]
$I$ :	total rainfall depth [cm]
$j$ :	subscript used to denote incremental position [dimensionless]
$k_c$ :	convection coefficient [ $W/m^2 \cdot K$ ]
$k_{conv,pv}$ :	convection coefficient for pavement surface [ $W/m^2 \cdot K$ ]
$k_{convatmv}$ :	convection coefficient for pavement surface (Eq. B.9) [ $W/m^2 \cdot K$ ]
$k_s$ :	thermal conductivity of soil or pavement [ $W/m \cdot K$ ]
$k_w$ :	thermal conductivity of water [ $W/m \cdot K$ ]
$K$ :	hydraulic conductivity of soil [cm/h]
$K_s$ :	saturated hydraulic conductivity of soil [cm/h]
$L$ :	length of parking lot, or section of lot being modeled [m]
$L_v$ :	latent heat of vaporization of water [J/kg]
$m$ :	flow parameter in kinematic wave equation [dimensionless]
$n$ :	surface roughness, used in Manning's Equation []
$N$ :	total number of sub-soil layers [dimensionless]
$N_{uL}$ :	Nusselt number [dimensionless]
$p$ :	precipitation intensity [cm/h]
$p_i$ :	initial precipitation intensity [cm/h]
$P$ :	total precipitation depth [cm]
$Pr$ :	Prandtl number [dimensionless]
$q$ :	runoff flow rate [ $m^2/s$ or $m/s$ ], also specific humidity (Eq. B.12) [ $kg_w/kg_a$ ]
$q_i$ :	flow rate of infiltration [cm/h]
$q_{ro}$ :	per-width runoff flow rate at the lot outlet [ $m^2/s$ ]
$Q_{ro}$ :	volumetric runoff flow rate [ $m^3/s$ ]
$r_a$ :	aerodynamic resistance [h/cm]
$R_s$ :	observed solar radiation [ $W/m^2$ ]
$R_{s0}$ :	maximum possible solar radiation [ $W/m^2$ ]

$Re_L$ :	Reynolds number [dimensionless]
$RH$ :	relative humidity [percent]
$S_E$ :	slope of the energy grade line [dimensionless]
$S_f$ :	friction slope [dimensionless]
$S_0$ :	slope of the bottom of the channel / parking lot [dimensionless]
$S1...S4$ :	refer to specific values of the slope-roughness parameter, $S^{1/2}/n$
$S^{1/2}/n$ :	slope-roughness parameter [dimensionless]
$t$ :	time [h]
$t_c$ :	time of concentration [h]
$t_d$ :	duration of rainfall [h]
$t_p$ :	time to ponding [h]
$t_{ro}$ :	time from onset of rainfall to cessation of runoff [h]
$T_a$ :	air temperature [ $^{\circ}C$ ]
$T_{af}$ :	characteristic air-vegetation temperature [ $^{\circ}C$ ]
$T_g$ :	ground surface temperature [ $^{\circ}C$ ]
$T_m$ :	average of air temperature and surface temperature [ $^{\circ}C$ ]
$T_p$ :	precipitation temperature; assumed equal to dew-point temperature [ $^{\circ}C$ ]
$T_{ref}$ :	reference temperature for heat export calculation [ $^{\circ}C$ ]
$T_{ro}$ :	temperature of the runoff on the pavement surface [ $^{\circ}C$ ]
$T_s$ :	soil temperature; sometimes refers to soil surface temperature [ $^{\circ}C$ ]
$T_s(0)$ :	initial surface temperature [ $^{\circ}C$ ]
$T_{sp}$ :	temperature of surface of pavement [ $^{\circ}C$ ]
$T_{soil}$ :	composite soil-moisture temperature over some depth [ $^{\circ}C$ ]
$T_v$ :	virtual air-ground temperature [ $^{\circ}C$ ]
$T_w$ :	temperature of the standing water on the pavement surface [ $^{\circ}C$ ]
$u_{af}$ :	characteristic ground-canopy wind speed [m/s]
$U$ :	wind speed [m/s]
$U_2$ :	wind speed evaluated at a height of 2m [m/s]
$V$ :	mean flow velocity [m/s]
$W$ :	width of paved surface [m]
$x$ :	horizontal spatial coordinate [m]
$y$ :	depth of runoff or standing water on pavement surface [cm]
$y_{ave}$ :	average depth of runoff over entire pavement surface [cm]
$z$ :	effective rainfall [cm/h]
$z_a$ :	height of air temperature and wind speed measurements [cm]
$z_{oh}$ :	surface roughness height of heat transfer [cm]
$z_{om}$ :	surface roughness height of momentum transfer [cm]
$z_n$ :	height of channel base above a given datum at point n [m]

## 1. INTRODUCTION

Urbanization affects the temperature of cold water resources, streams and rivers in particular. Cold-water streams typically exist in well-shaded watersheds with large water inputs from groundwater. They are ecologically significant because they support coldwater fisheries and other wildlife that would be unable to survive in warmer streams. Of particular interest is the conversion of land from existing agricultural use or natural conditions. Urban expansion usually requires removing crops and trees and replacing them with parking lots, roads, lawns, and buildings. These changes affect shading, heat transfer, and hydrology within the watershed. Currently, there are few tools available to project to what extent stream temperatures are influenced by development in the watershed.

The main focus of this research is to create a model that would be useful for making decisions on land use and zoning in the watersheds of coldwater streams, to ensure that urbanization does not negatively impact the fragile nature of these ecosystems. Ease of use is essential if the model is to be used for planning and permit decisions. The ideal model would be able to accept standard climate data (solar radiation, air temperature, relative humidity, and wind speed) along with parameters concerning land usage to predict the changes in surface and subsurface runoff temperatures, and ultimately, stream temperature.

One small but significant portion of this overall model is the creation of a sub-model that can predict the runoff volume and temperature from paved portions of watersheds (such as parking lots and roads) during a rainfall event. The increase in impervious surface area in a watershed will increase the volume and temperature of storm water runoff. This is a growing concern in the watersheds of coldwater resources (Van Buren et al., 2000a, 2000b). A number of models are currently available for the prediction of runoff temperature from paved surfaces, and even from entire urban or partially-developed watersheds. These models will be reviewed in more detail in the next section.

This report is intended to give an overview of the heat transfer processes that contribute to the heating of rainfall runoff from a land surface, with particular emphasis on runoff from an impervious surface. With the information on heat transfer processes a model is developed to predict the temperature and flow rate of runoff from such a surface. The bulk of the paper is devoted to the description and derivation of the necessary equations. The intent is to develop a conceptual framework and to compare our formulations with the models developed in earlier work by Van Buren, et al. (2000a, 2000b), Ul-Haq and James (2002), Roa-Espinosa, et al. (2003), and others. Improvements will be made where possible, e.g. by including the effects of radiation and evaporation before, during, and after rainfall events. A fairly complete model will be developed, and then used to determine which terms can be neglected without seriously affecting the accuracy of the model. A sensitivity analysis will also be conducted.

The model needs to address how the rainfall duration and intensity can affect the volume and temperature of the runoff. For example, during a daytime storm of small intensity

with very little runoff, most of the initial rainfall may evaporate and carry heat away from the pavement surface. Runoff will thus not be as thermally-enhanced as it might be if the intensity were higher. Likewise in an event of high intensity and duration, the water reaching a stream will likely not be at an elevated temperature for a long duration, as the thermal signal carried from the pavement will diminish quickly in a large volume of outflow. The model described in this paper should include enough detail to be able to predict the interaction of various processes realistically.

## **2. PREVIOUS STUDIES AND MODELS**

The models for runoff and heat transfer developed by Ul Haq and James (2002), Van Buren, et al. (2000a), Roa-Espinosa, et al. (2003) and Jia, et al. (2002) are perhaps the most relevant to this paper, although certainly not the only models available. The models of Ul Haq and James (2002) and Van Buren, et al. (2000a) have focused on prediction of heating of runoff over impervious surfaces, and do not include the ability to model discharge from an entire watershed. The models by Roa-Espinosa, et al. (2003) and Jia, et al. (2002) were created with the intention of predicting the effects of land-use changes on the temperature and volume of runoff from a watershed.

The model of Ul Haq and James (2002) was developed with the intention of predicting changes in temperature of streams in watersheds with a large storm sewer input. The only heat transfer considered is that within a one-dimensional soil-pavement-air column. A separate program, PCSWMM, was utilized to compute a water balance as input to the model. Key assumptions in this model included a rainfall temperature equal to that of the air and neglect of all heat transfer terms except convection from the ground into the runoff, advection from the rain itself, and evaporation. The model was applied to a stormwater discharge on a cold water stream in Portage, Michigan. Although acceptable correlation was found between simulation results and observed data, it could be argued that the model would have limited applicability due to a number of factors. First, heat transfer with runoff from pervious surfaces was ignored. The effects of both short- and long-wave radiation were neglected, and the heat carried away by the runoff was determined by treating runoff as uniform-depth flow over a flat plate of constant heat flux. Runoff depth and pavement temperature would be expected to vary spatially along any paved surface of considerable length, and the contribution of heat from pervious surfaces should be significant.

The impervious surface runoff model TRMPAVE by Van Buren, et al. (2000a) includes a more rigorous treatment of the surface energy balance than that of Ul Haq and James. Again, heat transfer was treated as one-dimensional in a soil-pavement-air column. TRMPAVE includes the capability to model both dry and wet weather periods, and the energy balance is different for each case. In the dry weather model, the energy balance includes conduction, convection, and net radiation. The wet weather energy balance includes conduction, convection into runoff, convection from runoff into the atmosphere, net radiation, and evaporation, and neglects any heat transferred by the rain itself. A finite difference approximation is used to determine the unsteady heat conduction into the

pavement and soil layers of the subsurface. Using a setup on a large parking lot that included a sprinkler system (for rainfall simulation) and instrumentation at the outlet, the model was tested against observed data for several rainfall events. A number of actual storm events were tested, as well. The model was found to be a good predictor of runoff temperature. It could be argued that the empirical equations used to estimate convection from the pavement into the runoff might not be applicable under all conditions. The spatial variation of runoff depth and pavement temperature was neglected.

The other two models mentioned at the beginning attempt to couple heat and water budgets for both pervious and impervious surfaces. The model TURM, under development by the University of Wisconsin-Madison and the Wisconsin Department of Natural Resources, is the simpler of the two (Roa-Espinosa, et al., 2003). The motivation is to create a tool that can be easily used by developers to plan land use changes in the watersheds of coldwater streams, and specifically to assess measures that can be taken to mitigate the effects of heated runoff. The model attempts to take into account a number of factors, including percentage imperviousness of land uses, air and surface temperatures, soil temperature profiles, heat exchange due to presence or absence of vegetation, and times of concentration of the runoff from different land use types. A large amount of data was taken for a partially-urbanized watershed north of Madison, Wisconsin to validate the model, and good correlation was found between predicted and modeled flow rates and temperatures. A major limitation of the model is that rainfall events are treated as having uniform intensity, a consequence of using the Soil Conservation Service (SCS) curve number method for prediction of runoff hydrographs. The model has been developed to predict changes in runoff regime and temperature on an event scale. Thus it may not be useful for long-term, continuous simulations investigating the extent to which reduced infiltration decreases base flow.

The fourth model is the Water and Energy transfer Processes (WEP) model developed by Jia, et al. (2002). This model has as its goal the prediction of change in water and energy budgets associated with land use changes in an entire urban or partially-urban watershed. WEP includes many details not found in any of the other models, as it can be used to model groundwater flow in addition to surface runoff and temperature. The model treats the watershed as a two-dimensional grid of cells, within which heat transfer is treated in the vertical direction only through a series of ten layers of differing composition. Surface and sub-surface flow is routed based on the average slope of the land surface into adjacent cells, and flow is routed in this way into rivers and other water bodies within the watershed. Water bodies, impervious surfaces, and soil-vegetation surfaces are treated separately, and the effects of evapotranspiration, convection, net radiation, advection, and conduction into the soil are considered, as well as the effects of shading and interception of both vegetation canopies and buildings. Due to the complex nature of the mass and energy balances utilized in this model, the input requirements are also quite extensive. Necessary inputs include detailed knowledge of topography and land use within the watershed, soil composition over a considerable depth, water table depths, and numerous soil and vegetation parameters in addition to the usual climate input data. The model has simulated with a great deal of accuracy a number of watersheds of different composition and sizes, including the western suburbs of Tokyo, the Tama watershed to the west of

Tokyo, and the Ebi River watershed (Jia and Tamai, 1998; Jia et al., 2001; Jia et al., 2002).

In general, most current models of runoff from paved surfaces appear to suffer from oversimplification in some areas. The model of Ul Haq and James (2002), for example, neglects the input of all forms of radiation during a rainfall event, and assumes a rainfall temperature equal to that of the air. In an actual storm event, however, the air temperature usually drops significantly, and it is more likely that rainfall temperature is closer to the dew-point temperature. The runoff model presented by Van Buren et al. (1999) was developed in greater detail and includes the effects of evaporation and radiation, but appears to neglect the heat brought into the runoff by the rain itself. The TURM model makes use of the SCS method for prediction of runoff. It could be argued that the SCS method is too approximate to work accurately in a wide variety of locations. However, TURM is still a work in progress. The WEP model developed by Jia et al. (2001) is far too complex to be applied to a single paved surface.

### **3. MODEL FORMULATION**

Three models are developed: an introductory case, a simplified runoff model, and a third more complete model. All three attempt to take into account the unsteady nature of rainfall events, but differ in their approximations of reality. In Model 1 a simple surface heat and water budget is developed. In Model 2 the main parameters such as runoff depth, runoff temperature, and the major heat fluxes are averaged over the area of the paved surface. Changes of these parameters occur only with time. Model 3 couples temporal variation of the main parameters with spatial variation along the length of the pavement surface. A main goal of this research is to determine whether assumptions made in the simpler models come at the expense of an acceptable level of accuracy.

#### **3.1. Model 1 for standing water without outlet**

##### **• *Description***

Model 1 is a simple model intended to serve as a starting point for the development of more complex mass and energy budgets. The pavement surface (parking lot) is treated as a level catchment with no outlet, with an unsteady but uniform pavement surface temperature and a rainfall of constant temperature and variable intensity (Figure 1). The depth of water is also assumed to be spatially uniform across the lot's surface.

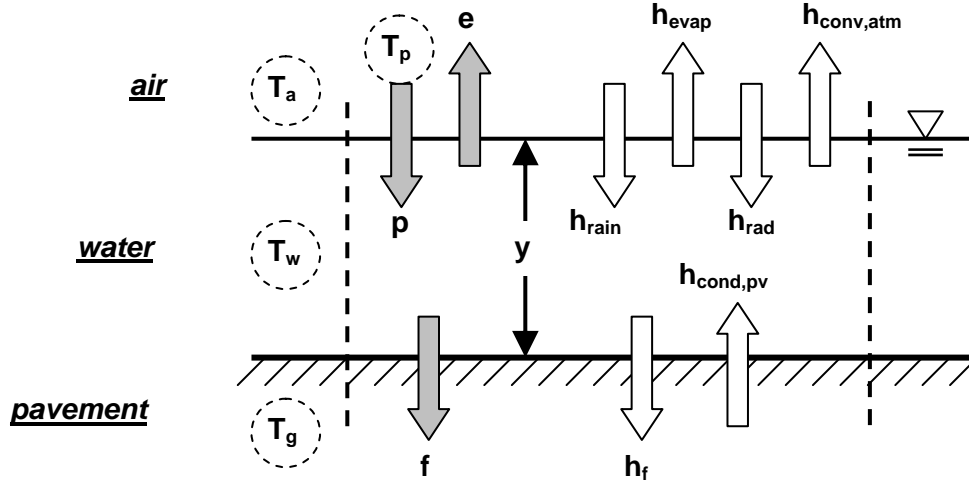


Figure 1. Water and heat fluxes in Model 1 (schematic).

In Figure 1,  $y$  is the water depth,  $T_w$  is the temperature of the standing water,  $p(t)$ ,  $e(t)$ , and  $f(t)$  are the precipitation, evaporation, and infiltration rates, respectively, and  $h_{cond,pv}$ ,  $h_{conv,atm}$ ,  $h_{evap}$ , and  $h_{rad}$  are the heat fluxes of conduction, atmospheric convection, evaporation, and net total (long wave and shortwave) radiation, respectively. Including the effects of evaporation and infiltration, the water mass budget is:

$$\frac{dy}{dt} = p(t) - e(t) - f(t). \quad (1)$$

It is assumed that the precipitation intensity would be known for time intervals of a particular storm event, and that the evaporation can be estimated using a number of equations that will be described in a later section. In the case of rainfall on a pavement surface, there is likely to be little infiltration beyond the initial abstraction for cracks and pores in the surface (thus  $h_f = 0$ ), and during a rainfall event evaporation is likely to be very small because the overlying air will be at or near saturation. Thus the only unknown in the mass budget is the water depth,  $y(t)$ .

The heat budget for the water standing on the pavement would include terms for the time-variable heat storage in the standing water, heat inflow from the falling rain, conduction between the pavement surface and water, net total radiation retained by the water, evaporation, and convection at the water surface:

$$\frac{d(y \cdot T_w)}{dt} \rho C_p = h_{rain} + h_{cond,pv} + h_{rad} + h_{evap} + h_{conv,atm}, \quad (2)$$

where  $T_w$  is the temperature of the standing water,  $\rho$  is the density of water,  $c_p$  is the specific heat of water,  $h_{rain}$  is the heat contribution of rainfall,  $h_{cond,pv}$  is the conduction between the pavement and water,  $h_{conv,atm}$  is the convection between the water and air,  $h_{rad}$

is the net solar and long wave radiation, and  $h_{\text{evap}}$  is the heat transfer due to evaporation, which will be negative and equal to the evaporation rate,  $e(t)$ , multiplied by the latent heat of vaporization of water,  $L_v$ . The rain heat flux will be the product of the heat capacity of water, the rainfall rate, and the difference in temperature between the rain ( $T_p$ ) and water ( $T_w$ ). The surface temperature gradient of the pavement will be needed for the calculation of the conduction term. Since this will be a common parameter needed in all models, its development will be described in a later section.

- ***Limitations***

The major limitation of this model lies in the assumption that there is no water outflow from the parking lot. A scenario in which a parking lot would essentially become a shallow storm water pond is highly unlikely, and also not useful for the purposes of predicting runoff volume and temperature. The assumption that a constant depth of water occurs throughout the lot means that no drainage slope is present. This is also an unrealistic simplification. However, this simple model can serve as a useful foundation for development of the next two models.

### **3.2. Model 2 for spatially-averaged runoff**

- ***Description***

Model 2 is essentially the same as the introductory model, but it includes a runoff term in the water balance. The depth of runoff and all other heat and mass balance parameters are spatially-averaged values over the entire pavement surface. Furthermore, to simplify the heat budget, the entire pavement surface is treated as an isothermal flat plate at some temperature that is a spatial average of the actual surface temperature distribution. A more general model might be necessary to determine accurate values of average runoff depth and average pavement temperature, but the aim of Model 2 is to maintain ease of calculation. A schematic is shown in Figure 2.

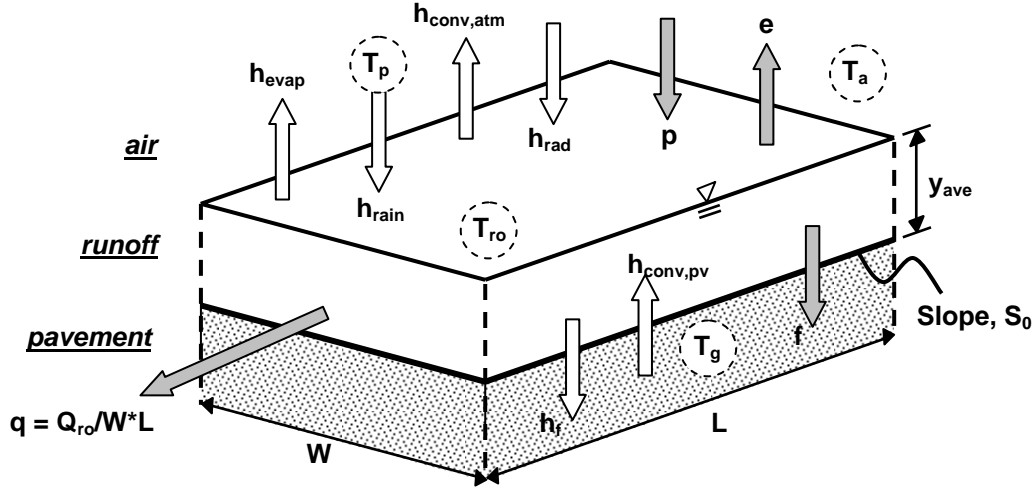


Figure 2. Water and heat fluxes in Model 2 (schematic).

- Water Mass Balance -

The first step in developing Model 2 was to add a runoff term,  $q$ , to the water mass balance of the introductory model, Model 1. Thus the water mass balance becomes

$$\frac{dy_{ave}}{dt} = p(t) - e(t) - f(t) - q(t). \quad (3)$$

A subscript, *ave*, has been added to the water depth,  $y$ , to indicate that it is an average depth over the pavement area,  $A_s$  (the product of  $W$  and  $L$ ). All hydrologic terms are considered to be average values for the entire surface area of the pavement,  $A_s$ . The runoff is assumed to flow straight off the end of the pavement with a per-unit-area flow rate of  $q$ . The sum of the precipitation, evaporation, and infiltration terms is often called the effective rainfall,  $z$ :

$$z(t) = p(t) - e(t) - f(t). \quad (4)$$

The water mass balance can therefore be simplified to:

$$\frac{dy_{ave}}{dt} = z(t) - q(t). \quad (5)$$

As before, it is assumed that the precipitation term is an input to the model, and that the rainfall intensity versus time is known. Evaporation can be estimated using equations that are outlined in Appendix A. The infiltration term,  $f(t)$ , is defined in more detail in Appendix A. While significant for models of pervious surfaces, infiltration in this model is assumed to be negligible due to the presence of the paved surface. Thus the only remaining unknowns in the water balance are the outflow per unit area,  $q$ , and the

average runoff depth,  $y_{ave}$ . Manning's equation can be used to relate these two parameters for the case of sheet flow over a paved surface:

$$q = \frac{1}{n} \cdot (y_{ave})^{2/3} \cdot S_E^{1/2} \cdot y_{ave}, \quad (5)$$

where  $n$  is the Manning's roughness coefficient of the paved surface and  $S_E$  is the slope of the energy grade line. Rearranging Eq. (5) to solve for the depth,  $y$ , gives

$$y_{ave} = \left[ \frac{q \cdot n}{S_E^{1/2}} \right]^{3/5}. \quad (6)$$

The value of the roughness coefficient,  $n$ , can be found in the literature. A typical value would be on the order of 0.02 for a paved surface. The slope of the energy grade line,  $S_E$ , represents the head loss of the flow over the length,  $L$ , of the surface. It will be equal to the slope of the pavement surface,  $S_0$ , if the depth of runoff is assumed to be constant. As will be shown in the derivation of the next model, this condition is due to the fact that the energy slope is the difference between the slope of the pavement surface and the slope of the runoff surface relative to the pavement surface.

#### - Heat Budget -

The calculation of the various terms of the heat budget equation is simplified by making the assumption that the pavement surface can be treated as an isothermal flat plate. The temperature of the water on the paved surface is assumed to be uniform over the area,  $A_s$ , and equal to the runoff temperature,  $T_{ro}$ , which is a function only of time. The heat budget equation includes terms for the time rate of change of stored energy in the runoff, heat lost by the outflow of runoff, heat inflow from the rainfall, heat lost by water infiltrating into the surface, evaporative flux, conductive flux from the heated pavement into the runoff, convective flux from the runoff into the atmosphere, and heat input from radiation:

$$\frac{d(y_{ave} \cdot T_{ro})}{dt} \rho C_p = -h_{outflow} + h_{rain} - h_f + h_{cond,pv} + h_{rad} + h_{evap} + h_{conv,atm}, \quad (7)$$

where  $T_{ro}$  is the average temperature of water on the surface of the pavement,  $h_{outflow}$  is the heat transferred out via runoff,  $h_{rain}$  is the heat flux from rainfall,  $h_f$  is heat transfer associated with infiltration,  $h_{cond,pv}$  is the conduction from the heated pavement into the runoff,  $h_{rad}$  is the net radiation,  $h_{evap}$  is the heat flux associated with evaporation, and  $h_{conv,atm}$  is the convective heat flux from the atmosphere into the water. The net radiation and the evaporative and convective heat fluxes all depend on the unknown temperature of the water on the pavement,  $T_{ro}$ . The above equation (Eq. 7) has to be solved to give this unknown temperature. Weather parameters and a pavement temperature gradient with depth are also needed to complete the calculations of both the convective flux from the

pavement into the water and the net long wave radiation, as will be outlined in a later section.

- ***Limitations***

This model gives a conceptual framework for the determination of the desired outputs-- surface runoff and temperature versus time--for the purpose of estimating the effects of thermally-enhanced runoff on receiving waters. The major limitations of this model include the assumption of a spatially-averaged flow rate, depth, and temperature. The flow regime is not represented realistically. To accurately estimate average depth and temperature, the solution of a general case of spatially-variable temperature and depth distributions would be necessary. For this reason we formulate the more general Model 3.

Note: A slightly more sophisticated version of Model 2 has been developed that takes into account the variation in the flow depth using approximate functions. This model will be described in a separate document.

### **3.3. Model 3 for spatial and temporal variation in runoff**

- ***Description***

This model is considerably more complex than the one previously described. It attempts to take into account both spatial and temporal variation of temperature and water depth on the paved surface. Figure 3 gives a schematic of the water depth distribution on the paved surface in this model. The runoff depth and temperature vary both with time and with distance from the drainage end of the paved surface. If a single parcel of water is followed from the end of the lot (assumed to be the highest point) to the drain end (assumed to be the lowest point), it would be found to increase in depth, velocity and flow rate. It would also increase in temperature as it absorbs heat from the pavement, at least in the initial stages of runoff while the pavement remains warmer than the rainfall temperature. This phenomenon is significant because it could mean that the pavement temperature at the drainage end of the lot may decrease more rapidly than the temperature at the high end of the lot due to the presence of a greater volume of water. This trend could be reflected in a spatially-variable pavement convection term.

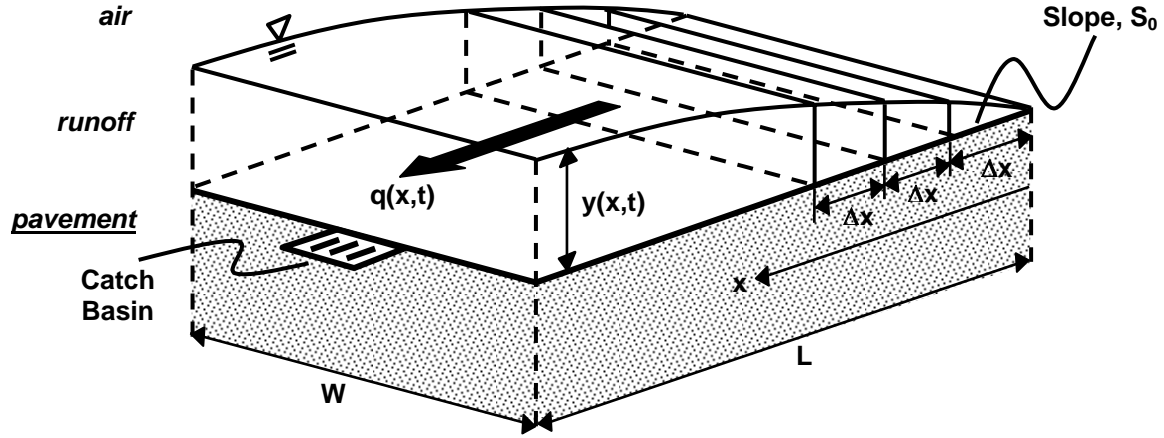


Figure 3. Water depth distribution for Model 3 (schematic).

- Water Mass Balance -

In the event that rainfall intensity remains constant over the total drainage area, at least for a given period of time, it can be assumed that the runoff flow rate reaches a quasi-equilibrium state during this interval, and that it would be found to vary only with the position in the parking lot rather than with both time and position. In this quasi-steady-state case, the water mass balance at any time,  $t$ , and distance,  $x$ , from the far end of the lot, is given as

$$\frac{\partial q(x,t)}{\partial x} = p(t) - f(t) - e(t) = z(t), \quad (8)$$

where  $q$  is the runoff flow rate per unit width,  $q = Q_{ro}/W$ , and  $\partial q/\partial x$  represents the change in flow rate along the slope of the parking lot. As before, the precipitation is assumed to be an input to the model, and the evaporation and infiltration calculations are outlined in Appendix A. In an actual storm event, rainfall intensity normally varies considerably with time, and steady-state is not a realistic assumption. In the case of unsteady state, the water mass balance becomes

$$\frac{\partial q(x,t)}{\partial x} + \frac{\partial y(x,t)}{\partial t} = z(t), \quad (9)$$

where the  $\partial y/\partial t$  term has been added to take into account water storage, i.e. the change in water depth,  $y(x,t)$ , with time,  $t$ .

Since the ultimate interest is in the flow rate and temperature of the runoff, it is useful to arrange the mass balance in a way that gives the runoff flow rate at any point,  $x$ , along the pavement surface. If it can be assumed that there is no spatial variation in the precipitation,  $p$ , infiltration,  $f$ , and evaporation,  $e$ , i.e. that they vary only with time, the runoff rate at any point,  $x$ , can be approximated as:

$$q(x, t) = z(t) \cdot x - \int_0^x \frac{\partial y(x, t)}{\partial t} dx, \quad (10)$$

where the term  $z(t)$ , as defined previously, is the effective rainfall. The above equation can be evaluated at the drainage end of the lot, where  $x=L$ , to give the outflow from the pavement surface. As was the case for Model 2, two unknowns exist: the outflow and the depth of water on the surface,  $y$ . In Model 2, each of these two variables was specified by a time-variable single average value for the entire paved surface. In Model 3, each varies also with distance,  $x$ , along the pavement.

The momentum equation is often used to relate flow and depth for sheet flow. If lateral inflow is neglected and a uniform velocity within the cross-section is assumed, i.e. Boussinesq coefficient = 1, the momentum balance is (Mays, 2001):

$$\frac{1}{A} \frac{\partial Q}{\partial t} + \frac{1}{A} \frac{\partial}{\partial x} \left( \frac{Q^2}{A} \right) + g \frac{\partial y}{\partial x} - gS_o + gS_f = 0, \quad (11)$$

where  $Q$  is the volumetric flow rate,  $A$  is the cross-sectional area of flow in a vertical section,  $y$  is the depth of flow,  $S_o$  is the pavement surface slope, and  $S_f$  is the friction slope. The first two terms are the local and convective acceleration terms, and describe the changes in flow velocity with time and with distance, respectively. The third term concerns the pressure forces due to change in depth with distance, the fourth term describes the gravity forces due to the pavement surface slope, and the last term describes frictional forces (Mays, 2001).

The momentum equation in its complete form is complex and difficult to solve. However, a number of assumptions can be made to simplify the equation. One common set of simplifications leads to the “kinematic wave” model. In a kinematic wave approximation for overland flow such as the runoff from a paved surface, inertial and pressure forces are assumed to be small compared to frictional forces, and the acceleration and pressure terms are neglected. This approximation is justified by the fact that in overland flow the depth of flow will be very small, such that pressure forces will be insignificant. Furthermore, overland surfaces tend to be relatively rough, so frictional forces will be large and flow should not appreciably accelerate downhill. With these assumptions, the momentum equation is simplified to

$$S_o = S_f. \quad (12)$$

The kinematic wave model simplifies the rating curve (plot of flow versus depth) for a surface; the rising and falling limbs of the outlet hydrograph are identical due to neglect of the pressure forces. The flow and depth for a surface can therefore be related by:

$$q = ay^m, \quad (13)$$

where  $q$  is the outflow per unit width and  $y$  is the depth of flow.  $a$  and  $m$  are parameters describing the nature of the surface and flow, and are dependent on slope, roughness, and turbulence. An estimate of these parameter values can be obtained from Manning's equation, given as follows:

$$q = \left[ \frac{1.0 \cdot S_f^{1/2}}{n} \right] y^{5/3}. \quad (14)$$

Thus, after applying the momentum equation ( $S_f = S_0$ ),

$$a = \left[ \frac{1.0 \cdot S_0^{1/2}}{n} \right] \text{ and } m = 5/3. \quad (15)$$

Flow,  $q$ , is now related to slope,  $S_0$ , roughness,  $n$ , and turbulence,  $m$ . In this case, the value of  $m$  (5/3) is for turbulent flow.

If this relation is solved for depth,  $y$ , it can be substituted into the continuity equation to give a complete description of the kinematic wave model. A common form of the equation is found by further introducing two parameters,  $\alpha$  and  $\beta$ , such that

$$\alpha = (1/a)^\beta, \quad (16)$$

$$\beta = 1/m = 3/5, \text{ and} \quad (17)$$

$$\frac{\partial q}{\partial x} + \alpha \beta q^{\beta-1} \frac{\partial q}{\partial t} = z(t). \quad (18)$$

This equation can then be solved by using a variety of numerical schemes to give flow per unit width of pavement,  $q$ , at any point along the pavement surface, for varying intensities of rainfall. With known  $q(x)$ -values for any time,  $t$ , water depths,  $y(x)$ , can be calculated from Eq. (13).

#### - Heat Budget -

The heat budget equation is similar to that introduced in Model 2 (Eq.7). As before, it is necessary to take into account the net advection effects for a control volume. The energy balance for a surface runoff control volume includes the time rate of change of heat storage in the water, the net horizontal advection by the flow over the pavement, heat inflow from the rainfall, heat lost via infiltration, convection from the heated pavement into the runoff, net radiation, evaporation, and convection between the water surface and the atmosphere:

$$\frac{\partial(y \cdot T_{ro})}{\partial t} \rho C_p = - \frac{\partial(q \cdot T_{ro})}{\partial x} \rho C_p + h_{rain} + h_f + h_{cond,pv} + h_{rad} + h_{evap} + h_{conv,atm}, \quad (19)$$

where  $T_{ro}$  is the temperature of the runoff water on the pavement,  $y$  is the depth of runoff, and  $q$  is the per-width runoff flow rate. All three are a function of both time and distance along the lot slope. The other terms have been defined previously.

It is important to note that in Model 3, the pavement surface is not treated as an isothermal flat plate, as it was in Model 2. Thus the calculation of the heat budget terms becomes more complex. As illustrated in Figure 3, the pavement surface is divided into a series of vertical columns, and heat transfer is assumed to occur in the vertical dimension only (1-D). The classical unsteady heat conduction equation is applied to the pavement material to estimate a pavement surface temperature and a convective heat flux from the pavement surface into the water. If the water column is completely mixed vertically, the pavement surface temperature is equal to the runoff temperature,  $T_{ro}$ . A complete description of the terms used in the heat budget can be found in Appendices B and C. Due to its importance in this model, the heat transfer between the runoff water and pavement is considered in more detail in the next section.

- ***Limitations***

The addition of spatial and temporal variation in both the runoff depth and temperature also adds considerable complexity to the model. Therefore, the most significant drawback of this model lies in its complexity, and in particular, the potential difficulty in solving the budget equations. The applied numerical schemes are approximations to more exact solutions, so some degree of accuracy is lost. In addition, the numerical methods require relatively short time steps and spatial scales in order to retain accuracy and stability, and an increase in computation time could be expected for more complex scenarios.

## **4. HEAT TRANSFER BETWEEN RUNOFF WATER AND PAVEMENT**

Under certain weather conditions, perhaps the most critical heat flux is the heat transfer from a hot pavement to storm water runoff. In this section the equations used to describe heat flux between the pavement and runoff are presented. Heat is transferred in two steps: first by conduction from the inside of the pavement or soil to the pavement surface, and second by convection from the pavement surface to the flowing runoff water on top of the pavement. The two processes are in series. Determination of the pavement surface temperature,  $T_s$ , is critical in estimation of the heat transfer rates by both processes.

### **4.1. Convective heat transfer from pavement surface to water**

A diffusive (thermal) boundary layer on top of the pavement will form if the pavement surface and the runoff water are of different temperature. The convective heat flux through that boundary layer, i.e. from the pavement surface to the runoff water, can be described by the following basic convection equation:

$$h_{conv,pv} = k_{conv,pv} (T_s - T_{ro}) \quad (20)$$

where  $k_{conv,pv}$  is the convection coefficient,  $T_{ro}$  is the runoff temperature, and  $T_s$  is the temperature of the pavement surface. The convection coefficient is not easily specified and is usually based on empirical relationships and data. Van Buren, et al. (2000) used a convection coefficient that was proportional to the rainfall intensity, which had been determined from a test plot used in their experimental setup. Such an approach would not be advisable for a general case. Ul Haq and James (2002) used a Nusselt number to estimate the average convection coefficient for the entire pavement length:

$$k_{conv,pv} = N_{uL} \frac{k_w}{L}, \quad (21)$$

where  $N_{uL}$  is the average Nusselt number,  $k_w$  is the thermal conductivity of water, and  $L$  is the length of the paved surface. The Nusselt number was approximated by the following empirical equation, which requires that the Prandtl ( $P_r$ ) and Reynolds ( $R_{eL}$ ) numbers be calculated for the given flow (Ul Haq and James, 2002):

$$N_{uL} = 0.68 P_r^{1/3} R_{eL}^{1/2}. \quad (22)$$

The Prandtl number is defined as

$$P_r = C_p \frac{\mu}{k_w}, \quad (23)$$

where  $C_p$  is the specific heat of water,  $\mu$  is the dynamic viscosity of water, and  $k_w$  is the thermal conductivity of water.

The Reynolds number for flow over the pavement can be determined from

$$R_{eL} = \frac{\rho \cdot V \cdot y_{ave}}{\mu}, \quad (24)$$

where  $V$  is the average flow velocity and  $y_{ave}$  is the average runoff depth (as used in Model 2). With the above set of equations, an average convective coefficient,  $k_{conv,pv}$ , can be estimated for an entire pavement surface.

The empirical equation (22) is only good for Prandtl numbers in the range of 0.6 to 50 (Ul Haq and James, 2002). For temperatures experienced in a temperate climate, e.g. in Minnesota, the Prandtl number of liquid water is in this range. Eq. (22) is for turbulent flow over an isothermal planar surface and gives an average value of the Nusselt number for that surface (Incropera and DeWitt, 2002). This assumption corresponds to Model 2.

In Model 3 spatial variations exist in runoff depth, flow velocity, and pavement surface temperature. Thus the pavement surface was divided into a series of cells in the

horizontal (x) direction along the pavement surface (Figure 3). Unsteady, vertical (1-D) heat transfer is assumed to occur in each cell. The convective equations outlined above are no longer valid for each element given the relatively short distances ( $\Delta x$ ) involved, so a different calculation scheme is needed. The pavement-runoff heat flux is calculated as a residual of the surface energy budget, and iterations are performed on this flux until the predicted pavement surface temperature and runoff temperatures are equal. This process will be explained in more detail in the next section.

#### 4.2. Conductive heat transfer from ground to pavement surface

Below the pavement, surface heat is typically conducted from the ground to the pavement surface during a rainfall event, and is a function of the sub-surface temperature gradient. The heat flux through the pavement surface,  $h_{cond,pv}$ , can be calculated from the heat conduction equation:

$$h_{cond,pv} = k_s \left. \frac{\partial T_s(z,t)}{\partial z} \right|_{z=0}, \quad (25)$$

where  $T_s(z,t)$  is the temperature distribution in the soil, and  $k_s$  is the thermal conductivity of the pavement or soil. The temperature profile below the pavement surface can be obtained by solving the unsteady heat diffusion equation

$$\frac{\partial T_s(z,t)}{\partial t} = \frac{\partial}{\partial z} \left( \alpha_p \frac{\partial T_s(z,t)}{\partial z} \right), \quad (26)$$

where  $\alpha_p = k/\rho c_p$  is the thermal diffusivity of the pavement or soil. The solution of this equation requires an initial temperature profile  $T(z,0)$  in the ground at time  $t=0$ . It also requires two boundary conditions: one at the pavement surface ( $z=0$ ) and one at some depth below the surface. The boundary conditions can be either a heat flux or a temperature. A pavement surface temperature,  $T_s(t)$ , or a ground heat flux are suitable upper boundary conditions. A constant temperature equal to mean annual air temperature plus 1 or 2° C at 8m depth is a good approximation for the lower boundary condition. Other options for this boundary condition include specification of a mean monthly temperature at a depth of 2m, or a groundwater temperature, if a shallow aquifer is present.

A heat diffusion equation used to estimate the subsurface temperature profiles has to be applied to the entire pavement area in Model 2, or to each cell in Model 3. The latter requires significantly more computation, but is not more complex. The issue becomes one of scale: treating the entire paved surface as an isothermal plate versus applying the same equations to smaller, isothermal increments of the pavement surface. In the future, the treatment of a paved surface by the two approaches needs to be evaluated for accuracy, as the simpler scheme would involve significantly less computation time and allow for the model to be easily extended to larger and more diverse watersheds.

### 4.3. Pavement surface temperature and runoff temperature

At the pavement surface ( $z = 0$ ) the heat flux coming out of the pavement has to equal the heat flux into the water above the pavement. Equating the right-hand sides of Eqs. (20) and (25) gives a boundary condition that can be used to find the pavement surface temperature,  $T_s$ . As it turns out, with few exceptions, the convective heat transfer from the pavement surface into the water (Eq. 20) is much faster than the conductive heat transfer through the ground. As a result the temperature differential  $T_s - T_{ro}$  is typically very small. In the case of wet weather, a pavement surface temperature equal to that of the runoff temperature ( $T_s = T_{ro}$ ) is therefore imposed, and it is assumed that the runoff water is well-mixed and of uniform temperature throughout its depth. This situation is illustrated in Figure 4.

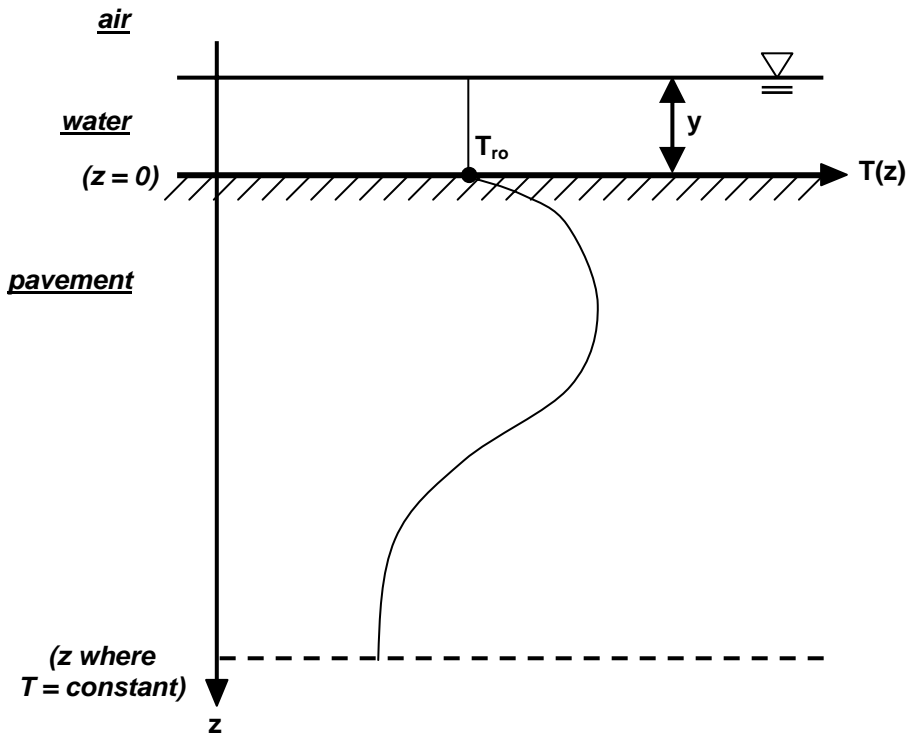


Figure 4. Assumed water/pavement temperature profile during wet weather (schematic).

The above model formulation was found to be suitable for the bulk of a rainfall event. However, the solution of the model equations proved to be highly sensitive and occasionally unstable at the very beginning and end of a rainfall event. The very small water depths present at these times, and the very high heat fluxes out of the pavement surface at the onset of a rainfall event are the probable causes of the issue. Unrealistically high or low water temperatures appear when the water depth,  $y$ , in Eq. (19) is near zero. Furthermore, at the beginning of a rainfall event when the dry pavement surface temperature may suddenly jump to a lower wet pavement surface temperature, the

temperature gradient at the pavement surface would be extremely large, and Eq. (25) may therefore give a very high heat flux. A more robust scheme therefore had to be developed to calculate the heat transfer from the pavement into the runoff, especially at the beginning and end of a rainfall event. This scheme will be outlined in the next section, which covers the numerical methods used to solve the governing equations.

## 5. METHODS USED TO SOLVE HEAT AND MASS BALANCE EQUATIONS

Analytical, exact solutions of the heat and mass budget equations of Model 3 are difficult or impossible to obtain. Numerical solution techniques are therefore required. The three main equations that have to be solved numerically are: (1) the kinematic wave equation used to determine the volumetric runoff rate during rainfall events, (2) the surface energy balance equation for wet weather conditions to obtain the runoff water temperature, (3) the heat diffusion equation to calculate temperature profiles in the soil for both wet and dry surface conditions.

The kinematic wave equation for runoff is solved by an implicit finite-difference method. The equation is discretized by dividing the surface into finite segments of length  $\Delta x$  and using small time steps of duration  $\Delta t$ , and applying Newton's method to linearize the equation. The surface energy balance is discretized by applying the same scheme, and the flows predicted by the kinematic wave solution are used as input. The 1-D unsteady heat diffusion equation is solved by using the Tri-Diagonal Matrix Algorithm (TDMA). In this method the subsoil is divided into layers which can have varying thicknesses and thermal properties, making it useful for layered soils or paved surfaces.

### 5.1. Numerical solution of the kinematic wave equation

The solution scheme applied to the kinematic wave equation (Eq. 18) is an implicit finite-difference method, as outlined by Wilson (2004). In this scheme, the runoff surface is divided into a number of increments of length  $\Delta x$ , as shown in Figure 3. Time is discretized into increments of duration  $\Delta t$ . Thus the kinematic wave equation can be approximated as:

$$\frac{q_j^i - q_{j-1}^i}{\Delta x} + \frac{\alpha(q_j^i)^\beta - \alpha(q_j^{i-1})^\beta}{\Delta t} = \frac{z_j^i + z_j^{i-1}}{2}, \quad (27)$$

where the index  $i$  indicates the time step,  $j$  indicates the cell number (or position along the surface), and  $q_j^i$  is the only unknown in a forward-marching scheme – the flow rate for time,  $i$  and position,  $j$ . Since this is a non-linear equation, Newton's method is applied to extract an explicit equation for the flow rate:

$$q_j^i = \frac{q_{j-1}^i \left( \frac{\Delta t}{\Delta x} \right) + \alpha \beta q_j^{i-1} \left( \frac{q_{j-1}^i + q_j^{i-1}}{2} \right)^{\beta-1} + \Delta t \left( \frac{z_{j-1}^i + z_j^{i-1}}{2} \right)}{\left( \frac{\Delta t}{\Delta x} \right) + \alpha \beta \left( \frac{q_{j-1}^i + q_j^{i-1}}{2} \right)^{\beta-1}}. \quad (28)$$

This equation can easily be applied at all positions along the surface, beginning at the upstream end, for all time increments of the storm event.

Water depths,  $y_j^i$ , can be obtained from Eq. (13) once the flow rates,  $q_j^i$ , are known.

## 5.2. Numerical solution of the runoff energy balance equation

The original energy balance equation (Eq. 19) was developed for a surface runoff volume, with the runoff and sub-surface pavement-soil volumes coupled only through the pavement-runoff heat flux term ( $h_{cond,pv}$ ). In the case of a pervious surface, an additional exchange of heat would result from infiltration of precipitation ( $h_{rain}$ ). Even for a paved surface where infiltration is negligible, the volume of runoff on the surface relative to the volume of soil will be small. As a result, significant numerical instability exists when considering all ‘atmospheric’ fluxes (i.e., net radiation, atmospheric convection) to act upon the runoff volume rather than on the underlying pavement.

In implementing a complete surface energy balance for wet weather, a critical assumption was made that the atmospheric fluxes could be considered to exchange heat with the pavement-soil volume rather than with the runoff itself. The presence of surface runoff modified surface properties such as albedo and emissivity, allowing the runoff to still exhibit some influence over the magnitude of these fluxes. Rainfall and runoff advection and pavement-runoff heat conduction remain in the runoff energy balance. Thus the surface heat budget is divided into two portions: one for the runoff volume, the other for the pavement-soil column. Neglecting infiltration, the modified runoff energy balance is written as:

$$\frac{\partial(y \cdot T_{ro})}{\partial t} \rho C_p = - \frac{\partial(q \cdot T_{ro})}{\partial x} \rho C_p + h_{rain} + h_{cond,pv}, \quad (29)$$

where, as before, the  $h_{cond,pv}$  term represents the pavement-runoff heat exchange. The pavement surface -soil column energy balance is:

$$h_{total} = h_{rad} - h_{conv,atm} - h_{cond,pv}, \quad (30)$$

where the sign convention used assumes that atmospheric convection will represent a heat loss from the surface, and the pavement-runoff term will have the opposite sign as in the runoff energy balance. The  $h_{total}$  term is the net heat flux at the top of the pavement-

soil column, and becomes the upper boundary condition for solving the 1-D heat diffusion equation, which is described in the next section.

As was mentioned in a previous section, estimating the pavement-runoff heat flux term requires a scheme more robust than using the temperature gradient near the surface. To make the computation more robust, we replace the instantaneous heat flux from the soil (Eq. 25) by the change in heat storage in the ground over a time step,  $\Delta t$ . The issue of an uncertain soil temperature gradient near the pavement surface is thus avoided. Instead of Eq. (25), we use the change in heat storage:

$$\int h_{cond,pv} dt = -\rho_s C_{p,s} \int \frac{\partial T(z,t)}{\partial t} dz, \quad (31)$$

which can be approximated by:

$$\int h_{cond,pv} dt = -\rho_s C_{p,s} \frac{\Delta T_s}{\Delta t} \delta_s C_1, \quad (32)$$

where  $\Delta T_s$  represents the change in pavement surface temperature over a time step  $\Delta t$ ,  $\delta_s$  is the depth of penetration of the temperature change (Figure 5), and  $\rho_s C_{p,s}$  is the heat capacity of the soil (or pavement). The factor  $C_1$  depends on the temperature profiles at the beginning and the end of a time step; values between 0.25 and 0.5 would be typical. The value of  $\delta_s$  can be estimated from the thermal diffusivity of the soil or pavement,  $\alpha_p$ , and the length of the time step,  $\Delta t$  (Incropera and DeWitt, 2002; Eckert and Drake, 1972):

$$\delta_s = 4(\alpha_p \Delta t)^{1/2}. \quad (33)$$

Substituting Eq. (33) into Eq. (32) and integrating gives the change in heat storage (average heat flux) as:

$$h_{cond,pv} = -4\rho_s C_{p,s} \frac{\Delta T_s}{\Delta t} (\alpha_p \Delta t)^{1/2} C_1. \quad (34)$$

Since the change in surface temperature,  $\Delta T_s$ , is also the change in runoff temperature,  $\Delta T_{ro}$ , over a time step,  $\Delta t$ , Eq. (34) can be used in a numerical form of Eqs. (29) or (30) to find runoff temperatures. Using the index notation as outlined in the previous section, the temperature difference,  $\Delta T_s$ , can be evaluated as:

$$\Delta T_s = T_{s,j}^i - T_{s,j}^{i-1} = T_{ro,j}^i - T_{ro,j}^{i-1}, \quad (35)$$

where it is assumed that  $T_s = T_{ro}$ . Discretized versions of the other heat flux terms in the runoff and pavement energy balances are not presented here, but equations used to evaluate these terms can be found in Appendices B and C.

Another discretization presented here is of the runoff heat storage term, which is the left-hand side of Eq. (29). If it is assumed that the runoff depth does not change significantly over a time step, the term can be discretized as:

$$\rho C_p \frac{\partial(y \cdot T_{ro})}{\partial t} = \rho C_p \cdot y_j^i \frac{T_{ro,j}^i - T_{ro,j}^{i-1}}{\Delta t}. \quad (36)$$

If a small enough time step is used, the assumption of a quasi-equilibrium depth will likely not result in large errors.

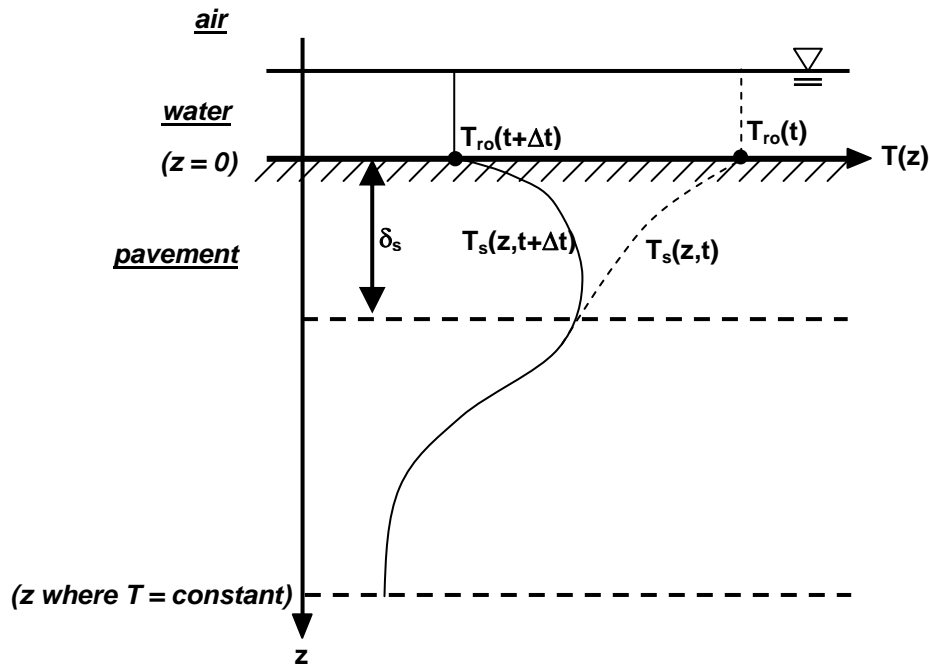


Figure 5. Depth of penetration of heat,  $\delta_s$ , during time step,  $\Delta t$ .

It is important to note that since the change in heat storage of the pavement is based on the change in surface temperature, the underlying assumption is that this temperature change is due only to the pavement-runoff heat exchange. However, in the current implementation this heat flux term is not the only flux acting on the pavement-soil volume; the atmospheric fluxes are also acting on this volume. Thus, in terms of a computation sequence,  $h_{total}$  must be evaluated first without inclusion of the  $h_{cond,pv}$  term (i.e., with only the atmospheric fluxes), and the 1-D heat diffusion equation solved to get an intermediate surface temperature,  $T_{ro}'$ . The  $h_{cond,pv}$  term can then be evaluated explicitly by substituting this intermediate surface temperature into Eq. (34) for  $T_{s,j}^{i-1}$ .

Solution of the runoff energy balance (Eq. 29) with  $h_{cond,pv}$  evaluated in this way results in a first guess at the new runoff temperature,  $T_{ro}$ ; solving the soil-pavement energy balance (Eq. 30) for  $h_{total}$  and applying this flux to the unsteady heat diffusion equation provides a

second guess at the new runoff temperature. If the two guesses do not agree, the  $h_{cond,pv}$  term can be adjusted and iterations performed until the guesses converge.

### 5.3. Numerical solution of the unsteady soil heat conduction equation

The unsteady 1-D soil heat conduction equation is applied to the pavement and its sub-layers. It can be written as:

$$\frac{\partial T}{\partial t} = \alpha \frac{\partial^2 T}{\partial z^2}. \quad (37)$$

There are several methods to solve this equation numerically. The current model uses a scheme known as the Tri-Diagonal Matrix Algorithm (TDMA) to solve a discretized version of the equation, which will be described briefly in this section.

The conduction equation is discretized by dividing the sub-surface vertically into a total of N discrete layers. Each layer, j, has some temperature,  $T_j$ , thickness,  $\Delta z_j$ , and thermal diffusivity,  $\alpha_j$ . Assuming that heat transfer between the layers occurs only via conduction, and integrating Eq. (37) over the entire volume of a layer, for a discrete time step,  $\Delta t$ , results in an equation of the following form (Patankar, 1980):

$$a_i T_{j-1}^{i-1} + b_i T_j^{i-1} + c_i T_{j+1}^{i-1} = d_i, \quad (38)$$

where i indicates the point in time, j is the layer number, and  $a_i$ ,  $b_i$ ,  $c_i$ , and  $d_i$  are time-dependent coefficients. The underlying assumption in this equation is that the temperatures at time i-1 persist throughout the time step until time i. The coefficients are defined as:

$$\begin{aligned} a_i &= \frac{\alpha_{j-1}}{\Delta z_j \cdot \delta z_{j-1}} \\ b_i &= \frac{1}{\Delta t} - \frac{\alpha_{j-1}}{\Delta z_j \cdot \delta z_{j-1}} - \frac{\alpha_j}{\Delta z_j \cdot \delta z_{j+1}}, \\ c_i &= \frac{\alpha_j}{\Delta z_j \cdot \delta z_{j+1}} \\ d_i &= \frac{1}{\Delta t} \cdot T_j^i \end{aligned} \quad (39-42)$$

where  $\delta z_{j-1}$  is the distance between the centers of layer j and layer j-1, and  $\delta z_{j+1}$  is the distance between the centers of layer j and layer j+1 (Patankar, 1980). The temperature of interest,  $T_j^i$ , is lumped into the  $d_i$  coefficient, and can be solved for using the TDMA method.

Boundary conditions, which will be necessary at the surface ( $j=0$ ) and at some finite depth in the soil column ( $j=N$ ), can be specified as a temperature or heat flux value. In the case of a specified temperature,  $a_i=0$ ,  $b_i=1$ ,  $c_i=0$ , and  $d_i$  equals the specified temperature. If a heat flux is specified as the boundary condition, which in this model is the case for the upper boundary (soil surface),  $a_i$  becomes zero,  $c_i$  remains unchanged from the general formulation (Eq. 41), and  $b_i$  and  $d_i$  are defined as follows:

$$b_i = \frac{1}{\Delta t} - \frac{\alpha_0}{\Delta z_0 \cdot \delta z_1}, \quad (43,44)$$

$$d_i = \frac{h_{net}}{\rho C_p \Delta z_0} + \frac{1}{\Delta t} \cdot T_0^i,$$

where  $h_{net}$  is the net surface heat flux, and  $\rho C_p$  is the heat capacity of the surface layer. In this model, an adiabatic condition is used at the lower boundary; Eqs. (43) and (44) can be used for this purpose by setting  $h_{net}$  equal to zero.

Writing the conduction equation for each layer results in a system of equations with as many unknown temperatures as equations; if the coefficients are placed in an array, they will be aligned along three diagonals of the matrix. In each layer the temperature of that layer can be written in terms of the temperatures of the two surrounding layers, which can then be substituted into the equation for the next layer down, and so on. At the bottom layer (N) the temperature is either specified (temperature boundary condition) or is the same as in the previous (N-1) layer (adiabatic boundary condition), and back-substitution provides values for the temperature at all layers above that.

An important feature of this method is that the layers can vary in thickness and thermal properties. This is an important, as the surface pavement layer typically rests on top of a sub-grade material, which in turn is above the local soil, all of which will have different properties. Using greater layer thicknesses at greater depths where soil temperature changes occur more slowly reduces computation time.

The TDMA can be used for both wet and dry weather energy balances. For the dry weather energy balance, the surface boundary condition is the ground flux, which is the residual of the surface energy balance. For wet weather conditions with surface runoff, the surface boundary condition is the ground-runoff heat flux, which is found for each runoff increment ( $\Delta x$ ), or cell, as has been discussed earlier.

#### 5.4. Computational sequence

The computational sequence for dry weather is fairly straightforward. For each time step, the net surface heat flux is found from a simplified version of Eq. (19):

$$h_{net} = h_{rad} - h_{evap} - h_{conv,atm}. \quad (45)$$

The 1-D unsteady heat diffusion equation (Eq. 37) is solved using this net flux as the upper boundary condition, resulting in a new sub-surface temperature profile.

The computational sequence for wet weather is more complicated. The sequence is as follows:

- (1) The kinematic wave equation (Eq. 18) is solved to obtain flow rates and water depths.
- (2) The energy balance equation for the soil-pavement volume is solved for the net flux into the ground (Eq. 30), taking into account only the atmospheric fluxes (net radiation and convection). Solving the 1-D unsteady heat diffusion equation (Eq. 37) results in an intermediate surface temperature. An estimate of the pavement-runoff heat flux ( $h_{cond,pv}$ ) is obtained from Eq. (34).
- (3) The runoff heat budget (Eq. 29) can then be solved to obtain a first guess of the runoff temperature at the end of the time step.
- (4) The first guess at the runoff temperature is used in Eq. (34) to find a modified value of the pavement-runoff heat flux ( $h_{cond,pv}$ ), which is then substituted into the complete soil-pavement energy balance (Eq. 30) to find  $h_{total}$ , which provides a second guess of the runoff temperature when combined with the unsteady heat diffusion equation (Eq. 37).
- (5) The two estimates of the runoff temperature, as obtained in Steps 3 and 4, should approximately agree. If not, the estimate as found in Step 4 is substituted into Eq. (34) to find a new  $h_{cond,pv}$ . This new value is weighted with the old value of  $h_{cond,pv}$  (as found in Step 4) to obtain a 'composite' pavement-runoff heat flux value. After substituting it into the pavement-soil energy balance (Eq. 30), and finding a new  $h_{total}$ , the diffusion equation is then solved again to find a new surface temperature (which is the same as the runoff temperature). If this estimate of runoff temperature agrees with that found in (3), the program proceeds to the next runoff cell.
- (6) Steps 2-5 are repeated for each runoff-pavement-soil cell for the current time step, starting at the upstream end. Then the calculation proceeds to the next time step, and begins with Step 2.

The use of an iteration scheme (Step 5) prevents fluctuations in the initial predictions of surface and runoff temperature that lead to instability, while also removing the need for an explicit equation for the pavement-water heat flux term, which is a difficult flux to characterize.

## 6. MODEL INPUT AND IMPLEMENTATION

To implement Models 2 and 3, boundary conditions and initial conditions must be specified, and both time and spatial scales must be chosen for numerical solutions of the equations. Operation of the model requires weather data, soil and pavement properties, and selection of significant parameter and coefficient values.

The upper boundary condition for the hydro-thermal model described above is a calculated heat flux through the water surface, while an adiabatic condition is used at the lower boundary, based on the assumption that at a great enough depth there will be no heat flux for the relatively short time scales involved. The temperature at this lower boundary, used to calculate an initial temperature profile, will be a necessary input.

Initial conditions are given by the dry weather temperatures of the pavement and ground prior to a rainfall event. The sub-surface pavement and soil temperature profiles can be simulated continuously with weather data as input; the wet weather equations outlined previously are used during rainfall events, while a simplified set of equations are used for dry weather conditions. Van Buren et al. (2000b) used eight days of dry weather prior to a rainfall event to prime a storm water pond model simulation, and five days of dry weather prior to a rainfall event to prime their urban runoff model (Van Buren et al., 2000a). Heat transfer processes on the ground surface during dry weather periods, and the computation of dry weather surface and ground temperatures for paved and other surfaces will be described in later work.

Time and distance scales for the numerical solution of the equations have to be related to the runoff velocities and the rainfall intensities and durations. Rainfall intensities are usually measured at weather stations at hourly intervals. Runoff velocities are typically on the order of 1 to 10 cm/s. With spatial scales on the order of 1 to 10m, time scales will therefore be on the order of seconds or minutes.

A description of surface topography is another necessary input to the model. The paved surface model will require a surface area and average slope for the usually well-delineated paved surface. A Manning's roughness will also need to be estimated for the paved surface, as well as any shading that might be present from buildings, trees, or vehicles.

Unless a pavement surface has a large number of cracks or is of a porous nature, it is likely that the infiltration term in the water mass budget can be neglected during a rainfall event. An initial abstraction of water, which describes the portion of the first rainfall that fills cracks and pores in the pavement surface, is still necessary. However, all rainfall could be assumed to become runoff after the initial abstraction has occurred, minus any evaporation that might occur.

Weather data from stations of the National Weather Service are available at 1-hour intervals. Weather stations operated by other organizations or individuals may give weather data (solar radiation, air temperature, relative humidity, wind speed, cloudiness) every hour, or perhaps less. An important question will be whether the weather data collected at an existing weather station are representative of another site where the paved surface will be located. Solar radiation and cloudiness between two stations not more than a few kilometers apart generally correlate well. Even air temperature and relative humidity (dew point) may correlate reasonably well, but wind speed may not. Wind sheltering and local variations in wind speeds will be a significant issue. Rainfall temperature can be approximated by the dew-point temperature of the air, but that

assumption may fall short of reality during hail storms. Rainfall temperature information needs to be collected.

During and often before a rainfall event solar radiation becomes blocked by a cloud cover resulting in a cooling of the ground surface; the net radiation term then becomes the balance between the long wave radiation emitted by the ground surface, and that emitted by the atmosphere. In some models, atmospheric radiation has been ignored during the course of a rainfall event. Although radiation may indeed be negligible during a rainfall event, it will be included in this model, because it is significant before and after rainfall.

Evaporation is largely a function of the relative humidity of the air, which approaches or is at 100% during a rainfall event. Therefore evaporation may be negligible during most of a rainfall event. However, it should be noted that evaporation may be significant between the onset of rainfall and the first sustained runoff; the initial rain may evaporate, especially if the pavement is hot, and the pavement surface temperature may consequently be lowered. After rainfall and runoff have ended, evaporation may again be significant, and it could remove the moisture remaining on the pavement surface. The associated heat loss may be significant, but is perhaps not of great significance as the focus of the model is on prediction of runoff temperature.

Important parameter and coefficient values that must be specified include albedos for short wave radiation, emissivities for long wave radiation, wind speed coefficients for convective heat transfer, and thermal conductivities of pavements. These parameters will influence the temperature conditions prior to the rainfall/runoff event simulations.

The necessary soil, pavement, and general surface properties can be difficult to estimate, especially if vegetation is present. Surface parameters such as albedo, emissivity, Manning's roughness, displacement height, and roughness lengths for momentum and heat transfer are a function of the land cover type. In the case of a paved surface the determination of these parameters can be simplified because of the lack of vegetation. The surface heat budget also requires thermal properties -- such as thermal conductivity and specific heat -- for both the pavement and the subsoil. For the pavement, thermal properties are largely a function of pavement type and temperature. For the soil, both thermal and hydraulic properties are a function of soil type, temperature, and moisture content, all of which can vary with depth below the surface. Thus estimation of soil properties can be complicated. Properties as used in this model are listed in Appendix E.

The depth of a shallow water table, or a depth at which the soil is saturated with groundwater, can become an important parameter to identify in long-term studies. This information will be necessary to fix the lower boundary condition in a soil moisture model. If data on a shallow ground water table are scarce, a ground water model may become necessary. It should be noted that for an event-based simulation the bottom boundary condition is not as critical as it is for a long-term simulation (e.g., for a season or multiple events), and in the case of the model described in this report, which is concerned with runoff from a paved surface, a soil moisture model is not implemented.

It is interesting to speculate about the effect of rainfall intensity on thermal enrichment of the runoff. Events with a low intensity and duration of rainfall may result in little runoff. In that case it may be found that most of the rainfall evaporates and that the small and possibly very warm amount of water does not represent a significant heat flux. Likewise, in a rainfall event of large magnitude, the heat absorbed by the runoff from the pavement may not be large enough to significantly change the temperature of the runoff, and especially not for a prolonged period of time. The thermal impact of runoff in such a case will be extremely sensitive to the rainfall temperature. Therefore it might be expected that the most thermally-enhanced runoff could be produced by a rainfall of intermediate intensity. Such a rainfall event could absorb a large enough quantity of heat from the pavement to significantly increase the runoff temperature, with a substantial enough volume of water to impact receiving waters. A sensitivity analysis was performed on the current model in order to investigate the effect on runoff temperature of rainfall intensity and duration, as well as other factors. The results are presented in the next section.

## 7. MODEL RESULTS/ SENSITIVITY STUDY

### 7.1. Objectives of the sensitivity study

A sensitivity study was performed using model responses/results to address four issues:

- (1) What physical parameters of the paved surface exhibit the most influence on heating of the runoff?
- (2) What type of rainfall event (i.e., intensity, duration, and rainfall temperature) is likely to contribute the largest amount of heating?
- (3) How significant are lengthwise effects? Are significant horizontal gradients present in runoff depth and temperature? Is a simpler 1-D model (i.e., Model 2) likely to perform as well as a quasi-2-D model such as Model 3?
- (4) How does the difference between initial pavement temperature and rainfall temperature affect the amount of heat that can be extracted from the pavement by the runoff?

The output of interest for a single event includes: 1) horizontal distributions of runoff depth and water temperature with time, and 2) a ‘thermograph’, or time-series of temperature and flow rate of runoff values at the parking lot outlet. With this information, an instantaneous ‘heat export rate’ from the parking lot can be defined as

$$h_{exp} = \rho_w C_{p,w} \cdot \frac{q_{ro}}{L} \cdot (T_{ro} - T_{ref}) \quad (46)$$

where  $h_{exp}$  is in Watts per square meter of parking lot surface area.  $L$  is the lot length,  $q_{ro}$  is the per-width flow rate at the outlet,  $T_{ro}$  is the outlet runoff temperature, and  $T_{ref}$  is some reference temperature. As defined here,  $h_{exp}$  is an instantaneous rate of heat export.

If integrated with respect to time over the duration of the entire runoff event, i.e. until runoff ceases, a total heat export,  $H_{\text{exp}}$ , can be found:

$$H_{\text{exp}} = \int h_{\text{exp}} dt = \frac{\rho_w C_{p,w}}{L} \int_0^{t_{ro}} q_{ro} \cdot (T_{ro} - T_{ref}) \cdot dt \quad (47)$$

where  $t_{ro}$  is the time between onset of rainfall and cessation of runoff, and  $H_{\text{exp}}$  will have units of energy per surface area (e.g.,  $\text{J}/\text{m}^2$ ). The choice of a reference temperature will determine the magnitude of the heat export, so its selection is not trivial. One option is to make the rainfall temperature the reference temperature. In that case the heat export indicates the extent to which the paved surface is heating the rainfall relative to a case in which the paved surface was not present. Another option, and the one used in the current implementation, is selecting a temperature near the upper limit of the temperature tolerance range of trout. For most species of trout in Minnesota, a stream temperature of much higher than  $20\text{ }^\circ\text{C}$  induces stress, and can even be lethal for prolonged periods of time (Eaton et al., 1995). A reference temperature of  $20\text{ }^\circ\text{C}$  is used in this sensitivity study, as it results in a heat export that indicates the potential heating load that could result in stress for trout if no mitigation or management practices were present. In this sense the heating load represents a worst-case scenario.

A number of model input parameters have to be specified. In general, the parameters fall into three categories: (1) physical characteristics of the paved surface (lot length, slope, and roughness), (2) parameters that characterize the rainfall event (intensity, duration, and temperature of the rainfall), and (3) antecedent conditions (initial paved surface temperature and sub-surface temperature profile). To reduce the number of potential simulation combinations, a few simplifications are introduced:

- (1) Lot slope and roughness are lumped into a single parameter ( $S^{1/2}/n$ ), which appears in Manning's equation and the kinematic wave equation.
- (2) The rainfall temperature is fixed for the duration of the event at  $20^\circ\text{C}$ . This value was chosen by assuming that rainfall temperature is well-approximated by dew point temperature.  $20\text{ }^\circ\text{C}$  is similar to the mean July wet-weather dew point temperature of  $18.5\text{ }^\circ\text{C}$  observed over a period of 6 years at the Minnesota Department of Transportation's MNRoad project site.
- (3) An initial lot surface temperature of  $30\text{ }^\circ\text{C}$  is specified. This value was chosen based on an observed difference between pavement surface and dew point temperatures at the onset of precipitation at the MNRoad site (around  $8\text{ }^\circ\text{C}$ ). Again, this is a mean July value observed over a 6-year period. A value of  $10^\circ\text{C}$  was chosen for the purposes of the sensitivity study, resulting in an initial lot surface temperature of  $30\text{ }^\circ\text{C}$ . A roughly exponential sub-surface temperature profile down to a value of  $26.6\text{ }^\circ\text{C}$  at a depth of 60 cm is assumed (Figure 6), where  $26.6\text{ }^\circ\text{C}$  is the mean July temperature observed at a 60 cm depth over the same 6 year period at the MNRoad site. Other initial temperature profiles could be used, based on specification of the initial surface temperature. These are also illustrated in Figure 6, and details on how the profiles were determined can be found in Appendix D.

- (4) Rainfall event duration is held constant at one hour, and the magnitude of the intensity is changed between events. Each event would thus consist of a one-hour, constant intensity rainfall.

With these simplifications in place, the number of simulations required for a sensitivity study became more manageable.

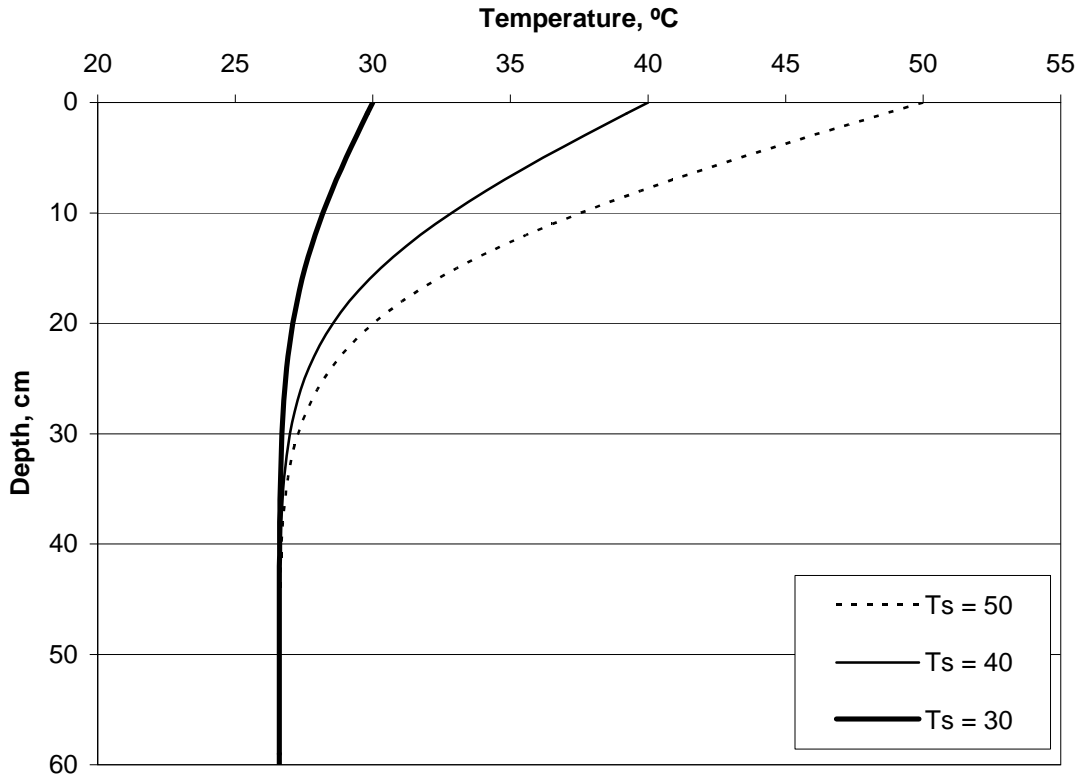


Figure 6. Initial sub-surface temperature profiles, as a function of specified surface temperature. Temperature fixed at 26.6°C at a depth of 60cm.

A simulation plan was developed as follows. Two different lengths (25m and 100m) were selected to investigate the effect that lot length has on horizontal gradients of runoff temperature. In terms of roughness and slope, it was assumed that lot slopes would be in the range of 0.33% to 3.5%, and that Manning's n would range from 0.022 to 0.088 (0.022 represents a fairly new and smooth surface area, while 0.088 is representative of a rough and worn surface area). This resulted in a range of  $S^{1/2}/n$  of 0.65 to 8.50, with 0.65 representing a nearly flat, rough surface and 8.50 representing a steep, relatively smooth surface. These two extreme values bracket the likely range of lot roughnesses and slopes. The remaining input parameter was the rainfall intensity; 0.8cm/h, 2.5cm/h, and 7.5cm/h were chosen to represent a range of likely events. The pavement was assumed to be 10cm thick, with 50cm of subgrade below that. Thermal conductivities for the pavement and soil were assumed to be 0.8 W/m\*K and 1.0 W/m\*K, respectively (see Appendix E). In terms of model parameters, the model used a vertical layer thickness ( $\Delta z$ ) of 1cm for a

total of 60 layers, a runoff cell width ( $\Delta x$ ) of 1m, and a time step of 5 seconds. In the sensitivity simulations, the atmospheric heat input was set to zero, i.e. no weather input was used, and the only heat sources are the rainfall and the paved surface. This was done to isolate the heating effect of the pavement on the runoff. A summary of the simulation plan for the sensitivity study is given in Table 1.

Table 1. Parameter selection for sensitivity study.

<b>Modified Parameters</b>	
Rainfall Intensity (constant over event):	0.8 cm/h, 2.5 cm/h, 7.5 cm/h
Lot length:	25 m, 100 m and 5m
$S^{1/2}/n$ :	0.65, 8.50
<b>Constant Parameters</b>	
Event duration:	1 hour
Rainfall Temperature:	20 °C
Initial Pavement Temperature:	30 °C
Initial lower-boundary Temperature:	26.6 °C (60 cm)
Reference Temperature:	20 °C
<b>Model parameters</b>	
$\Delta t$ :	5 sec
Runoff cell width, $\Delta x$ :	1.0 m
Number of sub-surface layers:	60
Sub-surface layer thickness, $\Delta z$ :	1 cm

## 7.2. Results of the sensitivity study: Horizontal distributions of water (runoff) depth and temperature

The first set of simulations was for a rainfall intensity of 2.5cm/h, varying the lot length, L and slope-roughness factor,  $S^{1/2}/n$ . A sample of the output for the short lot and low slope-roughness is shown in Figure 7.

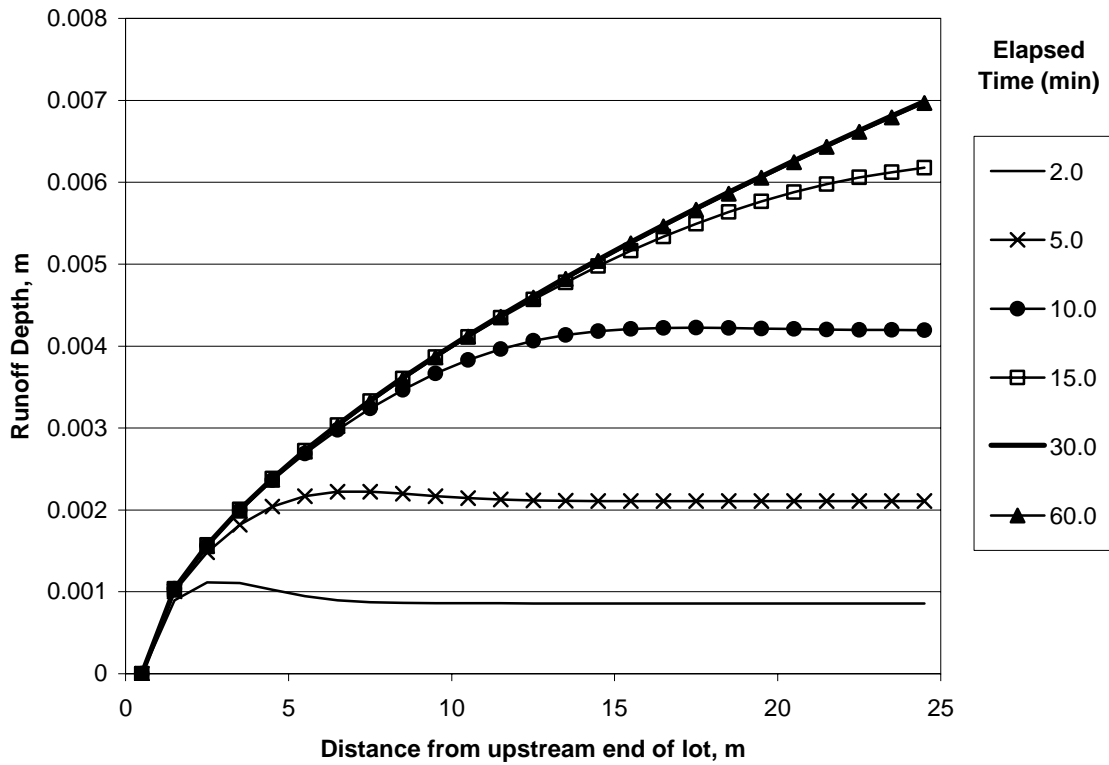


Figure 7. Horizontal distributions of runoff depth vs. time, for a one-hour 2.5cm/h intensity event. Lot length = 25m,  $S^{1/2}/n = 0.65$ .

On this flat, rough surface ( $S^{1/2}/n = 0.65$ ), a quasi-steady state water depth profile is reached between 15 and 30 minutes. This is also known as the time to equilibrium,  $t_e$ . At that time the water depth at the outlet of the lot is 7mm. A water (runoff) temperature vs. distance plot for the same event is shown in Figure 8.

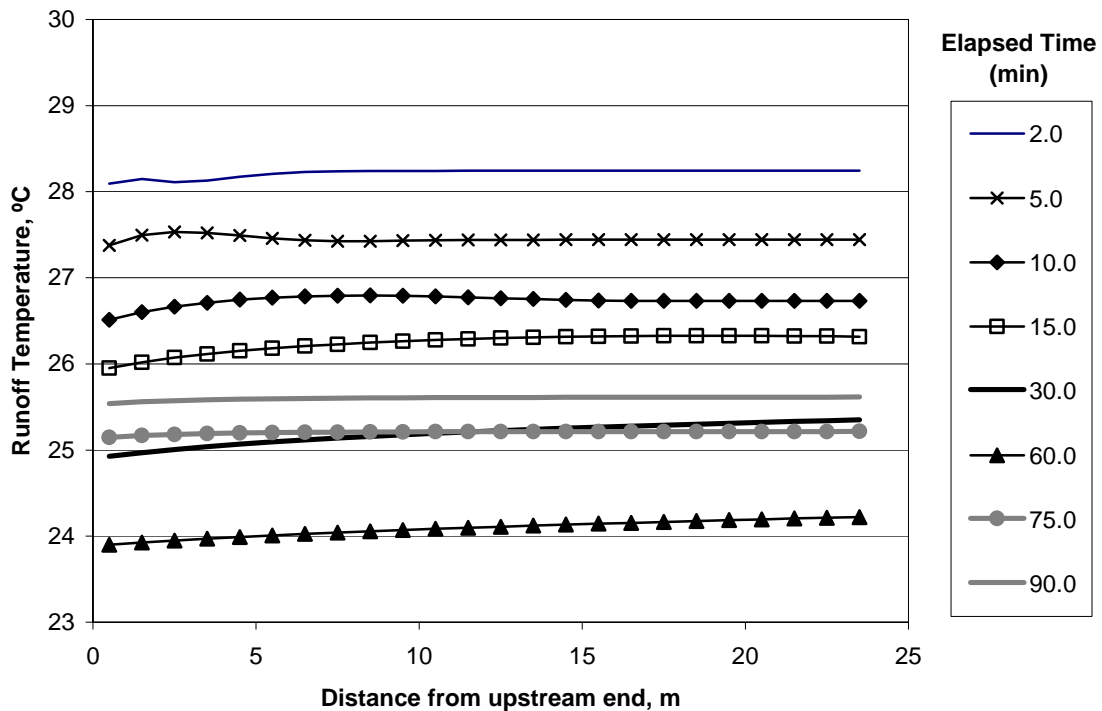


Figure 8. Horizontal distributions of runoff temperature vs. time, for a one-hour 2.5cm/h intensity event. Lot length = 25m,  $S^{1/2}/n = 0.65$ , rainfall temperature is 20.0 °C, initial pavement surface temperature is 30.0°C.

Near the beginning and the end of a rainfall event, the temperature gradient along the slope of the lot is very small. A maximum difference of around 0.4 °C exists between the upstream and downstream ends, at 30 minutes into the rainfall event. The gradients are particularly strong in the first 5 m of the lot, while the runoff temperature is approximately uniform in the lower portion of the lot length. This holds true for most of the event. Other important features of the plot are (1) the minimum runoff temperature occurs at the very end of the event, and (2) the runoff temperature increases after the rainfall has ended. Since there is no weather input in this particular case, this heating of the runoff occurs solely as a result of conduction from the pavement and subgrade.

Plots made for other slope-roughness conditions showed very similar results. Figures 9 and 10 give water depths and water temperatures for a steep and smooth lot ( $S^{1/2}/n = 8.5$ ) with all other conditions the same as for Figures 7 and 8. For the steep slope-low roughness condition, a ‘steady-state’ depth profile was reached in less than 5 minutes, i.e. much sooner than in the case of low slope-high roughness. The water depths on the steeper slope lot were smaller, as to be expected. The temperature gradients along the lot are less severe in the high slope case, most likely because of smaller water depth and shorter time to equilibrium relative to the low slope case. The magnitudes of the runoff temperatures were very similar for the downstream portions of the lot in both cases. Slope and roughness of the lot obviously influenced the water depth distributions, but appeared to have very little effect on the temperature distribution of the runoff.

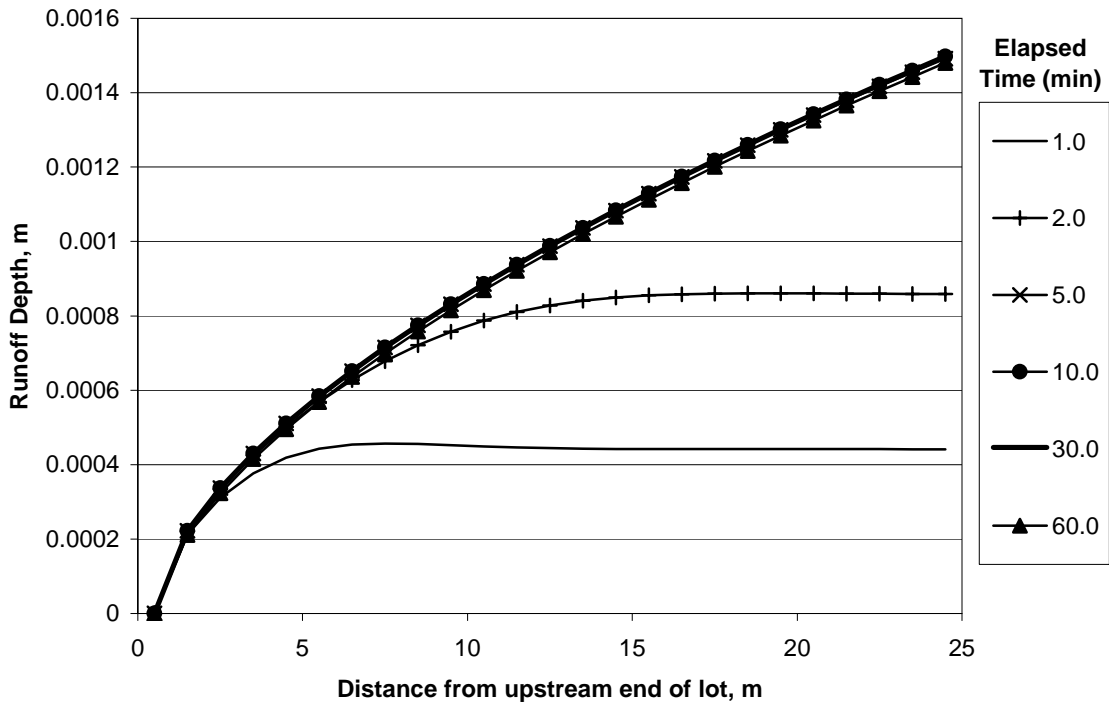


Figure 9. Horizontal distributions of runoff flow rate vs. time, for a one-hour 2.5cm/h intensity event. Lot length = 25m,  $S^{1/2}/n = 8.5$ .

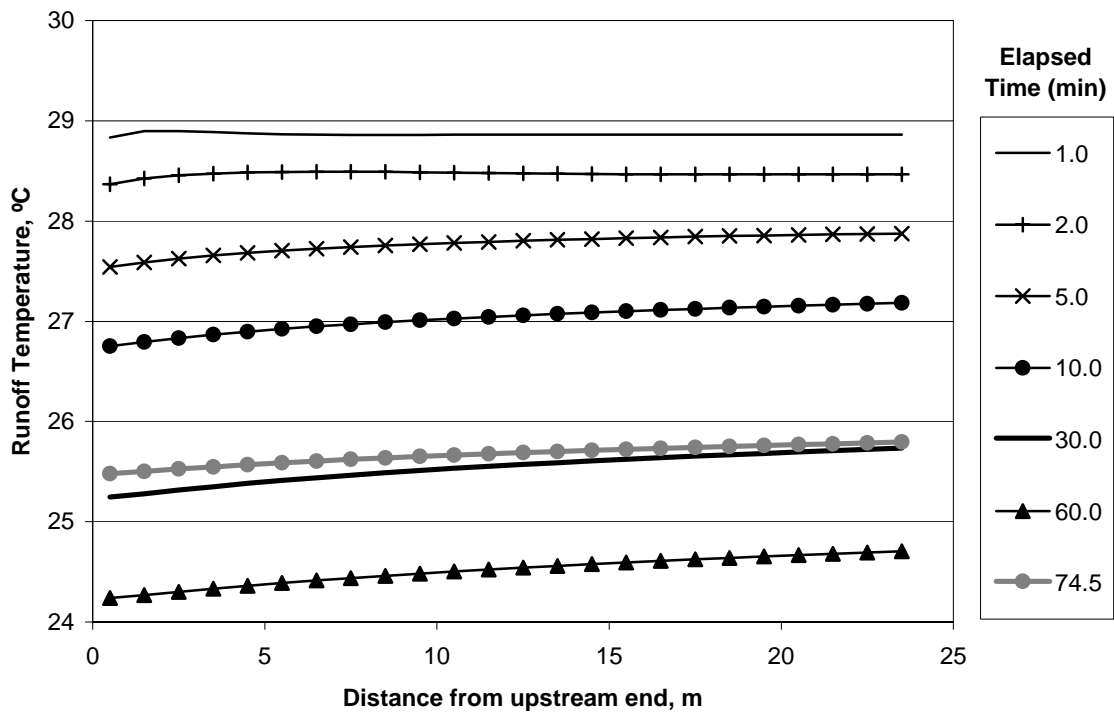


Figure 10. Horizontal distributions of runoff temperature vs. time, for a one-hour 2.5cm/h intensity event. Lot length = 25m,  $S^{1/2}/n = 8.5$ , rainfall temperature is 20.0 °C, initial pavement surface temperature is 30.0°C.

When the same set of simulations ( $S^{1/2}/n = 0.65$ ) was repeated for a lot length of 100m it was found that the temperature and depth distributions for the upstream 25m of the 100m simulations exactly matched the results of the previous 25m lot simulation (Figures 7 to 10). This is a logical result, given that there are no ‘backwater’ effects in the kinematic wave model that routes runoff water from one cell to the next. It was therefore concluded that it would not be necessary to run separate simulations for short lot lengths, because information could be extracted from the simulation of the longer lots.

A plot of the water depth distributions for a 2.5cm/hr event on a low slope-high roughness lot ( $S^{1/2}/n = 0.65$ ) of length 100m is given in Figure 11. As the plot shows, a quasi steady-state depth is reached at approximately 60 minutes (i.e., at the end of the rainfall event), compared to 30 minutes for the 25m lot for the same conditions. The maximum water depth at the end of the 100m lot was 1.65cm, while for the 25m lot it was only about 0.7cm.

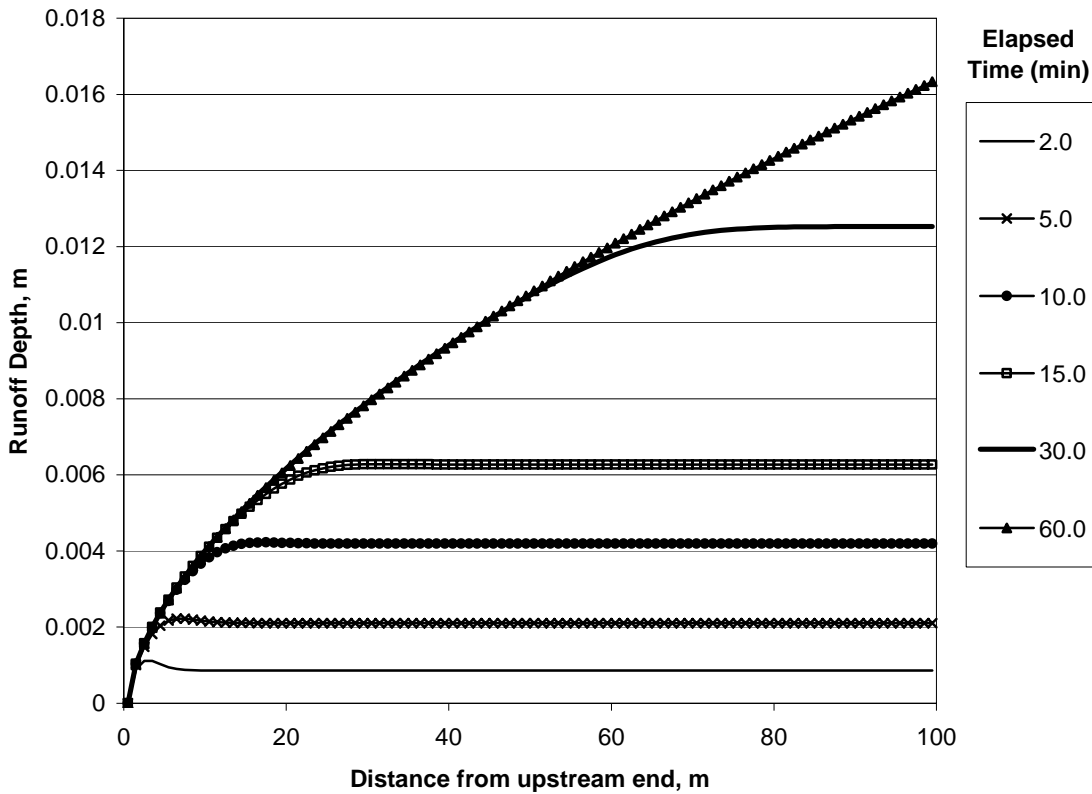


Figure 11. Horizontal distributions of runoff depth vs. time, for a one-hour 2.5cm/h intensity event. Lot length = 100m,  $S^{1/2}/n = 0.65$ .

The temperature distributions for the 100m lot showed that, as for the shorter lot, the longitudinal (horizontal) temperature difference was always small, reaching a maximum of 0.7 °C near the end of the rainfall event (Figure 12). It is concluded that the total

temperature difference along the length of the lot was almost negligible, regardless of lot length, with the lower temperatures occurring at the upstream end.

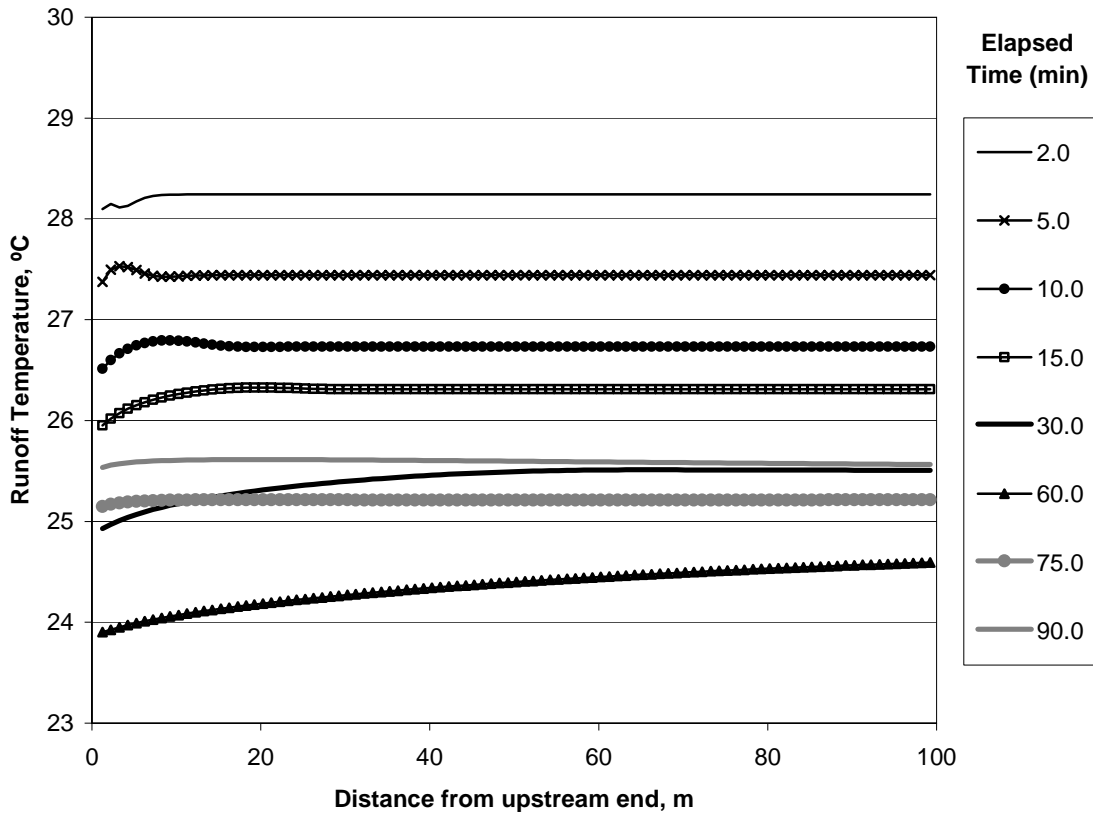


Figure 12. Horizontal distributions of runoff temperature vs. time, for a one-hour 2.5cm/h intensity event. Lot length = 100m,  $S^{1/2}/n = 0.65$ , rainfall temperature is 20.0 °C, initial pavement surface temperature is 30.0°C.

A change in slope or roughness of the lot to  $S^{1/2}/n = 8.5$  again had a significant effect on water depths, but an insignificant effect on water temperatures. The water temperatures for the  $S^{1/2}/n = 0.65$  and the  $S^{1/2}/n = 8.5$  case differed by less than 0.90 °C at all locations, with a mean difference of 0.55 °C (not shown). It is therefore expected that slope and roughness of a paved lot are not crucial input parameters for the runoff temperature and heat export simulation. Further analysis will be conducted.

### 7.3. Results of the sensitivity study: Hydrographs, thermographs and heat export rates

Perhaps of greater interest than the spatial distributions of water depth and water temperature along the along the paved surface are the hydrographs and thermographs (time series of flow rate and water temperature) at the outlet from the parking lot. With these two pieces of information the time series of heat export, as well as the total amount of heat exported from a paved lot during a rainfall event can be determined. Simulation

results of hydrographs, thermographs and heat export rates will be presented and interpreted in this section.

To illustrate the hydrologic behavior of a paved surface, the hydrographs for two lot lengths (25m and 100m) and two rainfall intensities (0.8cm/h and 7.5cm/h) are presented in Figure 13 (flow rate is in cubic meters per second per unit width, or  $m^2/s$ ). Rainfall duration is fixed at one hour, and a low slope-high roughness condition ( $S^{1/2}/n = 0.65$ ) is assumed. The results show the expected trends. For the low intensity rainfall, the peak flow and total volume of runoff were far less than those for the high intensity event. The shorter lot reached its peak or steady-state flow in a much shorter time. This time-to-steady-state flow is also known as time to equilibrium,  $t_e$ . The effect of slope-roughness, length, and rainfall intensity on  $t_e$  will be addressed later.

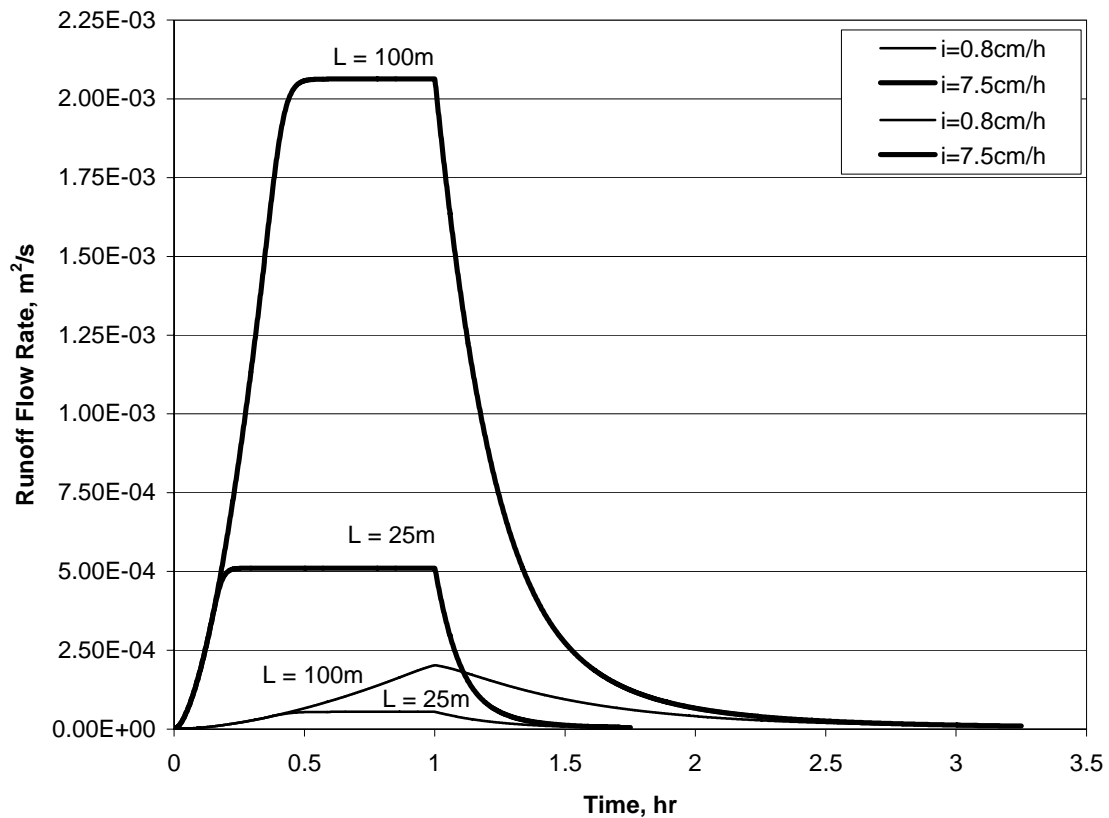


Figure 13. Runoff hydrographs for two lot lengths and two rainfall intensities. Rainfall duration = 1 hour,  $S^{1/2}/n = 0.65$ .

Slope and roughness play a role in the hydrology of a paved surface. Hydrographs for several values of  $S^{1/2}/n$  are plotted in Figure 14, for a 2.5cm/h rainfall of one hour duration on a lot of 25m length. The total volume of runoff is the same in all cases, since lot size and rainfall intensity are constant. The peak flow for all four slope-roughness cases is exactly the same, but the time to equilibrium increases as the slope-roughness parameter decreases (i.e., lower slope or higher roughness). The duration of runoff,  $t_{ro}$ , likewise increases as the slope-roughness becomes smaller. All trends in this plot are as expected.

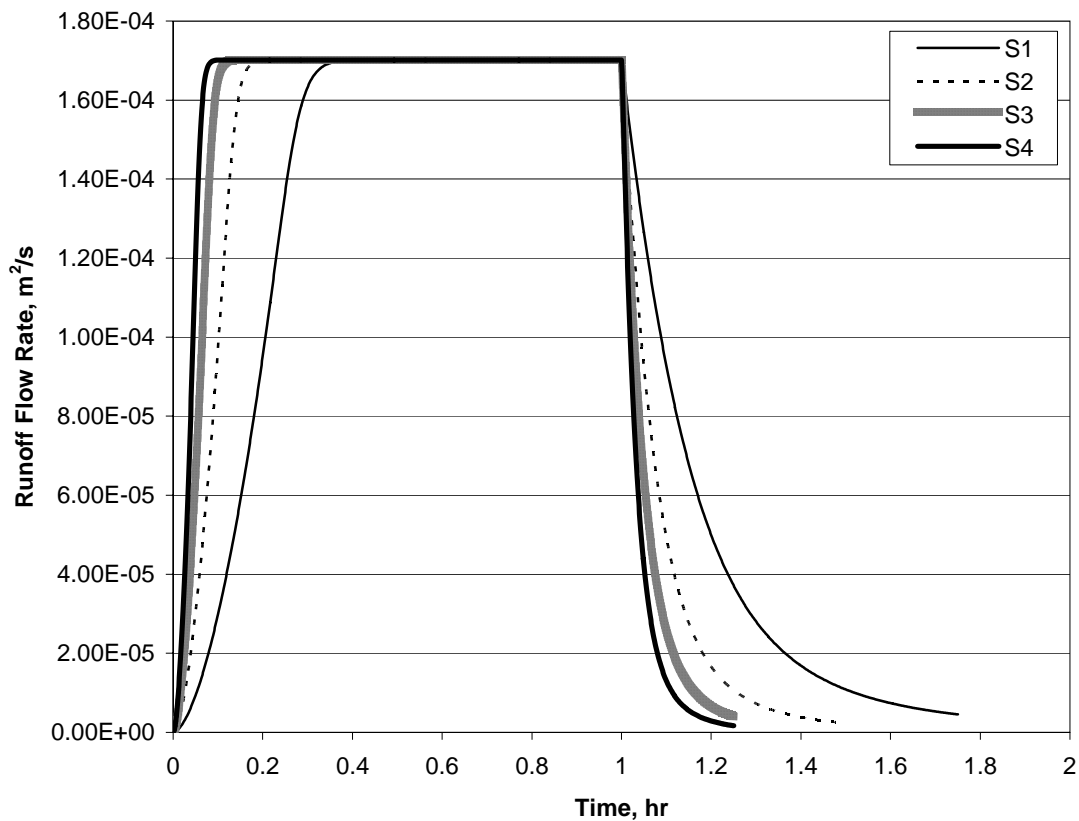


Figure 14. Outlet hydrographs for variation in the slope-roughness parameter ( $S^{1/2}/n$ ). Intensity = 2.5cm/h,  $t_d = 1$  hr,  $L = 25$ m. S1 =  $S^{1/2}/n$  of 0.65, S2 =  $S^{1/2}/n$  of 2.13, S3 =  $S^{1/2}/n$  of 4.55, S4 =  $S^{1/2}/n$  of 8.50.

Time to equilibrium is obviously affected by the three parameters investigated here. To summarize this effect the time to equilibrium for various values of rainfall intensity, lot length, and slope-roughness are listed in Table 2. The values were determined graphically from the hydrographs. In general, time to equilibrium decreased with increasing rainfall intensity or with an increase in slope-roughness, meaning that steady-state flow develops more quickly on steeper slopes with higher-intensity rainfall. Not surprisingly, time to equilibrium increases with increasing lot length.

Table 2. Approximate time to equilibrium (hours) for various values of input parameters.

i (cm/h)	L=25m		L=100m	
	S <sup>1/2</sup> /n		S <sup>1/2</sup> /n	
	0.65	8.5	0.65	8.5
0.8	0.6	0.15	--	0.3
2.5	0.4	0.12	0.8	0.2
7.5	0.25	0.05	0.5	0.15

The parking lot outflow thermographs and heat export rates show similarly logical trends. A sample thermograph is shown in Figure 15, for a one-hour 2.5cm/h rainfall on a low slope-high roughness lot of 100m length. As before, rainfall temperature is held constant at 20 °C, and there is no atmospheric heat exchange.

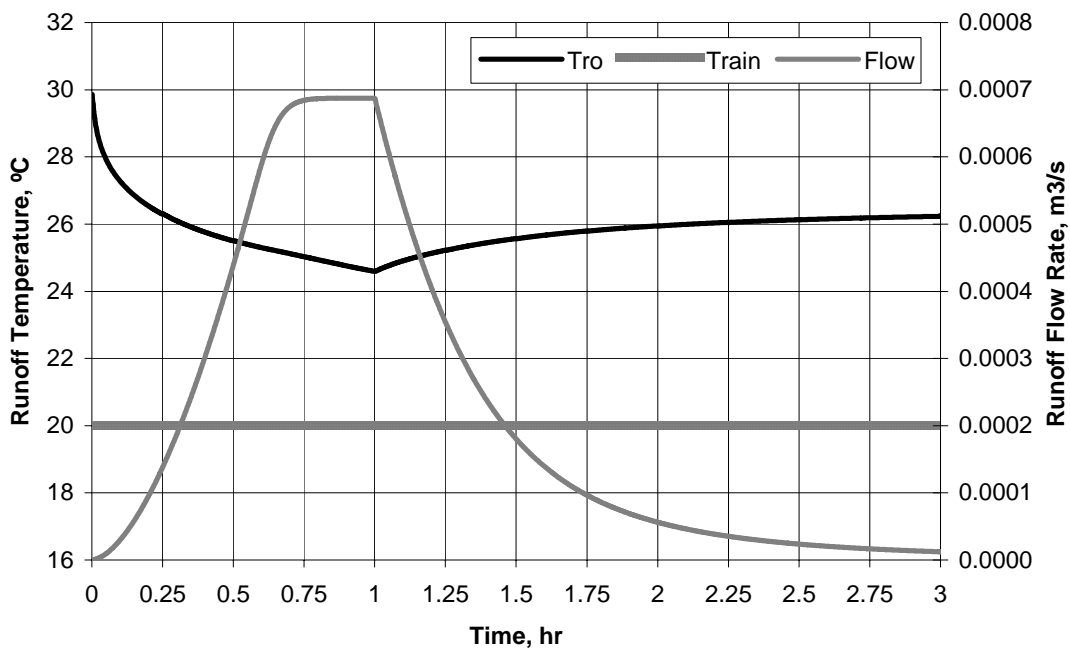


Figure 15. Runoff temperature and flow rate, for a one-hour 2.5cm/h intensity rainfall. Lot length = 100m, S<sup>1/2</sup>/n = 0.65, rainfall temperature is 20.0 °C, initial pavement surface temperature is 30.0°C.

The plot in Figure 15 shows a large decrease in runoff temperature in the first few minutes of the rainfall; later in the event the decrease in temperature is not as rapid. After the rainfall ceases, the runoff temperature rebounds due to continued heat conduction from the pavement into a water layer of diminishing depth.

For the same event and parameters, a plot of instantaneous heat export versus time (Figure 16) shows that the maximum heat export rate occurs near the beginning of the rainfall event, i.e. when the pavement cools rapidly and gives off the most heat to the runoff. The similarity between the hydrograph and the heat export time series is remarkable and suggests that export of water and heat from the parking lot can perhaps be described by similar (normalized) functions. Figure 16 gives only one example and others need to be explored before the similarity is proven.

Heat fluxes are calculated with reference to the rainfall temperature of 20°C. When integrated over the entire rainfall event, the total heat export is 514 kJ per m<sup>2</sup> of lot area. This represents the total heat load that would be supplied by the runoff to a receiving water body that has a temperature of 20 °C.

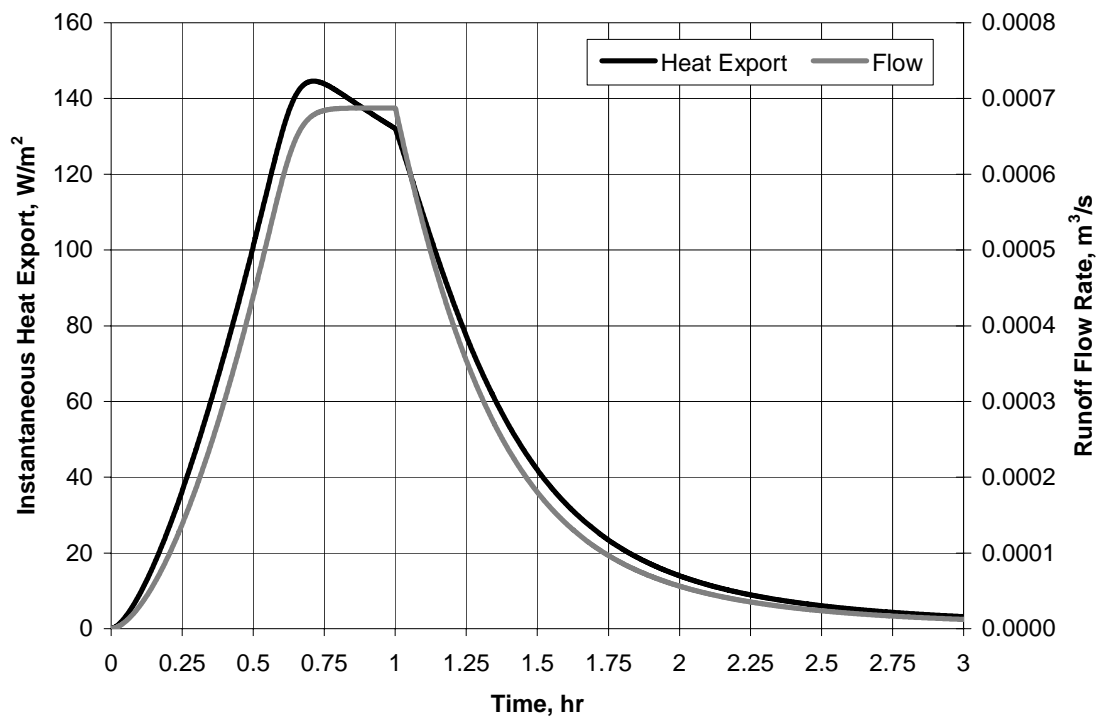


Figure 16. Heat export rate and outlet flow rate, for a one-hour 2.5cm/h intensity rainfall. Lot length = 100m,  $S^{1/2}/n = 0.65$ , rainfall temperature is 20.0 °C, initial pavement surface temperature is 30.0°C, total heat export = 464 kJ/m<sup>2</sup>.

The effects of surface slope and roughness on the runoff temperatures from a paved surface are illustrated in Figure 17 for a one-hour event of 2.5cm/h intensity. The runoff temperatures were remarkably similar for all four slope-roughness cases investigated. The mean runoff temperature difference between the two extreme slope-roughness cases was 0.11 °C, and the maximum difference was 0.31 °C. These results suggest that surface slope and roughness of the paved surfaces have negligible influence on runoff temperature.

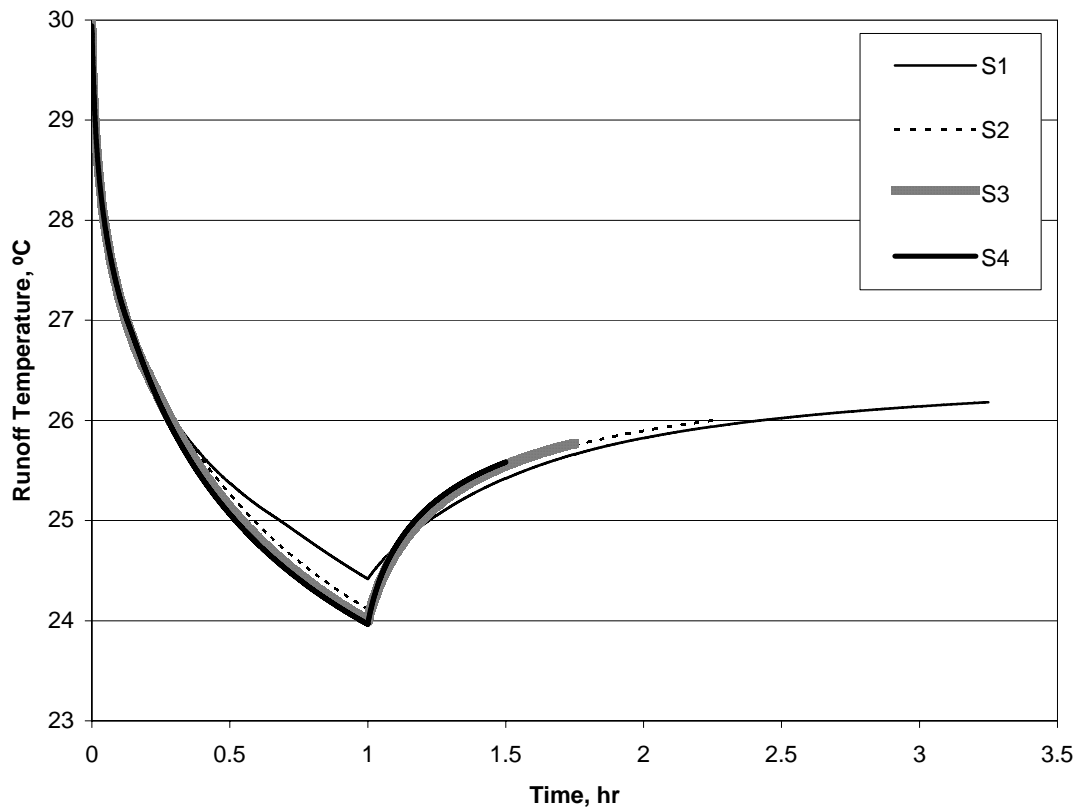


Figure 17. Runoff temperatures from four paved surfaces with different slope-roughness values, for a one-hour 2.5cm/h intensity rainfall. Lot length = 100m.  $S1 = S^{1/2}/n$  of 0.65,  $S2 = S^{1/2}/n$  of 2.13,  $S3 = S^{1/2}/n$  of 4.55,  $S4 = S^{1/2}/n$  of 8.50, rainfall temperature is 20.0°C, initial pavement surface temperature is 30.0°C.

The effect of lot length on runoff temperature is illustrated in Figure 18. This graph shows that trends in runoff temperature were again remarkably similar for all cases investigated. The extreme trends correspond to the case of a long lot (100m) with low slope-roughness (0.65), and the case of a short lot (5m) with high slope-roughness (8.5). The maximum difference in temperature between these two cases was only 0.51°C, with a mean difference of 0.17°C, suggesting that both length and slope have a small influence on runoff temperature.

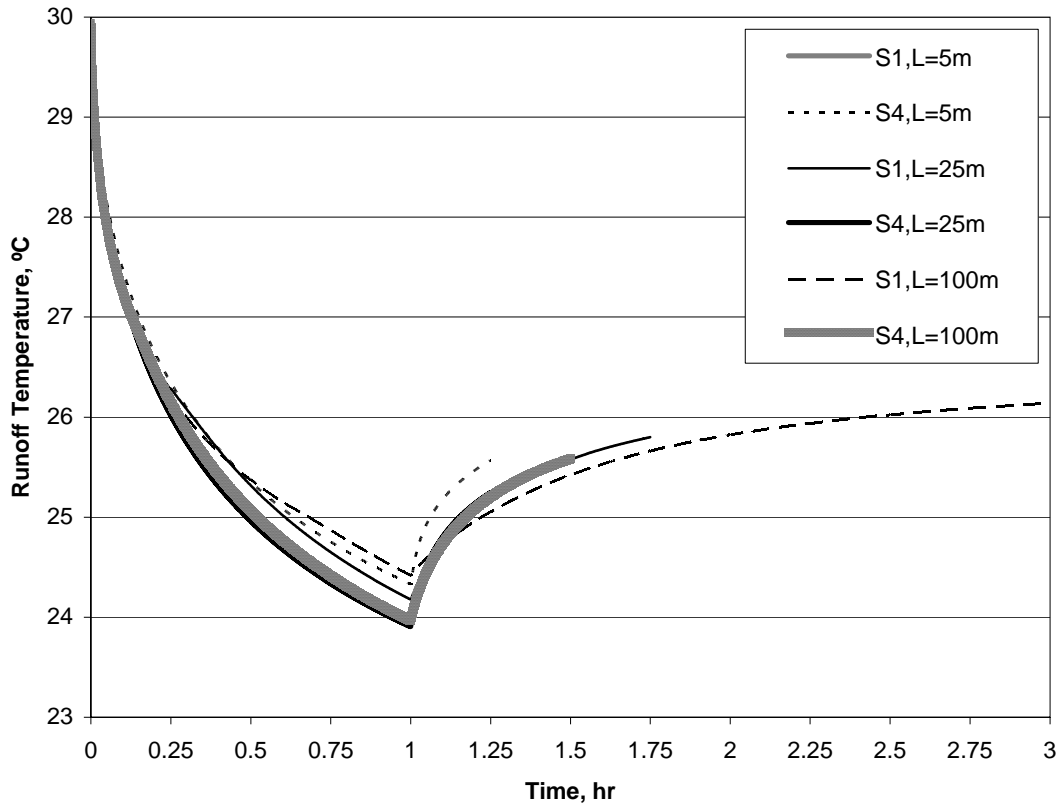


Figure 18. Runoff temperatures from six paved surfaces of three lengths (5m, 25m and 100m) and with two different slope-roughness values, for a one-hour 2.5cm/h intensity rainfall.  $S1 = S^{1/2}/n$  of 0.65,  $S4 = S^{1/2}/n$  of 8.50, rainfall temperature is 20.0 °C, initial pavement surface temperature is 30.0°C.

Since Figures 17 and 18 show that runoff temperatures are not greatly influenced by pavement/lot parameters such as lot length, slope, and roughness. It is of greater interest to explore the effect of the rainfall event parameters and antecedent conditions. Time series of runoff temperature for three values of rainfall intensity are shown in Figure 19. Significant differences in the runoff temperatures can be seen for three different rainfall intensities (with lot length and slope-roughness held constant). The highest runoff temperatures occur with the low-intensity rainfall, and the lowest temperatures for the high-intensity event. The lower runoff temperatures occur with higher rainfall intensities because a larger amount of colder rain water (recall that  $T_{rain} = 20.0^{\circ}C$ ) is available for extracting heat from the pavement. The effect of this phenomenon on the heat export rate and total event heat export is investigated next.

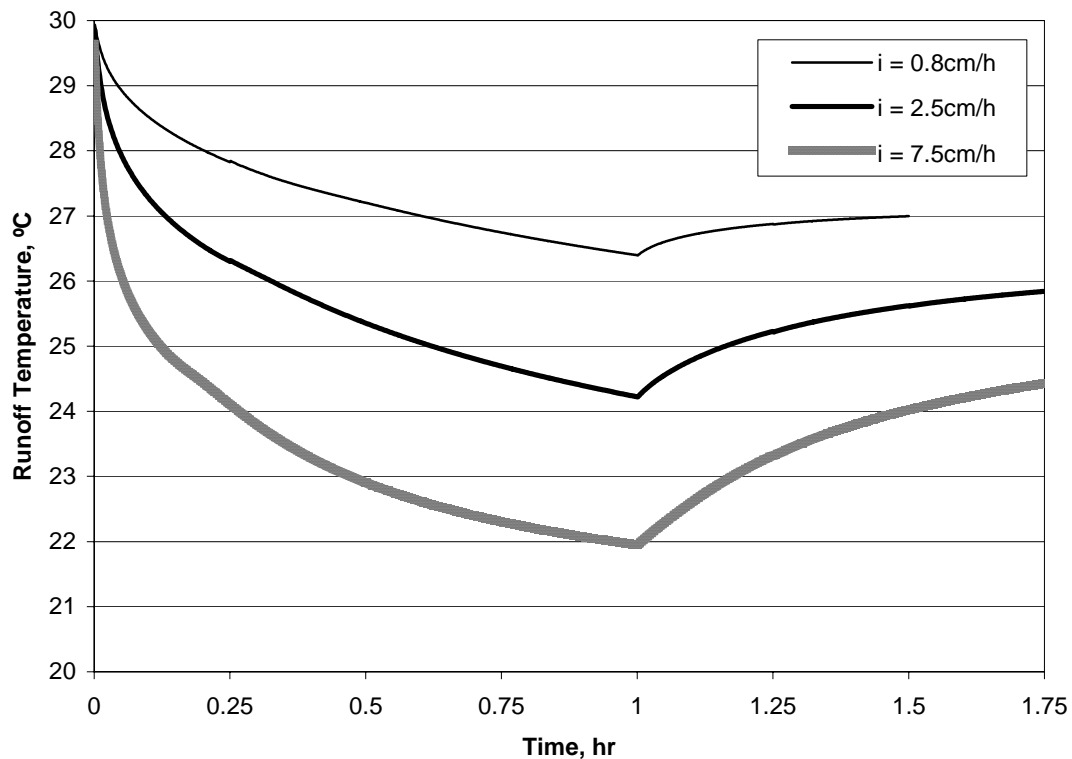


Figure 19. Runoff temperatures from a paved surface for three rainfall intensities (0.8cm/hr, 2.5cm/hr and 7.5cm/hr). Rainfall duration is one hour, lot length is 25m,  $S^{1/2}/n = 0.65$ , rainfall temperature is 20.0 °C, initial pavement surface temperature is 30.0°C.

Runoff temperatures give an incomplete and even erroneous idea of the amount of heat released from a pavement into the runoff. Instead, the heat export rate ( $\text{W}/\text{m}^2$ ), and most importantly the total event heat export amount ( $\text{J}/\text{m}^2$ ), have to be evaluated. Both are essentially the product of runoff flow rate and runoff temperature. As was mentioned previously, heat export calculations use a reference temperature of 20 °C, which is considered to be a limit of thermal stress for trout.

A plot of heat export rates vs. time for four values of the parameter  $S^{1/2}/n$  was made (Figure 20). Lot length was fixed at 25m, and a rainfall event of 2.5cm/h intensity and one hour duration was used. Figure 20 illustrates the effect of pavement slope and roughness on heat export rates. Instantaneous heat export rates are significantly affected by slope-roughness. For the highest slope-roughness case, the maximum heat export rate occurs near the beginning of the rainfall event (after around 5 minutes elapsed time), while for the low slope-roughness case the maximum occurs near an elapsed time of about 20 minutes. The peak heat export rate for the high slope-roughness case was roughly  $60 \text{ W}/\text{m}^2$  higher than for the low slope-roughness case, a difference of 38%.

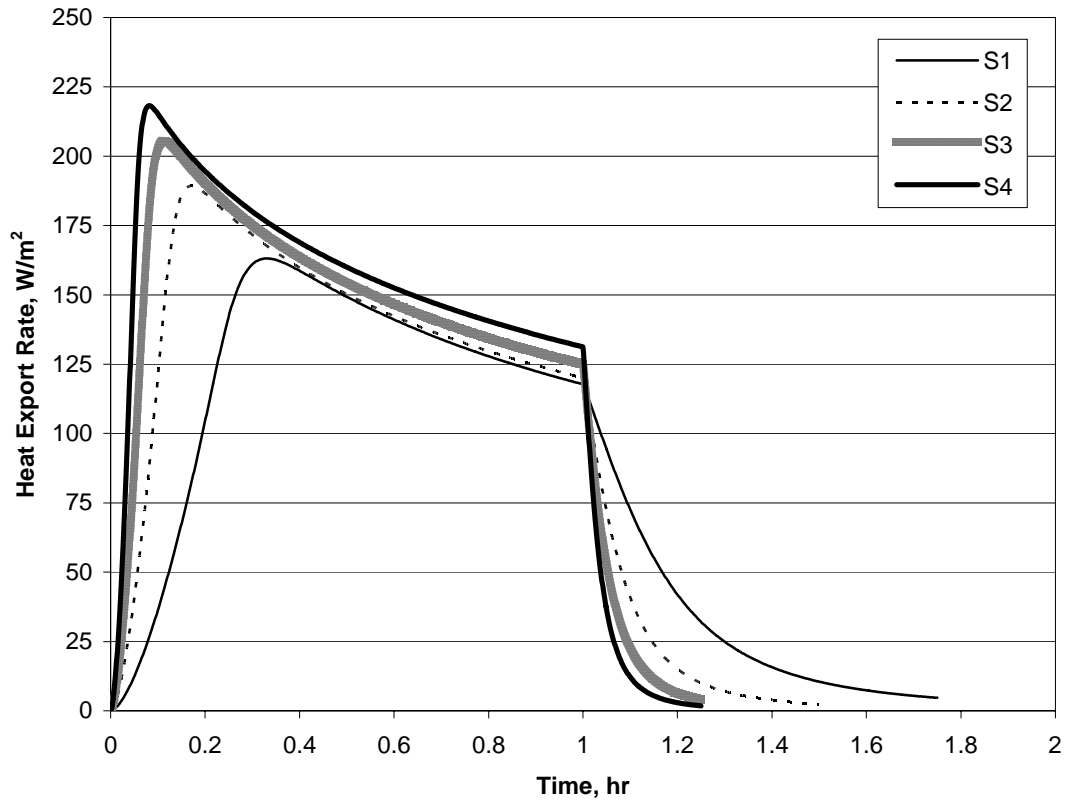


Figure 20. Heat export rates ( $W/m^2$ ) from four paved surfaces with different slope-roughness values, for a one-hour 2.5cm/h intensity rainfall. Lot length = 25m.  $S1 = S^{1/2}/n$  of 0.65,  $S2 = S^{1/2}/n$  of 2.13,  $S3 = S^{1/2}/n$  of 4.55,  $S4 = S^{1/2}/n$  of 8.50, rainfall temperature is 20.0 °C, initial pavement surface temperature is 30.0°C.

Next, the effect of lot length on heat export rate was investigated. Figure 21 shows time series of heat export rate versus time for three lot lengths, for a slope-roughness of 0.65 and a one-hour, 2.5cm/hr rainfall event. Again, significant variation in the heat export rates results from a change in lot length. The highest peak rate ( $164 W/m^2$ ) was observed for the shortest lot (5m), while the lowest peak rate ( $145 W/m^2$ ) occurred for the longest lot (100m). The difference amounted to only 13% of the lowest peak rate.

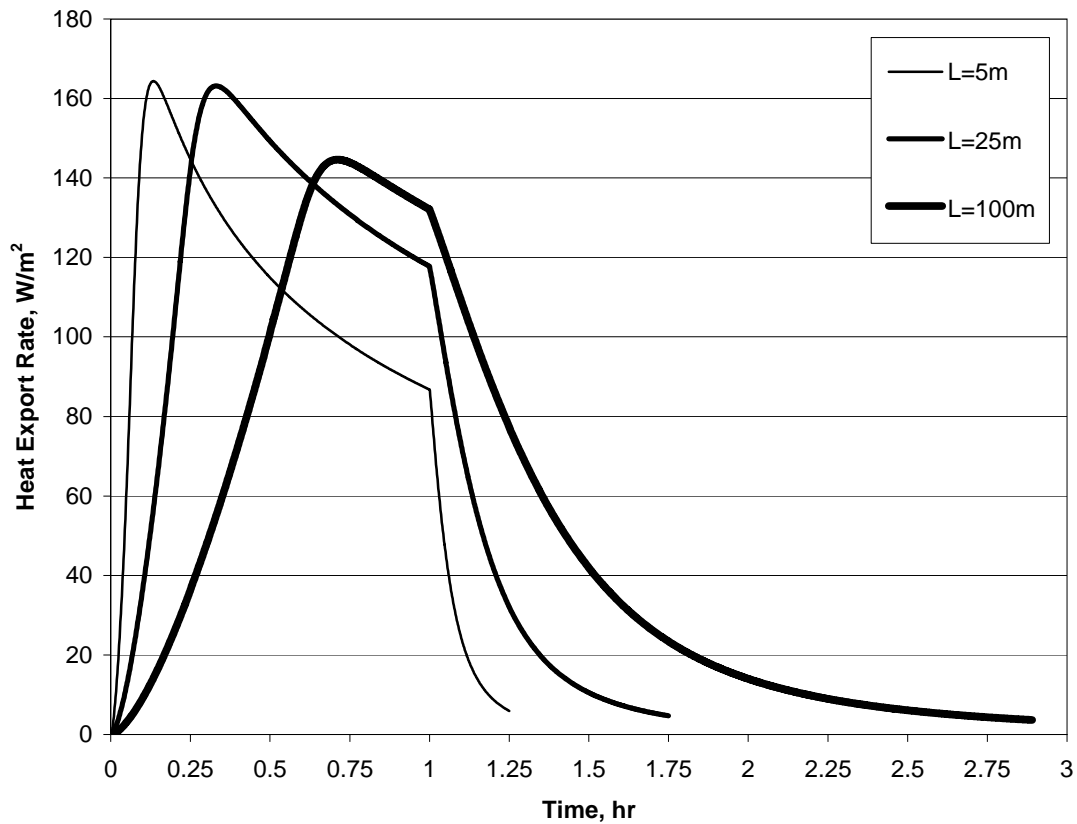


Figure 21. Instantaneous heat export rates from three paved surfaces of lengths  $L=5\text{m}$ ,  $25\text{m}$  and  $100\text{m}$  for a one-hour  $2.5\text{cm/h}$  intensity rainfall.  $S=S^{1/2}/n$  of  $0.65$ , rainfall temperature is  $20.0^\circ\text{C}$ , initial pavement surface temperature is  $30.0^\circ\text{C}$ .

The dependence of heat export rate on rainfall intensity is very pronounced (Figure 22). As in the case of Figure 19, a constant length ( $25\text{m}$ ), slope-roughness ( $0.65$ ), and rainfall duration ( $1$  hour) was used. Heat export rates were generally higher for higher rainfall intensities – an interesting result considering that runoff temperatures were lower for the higher intensity rainfall. This situation illustrates well the coupling between the runoff itself and the runoff temperature; both must be taken into account to assess the heat extracted from the pavement by the runoff.

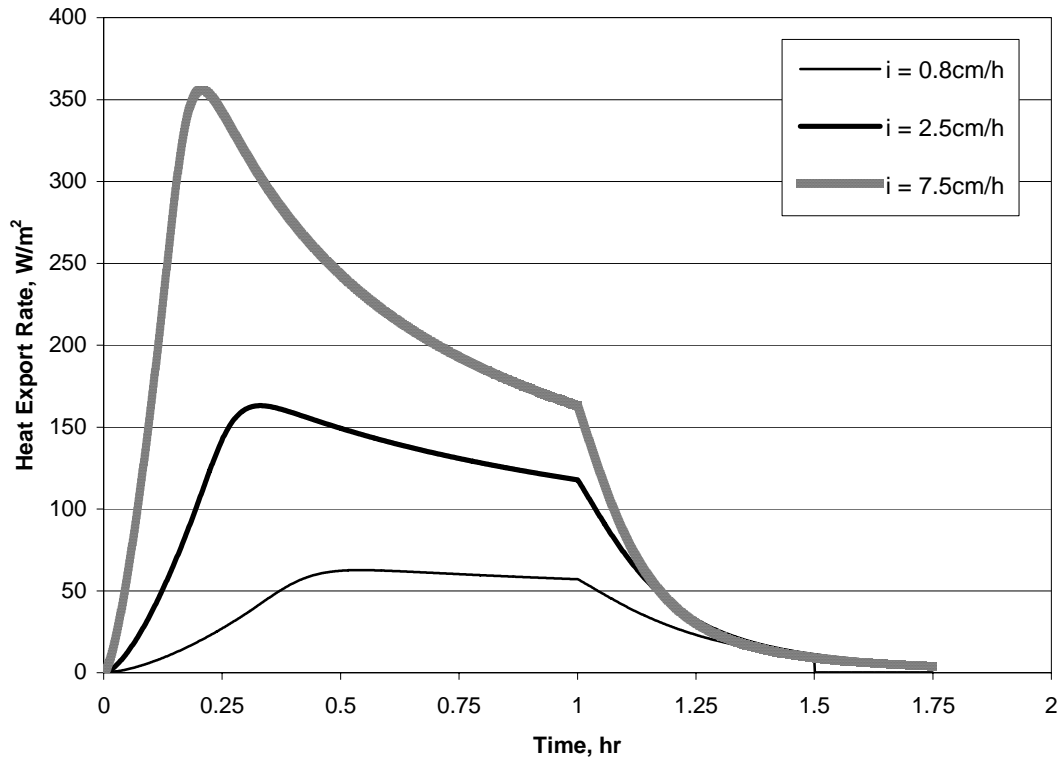


Figure 22. Heat export rate from a paved surface for three rainfall intensities (0.8cm/hr, 2.5cm/hr and 7.5cm/hr). Rainfall duration is one hour, lot length is 25m,  $S^{1/2}/n = 0.65$ , rainfall temperature is 20.0 °C, initial pavement surface temperature is 30.0°C.

While the timing of the heat export rate is of importance if no mitigation is present between a paved surface lot and a trout stream, the most significant numerical simulation result presented so far is the total event heat export (Eq. 47). The total event heat export represents the total amount of heat (with a reference temperature of 20 °C) contributed by the runoff from an entire rainfall event to a receiving water body that is at 20 °C. The effect of physical parameters (lot length, slope, and roughness) and of rainfall intensity on the event heat export is shown in Table 3. As before, a one-hour duration event was used.

Table 3. Total event heat export, in  $\text{kJ/m}^2$ , for two lot lengths  $L$ , two slope-roughness parameter values  $S^{1/2}/n$ , and three total rainfall depths  $I$ . Rainfall duration,  $t_d$  is 1 hr, hence rainfall intensity  $i(\text{cm/hr}) = \text{rainfall amount } I(\text{cm})$ .

$I$ (cm)	$L=25\text{m}$		$L=100\text{m}$	
	$S^{1/2}/n$		$S^{1/2}/n$	
	0.65	8.5	0.65	8.5
0.8	212	228	216	228
2.5	508	518	514	515
7.5	846	836	874	840

According to Table 3, the physical parameters (slope-roughness and length) of the paved surface do not significantly impact the total event heat export from the pavement (per unit surface area). In general, an increase in slope-roughness tends to exhibit small influence on total event heat export, with a slight increase for the low-intensity and medium-intensity events and a small decrease for the high-intensity event. This trend is roughly the same for both lot lengths. Therefore, at least for the initial case simulated here, lot length and slope-roughness appear to be strongly tied to lot hydrology, but do not greatly affect event heat export.

The total event heat export per unit surface area predicted for a given slope-roughness and rainfall intensity was almost the same for the two simulated lot lengths (25m and 100m), with the longer lot producing negligibly higher heat export values (1.0% on average). Again, the difference tended to become larger with increasing rainfall intensity, but the overall impact of lot length is insignificant. The implication is that the nature of the rainfall event and antecedent heating conditions of a pavement will have a greater impact on heating of runoff than the surface parameters (slope, roughness and length) of the lot. It should be clarified that the magnitude of total heat export from a paved surface will be linearly proportional to the surface area of the lot, but that the heat export per unit area is only slightly impacted by lot size.

Total event heat export increases with rainfall intensity. This result seems logical, as the higher-intensity events contain a greater mass in which to store the heat removed from the pavement. The highest intensity rainfall events produce the lowest runoff temperatures, and the large volume of water leads to the largest heat export. Likewise, the runoff temperature is higher in the case of the low-intensity events, and the small volume of water present in these cases results in a relatively small heat export. However, the lower-intensity rainfall events appear to be more ‘efficient’ at removing heat from the surface, if efficiency is defined as heat export per unit area and per unit depth of rainfall. Table 4 summarizes the event efficiencies for the 1 hour duration, constant-intensity storms with no weather input (the same case as shown in Table 3). This efficiency is highest for the low intensity events and lowest for the high-intensity events, with the low-intensity events roughly twice as efficient as the high-intensity events.

*Table 4. Event ‘efficiency’, in kJ/m<sup>2</sup> per cm of rainfall, for two lot lengths L, two slope-roughness parameter values S<sup>1/2</sup>/n, and three total rainfall depths I. Rainfall duration, t<sub>d</sub> is 1 hr, hence rainfall intensity i(cm/hr) = rainfall amount I(cm). Event efficiency is a measure of heat export per unit depth of rainfall.*

I (cm/h)	L=25m		L=100m	
	S <sup>1/2</sup> /n		S <sup>1/2</sup> /n	
	0.65	8.5	0.65	8.5
0.8	265	285	270	285
2.5	203	207	206	206
7.5	113	111	117	112

To assess the affect of rainfall duration, the set of conditions in Table 3 (base case) was simulated again for a duration of 4 hours, with the total depth of rainfall,  $I$ , remaining constant (essentially reducing the intensity by a factor of 4). The results are presented in Table 5. It should be noted that for the low-intensity rainfall event on the low slope-roughness lots, no runoff was produced (marked by an ‘x’ in Table 5), i.e., the depth of water present on the surface never exceeded the minimum threshold value of 0.1mm required for runoff.

*Table 5. Total event heat export, in  $\text{kJ/m}^2$ , for two lot lengths  $L$ , two slope-roughness parameter values  $S^{1/2}/n$ , and three total rainfall depths  $I$ . Rainfall duration,  $t_d$  is 4 hr, hence rainfall intensity  $i(\text{cm/hr}) = \text{total rainfall depth } I(\text{cm})/4\text{hr}$ .*

$I$ (cm)	$L=25\text{m}$		$L=100\text{m}$	
	$S^{1/2}/n$		$S^{1/2}/n$	
	0.65	8.5	0.65	8.5
0.8	x	234	x	234
2.5	589	604	591	606
7.5	1180	1191	1188	1197

An overall increase in total event heat export was observed relative to the one hour rainfall events. The increase was not uniform, however; a mean increase of 3%, 18%, and 43% was observed for the 0.8cm, 2.5cm, and 7.5cm events, respectively. This trend shows that higher intensity events are able to extract more heat from the pavement with a longer duration rainfall event, but that the lower intensity events are nearly extracting as much heat as possible with just a one-hour duration. The longer duration allows the high-intensity events to become more ‘efficient’ (extract more heat per depth of rainfall) than for a one hour duration. The implication here might be that longer duration events, for a constant rainfall depth, will be a bigger problem in terms of total heating load than short, intense events.

Given that the physical lot parameters do not tend to greatly affect the total event heat export, it would be expected that initial conditions would play a significant role in determining heat export. Therefore another set of simulations was run to investigate the effect of an increase in the initial temperature difference between the pavement surface and rainfall. In this case, the temperature difference was  $20^\circ\text{C}$ , with an initial pavement surface temperature of  $40^\circ\text{C}$  and rainfall temperature again at  $20^\circ\text{C}$ . This represents a doubling of the initial pavement-rainfall temperature difference relative to the original case. A 1-hour rainfall duration was used, and slope-roughness, lot length, and rainfall intensity were varied as before. Heat input from the atmosphere was neglected. The total event heat export values were again calculated with  $20^\circ\text{C}$  as a reference temperature, and the results are summarized in Table 6 below.

Table 6. Total event heat export, in  $\text{kJ/m}^2$ , for two lot lengths  $L$ , two slope-roughness parameters  $S^{1/2}/n$ , and three total rainfall depths  $I$ . Rainfall duration,  $t_d$  is 1 hr, initial pavement temperature is  $40^\circ\text{C}$ , rainfall temperature is  $20^\circ\text{C}$ .

$I$ (cm)	$L=25m$		$L=100m$	
	$S^{1/2}/n$		$S^{1/2}/n$	
	0.65	8.5	0.65	8.5
0.8	350	385	342	381
2.5	845	876	831	871
7.5	1407	1407	1430	1402

As expected, a very significant increase in total event heat export was observed relative to the case of a  $10^\circ\text{C}$  difference between initial pavement and rainfall temperatures (Table 3). The increase in total event heat export varied little with rainfall intensity: 65%, 67%, and 66% for the 0.8cm/h, 2.5cm/h, and 7.5cm/h intensities, respectively. Slope-roughness and lot length also had very little impact on the increase in heat export associated with the increase in initial pavement temperature; increases in heat export were slightly larger (by a few percent) for the high slope-roughness cases than for the low slope-roughness cases, with almost no difference seen for a change in lot length. These results are an indication that heat export is significantly more dependent upon initial pavement temperature and rainfall temperature than on physical lot parameters or rainfall intensity. That a hotter pavement results in a greater total event heat export is an intuitive result, but further sensitivity analysis will be needed in the future.

#### 7.4. Results of the sensitivity study: Heat export including the effect of atmospheric heat transfer

Neglect of the atmospheric forcings present during a real rainfall event was for the purpose of assessing the relative importance of physical and event parameters. It is expected that the atmospheric heat fluxes will exhibit significant influence over runoff temperature, therefore a future sensitivity analysis will need to be conducted with the inclusion of atmospheric effects. An analysis investigating the sensitivity of the model to the atmospheric parameters themselves (e.g., air temperature, wind speed, solar radiation) will need to be conducted in the future as well. As a preliminary exercise, a set of simulations were run for the same event and physical parameters used previously (Table 1), this time including atmospheric heat fluxes. This was done in an effort to show that the atmospheric contribution is significant.

In order to calculate realistic values of the atmospheric heat fluxes, reasonable climate input parameters had to be determined. It is important to note that the parameters chosen do not represent a worst-case scenario or a so-called design storm; this issue will be addressed by future work due to the complicated aspects of design storm selection. The climate data collected over a period of six years (1999-2004) at the Minnesota Department of Transportation's MNRoad research site was used to determine the storm parameters for the sensitivity study. Values of solar radiation, air temperature, dew point temperature, and wind speed were determined by averaging hourly observations during

wet weather periods only, i.e. during times when observed precipitation depth was greater than zero. Mean values during the month of July were used, using six years of data, with the exception of the air and dew point temperatures. In the no-weather simulations completed previously, the rainfall temperature was held constant at 20 °C; for sake of continuity, the air temperature used in the constant-weather simulations was increased to 21 °C and dew point was fixed at 20 °C, which is the rainfall temperature. For solar radiation, the value was determined from storms that occurred only during daylight hours. The chosen parameters are shown in Table 7.

*Table 7. Climate parameters used in calculating atmospheric heat fluxes. Determined from rainfall events observed during July at MNRoad Project site, 1999-2005. Temperatures in parentheses are calculated from July rainfall events; temperatures in table are values used in the simulations, chosen for sake of continuity with the no-weather simulations.*

Parameter	Value	Units
Solar Radiation	113	W/m <sup>2</sup>
Air Temperature	21 (19.3)	°C
Rainfall Temperature	20 (18.5)	°C
Wind Speed	1.96	m/s
Starting Time	15:00	

Total event heat export values for the simulations including atmospheric heat fluxes are summarized in Table 8. Overall, climate forcing tends to decrease event heat export, but does not have a uniform effect; it is highly dependent on rainfall intensity. The heat export versus the ‘no weather’ cases decreased by roughly 34%, 21%, and 6% for the low, medium, and high-intensity events, respectively. This behavior would logically suggest that due to the relatively high heat capacity of water, a smaller amount of runoff is more likely to be influenced by atmospheric forcing than a large volume. As was observed before, the physical parameters appeared to have a less significant role.

*Table 8. Total event heat export, in kJ/m<sup>2</sup>, for simulations including atmospheric heat fluxes, for two lot lengths L, two slope-roughness parameters S<sup>1/2</sup>/n, and three total rainfall depths I. Rainfall duration, t<sub>d</sub> is 1 hr, initial pavement temperature is 30°C, rainfall temperature is 20°C.*

I (cm)	L=25m		L=100m	
	S <sup>1/2</sup> /n		S <sup>1/2</sup> /n	
	0.65	8.5	0.65	8.5
0.8	145	164	140	138
2.5	402	420	396	411
7.5	787	795	805	800

A time series plot of runoff temperature for both cases (i.e., with and without atmospheric forcing) for a given set of physical parameters is used to illustrate the effect of atmospheric heat exchange on runoff temperature. Figure 23 shows a plot for a low-

intensity event (0.8cm/h), slope-roughness of 0.65, and length of 25m. In this case, the atmospheric heat fluxes tended to mitigate the impact of runoff temperature, especially near the end of the event. This suggests that in this case the net atmospheric heat flux is negative, and has a significant impact on runoff temperature given the small amount of water present on the surface.

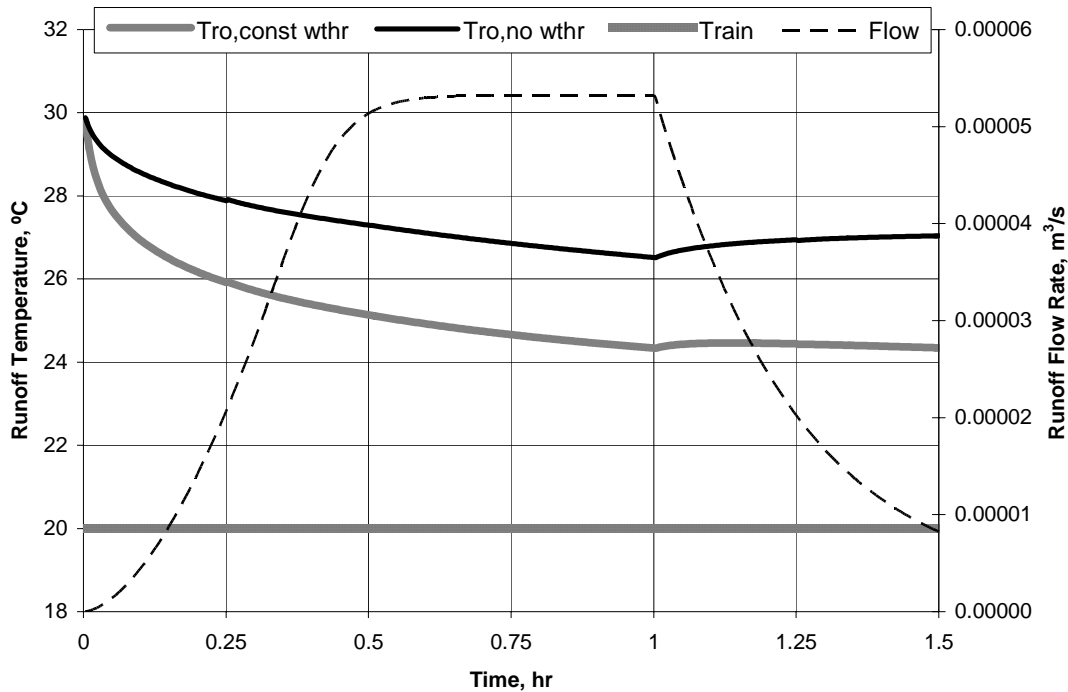


Figure 23. Runoff temperature and flow rate, for a one-hour 0.8cm/h intensity rainfall. Lot length = 25m,  $S^{1/2}/n = 0.65$ , rainfall temperature is 20.0 °C, initial pavement surface temperature is 30.0°C. Runoff temperature is calculated both with and without the effect of atmospheric heat fluxes.

In Figure 24, the same plot is shown for the high rainfall intensity; physical parameters remain the same as in Figure 23. In this case, the net atmospheric heat exchange is again negative, as the runoff temperature is generally lower than in the no-weather case. The cooling effect of the atmospheric forcing is diminished relative to the low-intensity event, however, due to the presence of a greater amount of water. This is especially true near the end of the event, when most available heat has been extracted from the pavement.

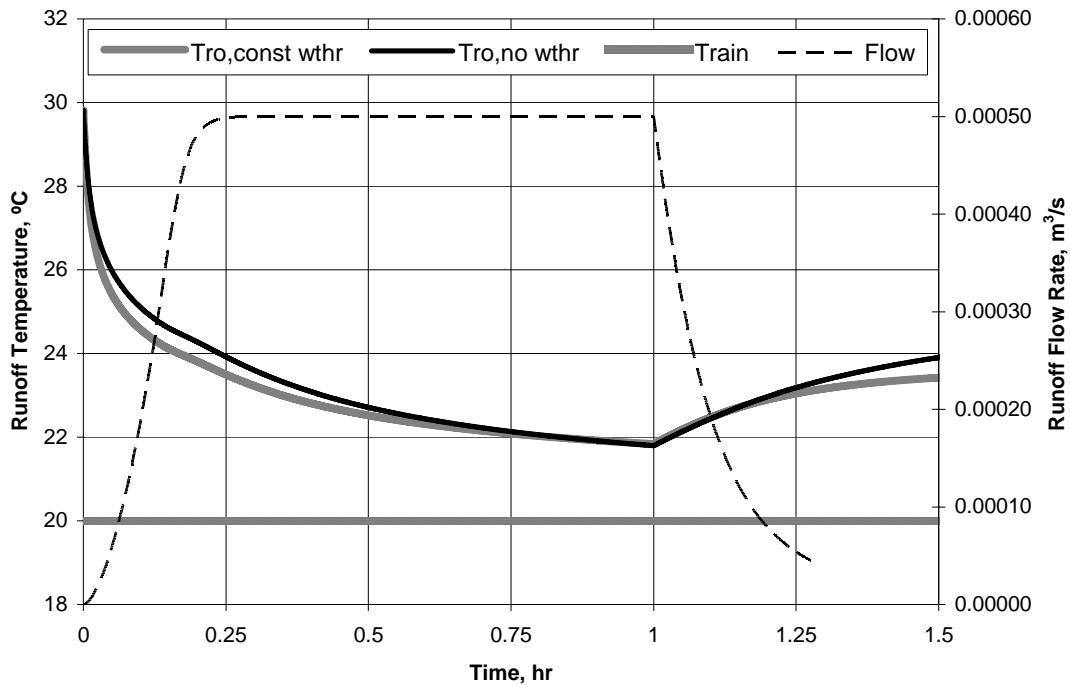


Figure 24. Runoff temperature and flow rate, for a one-hour 7.5cm/h intensity rainfall. Lot length = 25m,  $S^{1/2}/n = 0.65$ , rainfall temperature is 20.0 °C, initial pavement surface temperature is 30.0°C. Runoff temperature is calculated both with and without the effect of atmospheric heat fluxes.

### 7.5. Summary of sensitivity study

A sensitivity analysis was performed with Model 3. The only heat input to the runoff was from the rainfall and conduction from the pavement surface; atmospheric heat exchange was neglected. The purpose of running simulations with no weather input was to isolate the effect of the pavement on the heating of the runoff. For investigation of the effect of atmospheric heat exchange, another set of simulations were run for constant weather input. Three main issues were addressed in the study: 1) the effect of physical parameters of the paved surface on heating of runoff, 2) the effect of rainfall event parameters on heating of runoff, and 3) the significance of lengthwise effects (i.e., horizontal gradients of runoff depth and temperature) on heating of runoff. Simulation output included runoff flow rate and temperature (versus both time and position), instantaneous heat export rate, and total event heat export. Heat export was calculated with a reference temperature of 20 °C; thus total event heat export represented the amount of heat contributed by the runoff from an entire rainfall event to a receiving water body that is at 20 °C.

To reduce the simulation load, simplifications were introduced: rainfall duration, rainfall temperature, and initial pavement surface temperature were set at one hour, 20 °C, and 30 °C, respectively, with the exception of the third simulation set, which used an initial pavement temperature of 40 °C and a rainfall temperature of 20 °C. Also, only one lower

boundary condition (soil temperature of 26.6°C at 60cm depth) was tested so far. In spite of these simplifications, a few significant conclusions can be reached:

- Physical parameters of the paved surface, such as length, slope, and roughness, appear to have very little influence on runoff temperature. In general, runoff temperatures may be slightly higher for longer lots and for higher slope and/or roughness.
- The total heat export (energy per unit paved surface area) also appears to be negligibly influenced by length, slope, and roughness of the paved surface. The sensitivity to the thermal properties (thermal diffusivity) of the pavement has not been tested yet.
- Runoff flow rate and runoff temperature are both necessary pieces of information to accurately estimate heat export from a paved surface.
- Rainfall intensity has a significant influence on runoff temperature, heat export rates, and total event heat export. Interestingly, high-intensity rainfall events produce the lowest runoff temperatures but also the greatest total event heat exports because the large volume of water extracts the most heat from the pavement. Likewise, low-intensity events produce the highest runoff temperatures, but the total event heat export is smaller due to the smaller amount of water that runs off.
- Lower-intensity rainfall events appear to be more ‘efficient’ at removing heat from the surface, as heat export per unit depth of rainfall for the low-intensity event is roughly twice that of the high-intensity event.
- The effect of an increase in rainfall duration, for constant rainfall depth, is an increase in total event heat export. The greater the total depth of rainfall, the greater the increase in event heat export. The implication is that increased rainfall duration allows higher-intensity events to extract more heat from the pavement, meaning these types of events might be more troublesome than short, intense events.
- Hotter pavement or cooler rainfall temperature logically results in greater extraction of heat from the pavement by the runoff. A doubling of the difference between pre-rainfall pavement temperature and rainfall temperature, from 10°C to 20°C (a worst-case scenario), resulted in a roughly 66% increase in total event heat export.
- Slope and roughness of the paved surface obviously influence the lengthwise water depth distribution, but appear to have little effect on the water temperature distribution on the lot. Runoff temperature between the upstream and downstream ends of the lot varied by less than 1 °C most of the time. It is likely that horizontal temperature gradients can be neglected in a runoff temperature model without

sacrificing much accuracy. Should a simpler, 1-D model (i.e., Model 2) be developed, it is anticipated that it would perform similarly to the quasi-2-D model (Model 3). A simplification of the model described in this report will be the focus of future work.

- Atmospheric heat exchange appears to play a significant role in determining runoff temperature and heat export from a paved surface. In the limited set of simulations run in this study, the total event heat export was strongly tied to rainfall intensity, with a reduction in event heat export versus the ‘no-weather’ case observed for low-intensity events, and an increase in heat export observed for the high-intensity events.

Findings of lesser consequence are as follows:

- The timing and magnitude of heat export rates is significantly affected by physical lot parameters. For longer lots or milder slopes/higher roughness, the peak heat export rate for the event is observed to be diminished and to occur later in the event.
- The highest instantaneous heat export rates occurred for the highest intensity rainfall events, and the lowest peak rates occurred for the lowest intensity rainfall events.
- In most cases, the strongest horizontal runoff temperature gradients occur in the upstream portion of the lot, while the downstream portion is usually at a relatively constant temperature.

## **8. VALIDATION OF SURFACE RUNOFF MODEL**

A significant component in the development of any model is the collection of data for validation of the model. The data must include components for both model input and output. The input data are necessary to run the model as a predictive tool, and the output data are needed to ensure accuracy of computed values. For the paved surface model outlined in this paper, the required inputs include weather data, soil and pavement properties, and a description of the size and topography of the parking lot or paved surfaces being modeled. The surface heat budget requires weather data consisting of precipitation intensity, total solar radiation, wind speed, air temperature, and relative humidity or dew point temperature. This type of data is readily available from modern weather stations. Data time series have already been obtained for the years 2004 and 2005 from a weather station on the St. Paul campus of the University of Minnesota.

To validate the model it will be necessary to collect runoff flow and runoff temperature data from various points within a parking lot for which the necessary input parameters are also available. Runoff flow rates or temperatures can be measured at the outlet of a

parking lot to evaluate predictions made by the paved surface model. Surface and subsurface temperatures will be needed to validate the surface energy budget.

For the time being the overland runoff component of the model was validated with data from an experimental setup in which a sprinkler system was used to create a uniform-intensity rainfall event over a small test plot. In this experiment (Wilson, 2004), a 7.24 cm/h (2.85 in/h) event of 1.75-hour duration was generated over a bare soil plot of 9.14m (30ft) length, 1.22m (4ft) width, and slope of 34.8%. Volumetric flow rate in L/s was recorded for the event. Using the above information as input, the model was used to predict the observed runoff from the plot. Figure 23 shows the observed and simulated hydrographs.

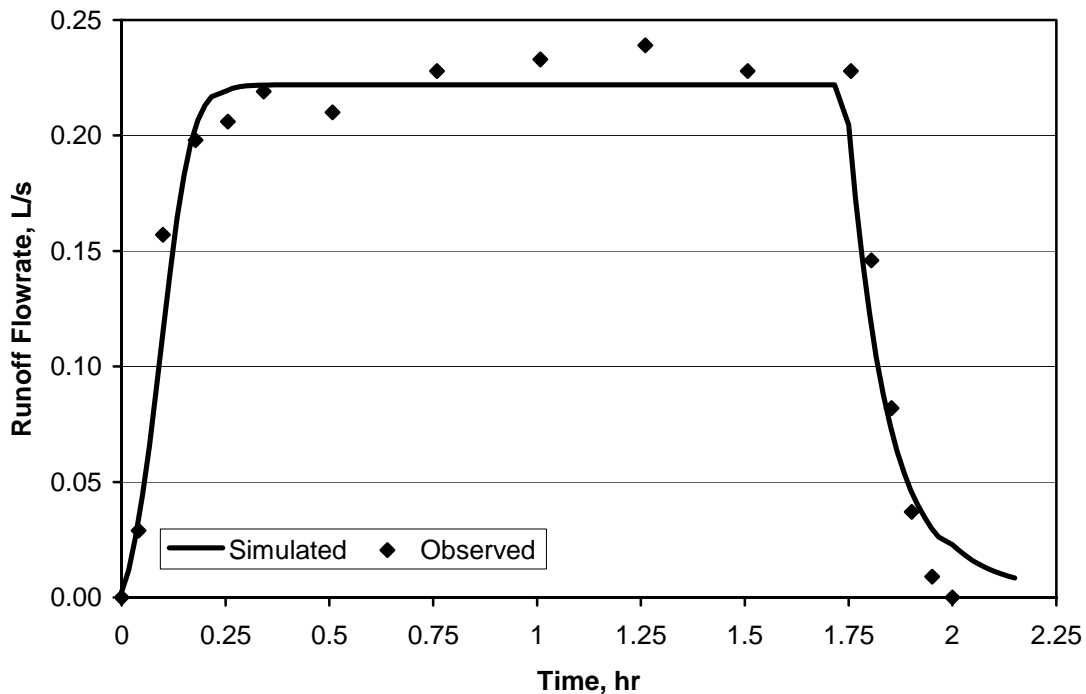


Figure 25. Observed and simulated hydrographs for an experimental rainfall event with duration of 1.75 h and intensity of 7.24 cm/h (2.85 in/h) (data from Wilson, 2004).

Visual inspection of Figure 25 shows that good agreement exists between the observed and the simulated flow rates. The RMSE was 0.0184 L/s, which is about 8% of the peak observed flow rate. The end behavior of the event is not predicted as well as the rest of the event, as the model uses the kinematic wave approximation for prediction of runoff. A consequence of using this method is that it will never predict a zero flow rate. Thus a minimum depth or flow threshold has to be introduced, i.e., flow will be set equal to zero below that value.

## 9. CONCLUSIONS

A computational model (Model 3) to predict the water temperature and flow rate of runoff from a paved surface has been introduced. The model uses a hydrologic (water) balance for the runoff water, and a heat balance for the runoff water as well as the pavement and sub-grade. To reduce the coupling of the heat and mass balances, a spatially-averaged water depth and water temperature model was also formulated (Model 2). The conceptual framework of the models and the results of a sensitivity study using Model 3 were presented herein. The results of this sensitivity study have been summarized in section 8.4. That summary leads to the following conclusions:

- (1) Physical parameters of the paved surface (slope, roughness and length) have little influence on simulated runoff temperature and total event heat export (per unit area).
- (2) Simulated water temperatures on the pavement surface, as predicted using the quasi-2-D model (Model 3), did not vary significantly in horizontal direction.
- (3) The lowest runoff temperatures are produced by rainfall events with high rainfall intensities and the highest runoff temperatures by low rainfall intensities.
- (4) Knowledge of both runoff flow and temperature is necessary to estimate heat export from a paved surface for a rainfall event.
- (5) The magnitude of heat export by runoff is strongly linked to rainfall event parameters (rainfall intensity, rainfall duration, and rainfall temperature).
- (6) The highest total heat export ( $\text{kJ}/\text{m}^2$ ) from a rainfall event is produced by the highest rainfall intensity, even though these events produce the lowest runoff temperatures.
- (7) The general effect of increasing rainfall duration was to increase the total event heat export, with a greater effect occurring for an increase in rainfall intensity.
- (8) Low-intensity rainfall events are more 'efficient' than high-intensity events in extracting heat from a pavement, where efficiency is measured by the total event heat export per depth of total rainfall ( $\text{kJ m}^{-2} \text{cm}^{-1}$ ).
- (9) The magnitude of total heat export from a rainfall/runoff event is also strongly linked to antecedent weather conditions.
- (10) Increasing the difference between initial pavement and rainfall temperature increases the total event heat export, a logical result given that warmer pavement or cooler rainfall would allow runoff to extract more heat from the pavement.

- (11) Atmospheric heat fluxes (i.e., solar radiation, longwave radiation, sensible heat flux, evaporation) appear to play a significant role in determining runoff temperature and total event heat export. With the parameters used in this study, the effect of atmospheric forcing was to reduce heat export relative to a ‘no weather’ case, with a greater reduction occurring for low-intensity rainfall events than for high-intensity rainfall events.

## 10. IMPLICATIONS

Implications of the above conclusions are as follows:

- (1) Conclusions (1) and (2) suggest that a simpler 1-D model such as Model 2 should be an appropriate tool to model runoff temperatures and total heat export from a rainfall event on a paved surface.
- (2) Conclusions (6) and (7) suggest that the rainfall event with the highest heat export per unit pavement surface area ( $\text{kJ}/\text{m}^2$ ) is an event with the largest rainfall intensity over the longest possible time.
- (3) Conclusions (3) and (7) suggest that the highest runoff temperature is produced by a rainfall event with the lowest intensity over the shortest time, i.e. the smallest rainfall volume that still produces runoff.
- (4) Conclusion (8) suggests that the rainfall event with the highest ‘efficiency’, i.e. heat export per volume of runoff water ( $\text{kJ}/\text{m}^3$ ), is a rainfall event of low intensity and short duration.
- (5) Conclusions (9) and (10) logically suggest the worst pre-rainfall pavement conditions with the largest impact on runoff temperature and heat export are those in which the warmest pavement temperatures exist down to the largest possible sub-surface depth.
- (6) Conclusions (7), (10), and (11) logically suggest that a realistic worst-case scenario would be a rainfall event of high intensity and long duration that occurs in late afternoon, when the initial pavement-rainfall temperature difference is at its maximum and a large amount of heat is stored in the sub-surface.

A design rainfall event should be selected based on implications (2), (3), and (4), even though the conclusions may contradict each other. An analysis therefore has to be made to determine the compounded effect of runoff temperatures and heat export rates on a receiving water body, and whether or not this is more important than the total event heat export. It is expected that such an analysis can assist in the selection of design rainfall events.

It is acknowledged that the sensitivity analysis performed here was not exhaustive. Among the primary goals were to assess the influence of physical lot parameters on heat export, and to determine if horizontal gradients in runoff depth and temperature are significant enough to warrant the use of a quasi-2-D model vs. a simpler 1-D model. The effect of rainfall duration or the effect of the difference in rainfall temperature and initial pavement surface temperature were not thoroughly investigated. Simulations including atmospheric forcing were included for sake of comparison, but more detailed analysis will be conducted in future work.

Furthermore, the model was run without first being validated by observations, which was not possible given the lack of available data. The hydrologic portion of the model was validated with observed flow rates for a generated rainfall event on a non-pavement test plot. Data of runoff water temperatures on parking lots will be collected in the near future for the validation of runoff temperatures.

Although emphasis in this paper has been on a paved catchment, the model(s) can also be applied to pervious surfaces with the modifications described. In site-specific applications the model simulation results can provide input to models of storm water detention ponds, wetlands, and streams in urban watersheds.

## **ACKNOWLEDGMENTS**

The authors thank the Project Officer, Bruce Wilson, of the Minnesota Pollution Control Agency (MPCA) for the opportunity to conduct this study. Data cited in this study were acquired from the MNROAD Project of the Minnesota Department of Transportation, from Prof. Bruce Wilson, Dept. of Biosystems and Agricultural Engineering at the University of Minnesota, and from David Ruschy, Dept. of Soil, Water and Climate at the University of Minnesota.

## REFERENCES

- Abu-Hamdeh, N.H., Reeder, R.C., Khdair, A.I., and Al-Jalil, H.F. (2000). "Thermal Conductivity of Disturbed Soils Under Laboratory Conditions." *Transactions of the Am. Society of Ag. Engineers*, **43(4)**: 855-860.
- Brutsaert, W. (1984). *Evaporation into the Atmosphere*, First Ed., Kluwer, Boston.
- Burman, R.D. (2003). "Evapotranspiration Formulas." In *Encyclopedia of Water Science*, 253-257.
- Chow, V.T. (1964). *Handbook of Applied Hydrology*. McGraw-Hill Inc., New York, NY.
- Deardorff, J.W. 1978. "Efficient Prediction of Ground Surface Temperature and Moisture with Inclusion of a Layer of Vegetation." *Journal of Geophysical Research*, **83**: 1889-903.
- Duffie, J.A. and Beckman, W.A. (1991). *Solar Engineering of Thermal Processes*. Second Ed., John Wiley and Sons, New York.
- Eaton, J.G., McCormick, J.H., Goodno, B.E., O'Brien, D.G., Stefan, H.G., Hondzo, M., and Scheller, R.M. (1995). "A Field Information-based System for Estimating Fish Temperature Tolerances." *Fisheries*, **20(4)**: 10-18.
- Eckert, E.R.G. and Drake, R.M., Jr. (1972). *Analysis of Heat and Mass Transfer*. McGraw-Hill, New York.
- Edinger, J., Brady, D.K. and Geyer, J.C. (1974). "Heat Exchange in the Environment". Report No. 14, Cooling Water Discharge Research Project RP-49, Electric Power Research Institute, Palo Alto, CA, 125 pp.
- Hermansson, A. (2001). "Mathematical Model for Calculation of Pavement Temperatures: Comparison of Calculated and Measured Temperatures." In *Transportation Research Record 1764*, National Research Council, Washington, D.C., 180-188.
- Incropera, F. P. and DeWitt, D. P. (2002). *Fundamentals of Heat and Mass Transfer*, Fifth Ed., John Wiley and Sons, New York.
- Jia, Y., Ni, G., Kawahara, Y. and Suetsugi, T. (2001). "Development of WEP Model and its Application to an Urban Watershed." *Hydrological Processes*, **15**: 2175-2194.
- Jia, Y., Ni, G., Yoshitani, J., Kawahara, Y., and Kinouchi, T. (2002). "Coupling Simulation of Water and Energy Budgets and Analysis of Urban Development Impact." *Journal of Hydrologic Engineering*, **7(4)**: 302-11.

- Jia, Y., and Tamai, N. (1998). "Integrated Analysis of Water and Heat Balances in Tokyo Metropolis with a Distributed Model." *Journal of the Japanese Society of Hydrology and Water Resources*, **11(2)**: 150-163.
- Kersten, M.S. (1948). "The Thermal Conductivity of Soils." *Proceedings of the Highway Research Board*, **28**: 210-218.
- Kustas, W.P. and Norman, J.M. (1999). "Evaluation of Soil and Vegetation Heat Flux Predictions Using a Simple Two-Source Model With Radiometric Temperatures for Partial Canopy Cover." *Agricultural and Forest Meteorology*, **94(1)**: 13-29.
- Langensiepen, M. (2003). "Evaporation and Energy Balance." In *Encyclopedia of Water Science*, 238-241.
- Luca, J. and Mrawira, D. (2005). "New Measurement of Thermal Properties of Superpave Asphalt Concrete." *Journal of Materials in Civil Engineering*, **17(1)**: 72-79.
- Mays, L.W. (2001). *Water Resources Engineering*, First Ed., John Wiley and Sons, New York.
- Monteith, J. L. (1973). *Principles of Environmental Physics*. Edward Arnold, London.
- Patankar, S.V. (1980). *Numerical Heat Transfer and Fluid Flow*. McGraw-Hill, New York.
- Rasmussen, A.H., M. Hondzo, and Stefan, H.G. (1995). "A Test of Several Evaporation Equations for Water Temperature Simulations in Lakes." *Journal of the American Water Resources Association*, **20(6)**: 1023-1028.
- Rawls, W.J., Ahuja, L.R., Brakensiek, D.L., and A. Shirmohammadi. 1993. "Infiltration and Soil Water Movement." In: D.R. Maidment (Editor), *Handbook of Hydrology*. McGraw-Hill, New York, pp. 5.1-5.51.
- Roa-Espinosa, A., Norman, J.M., Wilson, T.B., and Johnson, K. (2003). "Predicting the Impact of Urban Development on Stream Temperature Using a Thermal Urban Runoff Model (TURM)." *Proceedings, U.S. EPA National Conference on Urban Stormwater: Enhancing Programs at the Local Level*, February 17-20, Chicago, IL, 369-389.
- Ryan, P.J. and Harleman, D.R.F. (1973). "An Analytical and Experimental Study of Transient Cooling Pond Behavior." Report No. 161. Ralph M. Parsons Laboratory, Department of Civil Engineering, Massachusetts Institute of Technology, Cambridge, MA. January 1973.
- Solaimanian, M., and Kennedy, T.W. (1993). "Predicting Maximum Pavement Surface Temperature Using Maximum Air Temperature and Hourly Solar Radiation." In

*Transportation Research Record 1417*, National Research Council, Washington, D.C., 2001, 1-11.

Stefan, H.G., Gulliver, J.S., Hahn, M.G. and Fu, A.Y. (1980). "Water temperature dynamics in experimental field channels: Analysis and modeling". Proj. Rep 193, St. Anthony Falls Lab., University of Minnesota, Minneapolis, 171 pp.

Ul Haq, R. and James, W. (2002). "Thermal Enrichment of Stream Temperature by Urban Storm Water." *Proceedings, International Conference on Urban Drainage*. Portland, OR.

Van Buren, M.A., Watt, W.E., Marsalek, J., and Anderson, B.C. (2000a). "Thermal Enhancement of Stormwater Runoff by Paved Surfaces." *Water Resources*, **34(4)**: 1359-1371.

Van Buren, M.A., Watt, W.E., Marsalek, J., and Anderson, B.C. (2000b). "Thermal Balance of an On-stream Stormwater Management Pond." *Journal of Environmental Engineering*, **126(6)**: 509-517.

Wilson, B. (2004). *Hydrologic Modeling of Small Watersheds*, [Lecture Notes.] University of Minnesota, May 2005.

## APPENDIX A. COMPONENTS OF THE WATER BALANCE

The water mass balance used in Model 3 is given by equation 9:

$$\frac{\partial q(x,t)}{\partial x} = -\frac{\partial y(x)}{\partial t} + p(t) - f(t) - e(t) \quad (9)$$

The flow rate,  $q$ , and the runoff depth,  $y$ , are estimated using Manning's equation. The precipitation,  $p$ , is measured at a weather station, and is an input to the model. Precipitation is assumed to be constant over the runoff area. Thus the two unknowns in the mass balance are the infiltration,  $f$ , and evaporation,  $e$ . Estimation of these two parameters is as follows.

### Infiltration

For an impervious surface the infiltration rate,  $f$ , in equation 9 is zero, unless significant permeability/porosity is present in the pavement and sub-grade e.g. due to cracking or by design. To create a general model that is applicable to pervious surfaces as well, it is useful to review methods for the estimation of infiltration rates. A widely-accepted model for one-dimensional, unsteady infiltration in an unsaturated porous soil is the Richards' equation, which is derived from Darcy's law for steady, uniform flow in a porous medium (Mays, 2001). Richards' equation is

$$\frac{\partial \theta}{\partial t} = \frac{\partial q_i}{\partial z} = \frac{\partial}{\partial z} \left( D_s \frac{\partial \theta}{\partial z} + K \right), \quad (A.1)$$

where  $q_i$  is the infiltration rate,  $\theta$  is the soil moisture content (ratio of water volume in the soil to total volume of soil),  $D_s$  is the soil water diffusivity, and  $K$  is the hydraulic conductivity, which is a function of pore geometry as well as soil moisture content or suction head,  $\Psi$ . For a homogeneous soil in which the hydraulic conductivity is a constant with depth ( $\partial K/\partial z = 0$ ), the  $K$  term can be eliminated from Richards' equation (Mays, 2001). In spite of this simplification, this equation is not easily solved, given the difficulty in specifying the soil parameters. Further simplification is needed to make the computation manageable.

One common simplification of Richards' equation is known as the Green-Ampt method. In the Green-Ampt model, a uniform, saturated wetting front is assumed to pass downward into the soil as water infiltrates. Above this wetting front the soil is saturated, and below this front the soil has whatever residual moisture content existed before infiltration began. The method also assumes that the infiltration rate,  $f$ , reaches a maximum value when water begins to pond on the surface, which occurs when the surface soil layer becomes saturated. Thus up to this point in time, the infiltration rate is equal to the rainfall rate,  $p$ , minus any evaporation losses. By the Green-Ampt method, the infiltration rate is obtained as

$$f(t) = K_s \left[ \frac{\Psi_f \Delta \theta}{F(t)} + 1 \right]. \quad (\text{A.2})$$

The wetting front suction head,  $\Psi_f$ , is the suction pressure across the wetting front. The term  $\Delta \theta$  represents the difference in soil moisture across the wetting front, and is equal to the difference between the moisture concentration of saturated soil (equal to the porosity,  $\eta$ ) and the initial moisture content of the soil prior to the onset of infiltration.  $K_s$  is the saturated hydraulic conductivity of the soil, a readily-available soil property. The cumulative infiltration depth,  $F(t)$ , is the total depth of water (per unit area) that has infiltrated into the soil. It is important to distinguish this from the depth to which the water has penetrated into the soil, also known as the wetting front depth, which is equal to  $F/\Delta \theta$ . The cumulative infiltration depth is given by the Green-Ampt equation as

$$F(t) = K_s t + \Psi_f \Delta \theta \ln \left[ \frac{F(t)}{\Psi_f \Delta \theta} + 1 \right]. \quad (\text{A.3})$$

Since it is impossible to solve for  $F(t)$  explicitly,  $F(t)$  has to be found by successive substitution or a similar method. The key assumption for the use of this equation is that ponding has to occur on the surface from the onset of rainfall. In actuality it is likely that the initial rainfall will soak into the soil until saturation occurs, meaning that ponding happens at some duration of time after rainfall begins. This is known as the ponding time,  $t_p$ . In a low-intensity rainfall event, surface ponding might not occur at all if the rainfall intensity never exceeds the soil's saturated hydraulic conductivity,  $K_s$ . Thus to calculate the time to ponding,  $t_p$ , it is first necessary to check that  $p(t) > K_s$ , or else all rain that falls will soak into the unsaturated soil. For the case when  $p(t) > K_s$ , the ponding time is given by

$$t_p = \frac{\psi_f \Delta \theta}{(p_1 / K_s) - 1}. \quad (\text{A.4})$$

This equation is derived with the restriction that the rainfall intensity,  $p$ , remains constant at the initial intensity of  $p = p_1$ . This situation would rarely be expected to occur in an actual storm event, but calculation of the ponding time in this fashion serves as a way to determine the cumulative infiltration depth,  $F_p$ :

$$F_p = p_1 \cdot t_p. \quad (\text{A.5})$$

This quantity represents the amount of water that must infiltrate into the soil before ponding can begin. Thus in a more realistic case where the rainfall intensity varies with time, the cumulative infiltration can be tallied for each time step. When the cumulative infiltration depth reaches the ponding depth, it can be assumed that ponding begins at this point in time, and hereafter the Green-Ampt equation can be applied. The resulting Green-Ampt infiltration rate equation for all  $t > t_p$  and  $p > K_s$  is thus:

$$F(t) = F_p + K_s(t - t_p) + \Psi_f \Delta \theta \ln \left[ \frac{F(t) + \Psi \Delta \theta}{F_p + \Psi \Delta \theta} \right]. \quad (\text{A.6})$$

For a rainfall event of variable intensity with a time step  $\Delta t$ ,  $F_p$  is given (Wilson 2004) as:

$$F_p = \int_0^{t_p} p(t) dt = \sum_{j=1}^{t_p/\Delta t} p(t_j) \Delta t. \quad (\text{A.7})$$

As before, it becomes necessary to solve the Green-Ampt equation with a series of successive substitutions because the unknown quantity,  $F(t)$ , is present on both sides of the equation. The bisector or secant method can also be used.

### Evaporation

A number of equations exist for the calculation of the evaporation rate,  $e$ , in Eq. A.1. Most are empirical and are based on relative humidity and the wind speed over the surface. Ul Haq and James (2002) used the following equation to estimate the evaporation rate:

$$e = 2.909 A_s^{-0.05} (e_s - e_a) U_2 \quad (\text{A.8})$$

where  $A_s$  is the area of the water surface in  $\text{m}^2$ ,  $e_s$  is the saturation vapor pressure of the air in kPa (evaluated at the runoff temperature),  $e_a$  is the actual vapor pressure of the air in kPa,  $U_2$  is the wind speed in m/s measured at a height of 2m above the ground, and  $e$  is in mm/day. Other similar relations also exist, including one originally developed by Chow (1964) and used by Van Buren et al. (2000a) in the development of their runoff model:

$$e = 3.59 \cdot 10^{-7} (1 + 0.0447 U_2) e_{sa} (1 - RH) \quad (\text{A.9})$$

where  $e$  is the evaporation rate,  $U_2$  is the wind speed in m/s,  $e_{sa}$  is the saturation vapor pressure at the temperature of the air, in kPa, and  $RH$  is the relative humidity.

By no means are these two equations for estimation of evaporation rate the only ones available. Other equations have been proposed and used. Evaporation from lake and pond surfaces is usually calculated using an aerodynamic formulation, and can include terms for both free and forced convection (Rasmussen et al., 1995). The specific form of the equation used by Ryan and Harleman (1973) for pond evaporation is given by:

$$e = \left( \frac{8.64 \cdot 10^7}{\rho L_v} \right) \left( 27 \Delta \theta_v^{1/3} + 31 U_2 \right) (e_s - e_a) \quad (\text{A.10})$$

where  $\Delta\theta_v$  is the difference in virtual temperature between the water surface and the air in °C,  $\rho$  is the density of water in kg/m<sup>3</sup>,  $L_v$  is the latent heat of vaporization in units of J/kg°C,  $e_s$  is the saturation vapor pressure of the air in kPa (evaluated at the runoff temperature),  $e_a$  is the actual vapor pressure of the air in kPa. The vapor pressures  $e_s$  and  $e_a$  are in units of kPa, giving  $e$  in mm/day. Deardorff (1978) proposed a similar evaporation equation. It was developed for a generic soil surface covered by a vegetation canopy, and includes the effects of wind speed, vapor pressure difference between surface and atmosphere, and temperature difference between surface and atmosphere. The Deardorff equation can be put in a similar form as the convection equation (Eq. B.11) by assuming no vegetative cover (appropriate for a pavement runoff model) and utilizing the Ryan and Harleman (1973) equation above (A.10):

$$e = (C_{fc}U_2 + C_{nc}\Delta\theta_v^{1/3}) \quad (\text{A.11})$$

where  $C_{fc}$  is a forced convection transfer coefficient with a value of 0.0015,  $C_{nc}$  is a free (natural) convection transfer coefficient with a value of 0.0015 (m/s)(°C<sup>-1/3</sup>),  $e$  is the evaporation rate in m/s, and the other parameters are as defined previously. Other similar relations also exist, but the evaluation of multiple methods is beyond the scope of this report.

## APPENDIX B. HEAT FLUXES ACROSS THE WATER SURFACE

The heat budget for runoff over the pavement surface (Eq. 19) is used to obtain the temperature of the runoff,  $T_{ro}$ . All parameters in the equation therefore have to be known. The last three terms (heat fluxes) in Eq. (19) describe heat fluxes through the water surface, i.e. between the water and the atmosphere. They represent the net short and long wave radiation, the evaporative (latent) heat flux, and the convective (sensible) heat flux, and need to be calculated from measured weather parameters.

### Net radiative heat flux

The net radiation term,  $h_{rad}$ , represents the difference between the incoming solar and long wave radiation from the atmosphere, and that reflected and emitted from the water/pavement surface:

$$h_{rad} = h_s(1 - \alpha_s) + h_l(1 - \alpha_l) - \varepsilon\sigma T_s^4 \quad (\text{B.1})$$

where  $h_s$  is the net incoming shortwave (solar) radiation,  $\alpha_s$  is the reflectivity of the pavement surface for shortwave radiation,  $h_l$  is the net incoming longwave radiation (emitted by the atmosphere),  $\alpha_l$  is the reflectivity of the pavement surface for longwave radiation,  $\varepsilon$  is the emissivity of the pavement surface,  $\sigma$  is the Stefan-Boltzmann constant, and  $T_s$  is the temperature of the soil surface. When runoff is occurring,  $T_s$  will be set equal to the runoff temperature,  $T_{ro}$ .

The net solar radiation is often measured and included in climate data. During a rainfall event the solar radiation input is likely to be reduced by a cloud cover. Net long wave radiation is not measured and requires a more detailed and lengthy calculation. Often, however, the difference between the absorbed and emitted longwave radiation is small relative to the shortwave solar radiation, and is ignored in many simple models.

Net longwave radiation on a pavement or soil surface, encompassing both the surface and atmospheric contributions, can be described by (Jia, et al. 2001):

$$h_{lw,net} = [1 - (1 - \varepsilon_a)F_c] \sigma T_a^4 - \varepsilon_s \sigma T_s^4 \quad (B.2)$$

where  $\varepsilon_a$  is the atmospheric emissivity,  $F_c$  is a cloudiness coefficient,  $T_a$  is the air temperature,  $\varepsilon_s$  is the emissivity of the pavement or soil surface (which is that of water in the runoff case),  $\sigma$  is the Stefan-Boltzmann constant, and  $T_s$  is the temperature of the water on the pavement or the pavement surface. As before, when runoff is occurring,  $T_s$  will be equal to the runoff temperature  $T_{ro}$ . The cloudiness factor,  $F_c$ , is the square of the ratio of the measured solar radiation,  $R_s$ , to the maximum possible solar radiation,  $R_{so}$ :

$$F_c = \left( \frac{R_s}{R_{so}} \right)^2. \quad (B.3)$$

$R_{so}$  can be computed from latitude and date, i.e., time of year (see, for example, Edinger et al., 1974, Stefan et al., 1980, and Duffie and Beckman, 1991). The emissivity of the air,  $\varepsilon_a$ , can be estimated from the empirical relationship

$$\varepsilon_a = 1 - 0.261 \exp(-7.77 \cdot 10^{-4} T_a^2). \quad (B.4)$$

In this equation emissivity is a function of air temperature only, but it also depends on the moisture content of the air (Edinger et al., 1974; Stefan et al., 1980).

### Evaporative heat flux

The heat flux due to evaporation,  $h_{evap}$ , is a negative (loss) term. It is estimated from

$$h_{evap} = -L_v \cdot e \cdot \rho \quad (B.5)$$

where  $L_v$  is the latent heat of vaporization of water,  $\rho$  is the density of water, and  $e$  is the evaporation rate, usually in units of depth per time (the same units used to describe precipitation and infiltration). The latent heat of vaporization is a weak function of the water temperature,  $T_w$ :

$$L_v = 2.501 \cdot 10^6 - 2370 \cdot T_w. \quad (B.6)$$

This equation gives the latent heat of vaporization in units of J/kg, with the water temperature,  $T_w$ , in °C. In the case of evaporation from runoff, the water temperature equals the runoff temperature,  $T_{ro}$ . In the case of evaporation from a soil-vegetation surface, the water temperature will be approximated by the soil surface temperature. The Deardorff evaporation equation (Eq. A.11), can be used to find the evaporative heat flux in the following form:

$$e = \rho_a L_v (C_{fc} U_2 + C_{nc} \Delta \theta_v^{1/3}) (q_{sat} - q_a) \quad (B.7)$$

where  $\rho_a$  is the density of air,  $q_{sat}$  is the saturated specific humidity of the air,  $q_a$  is the actual specific humidity of the air, and the other parameters are as defined previously.

### Convective heat flux from air to water

The atmospheric convection term,  $h_{conv,atm}$ , represents the sensible heat flux from the atmosphere to the runoff or vice versa. Many formulations for this heat flux exist. A few equations will be outlined in this section.

The most general form of the convection equation is:

$$h_{conv,atm} = \frac{1}{r_a} (T_a - T_{ro}) (\rho C_p)_a \quad (B.7)$$

where  $T_a$  is the air temperature,  $T_{ro}$  is the runoff temperature,  $\rho c_p$  is the heat capacity of the air, and  $r_a$  is the aerodynamic resistance, or the resistance to heat transfer between the air and the water. A general form of the resistance, originally used by Monteith (1973), is referenced in a number of sources (Kustas and Norman, 1998; Burman, 2003; Jia et al., 2001):

$$r_a = \frac{\ln[(z_a - d) / z_{om}] \cdot \ln[(z_a - d) / z_{oh}]}{\kappa^2 U_a} \quad (B.8)$$

where  $z_a$  is the height above the ground at which air temperature and wind speed are measured,  $z_{om}$  is the surface roughness height of momentum,  $z_{oh}$  is the surface roughness height of heat transfer,  $\kappa$  is the von Karman constant,  $U_a$  is the wind speed, and  $d$  is the displacement height. The displacement height is defined as the average height of heat and mass exchange within a canopy, or the plane at which the logarithmic portion of a wind profile above a canopy would extrapolate to zero (Langensiepen, 2003). This height varies from a value of zero over a flat surface free of vegetation (such as a parking lot), to a value of several meters or more for a dense canopy of tall trees. The roughness height of momentum is often considered equivalent to the physical surface roughness (Brutsaert, 1984). Its value can be found in a number of literature sources. The roughness height of heat transfer,  $z_{oh}$ , is often assumed to be roughly one-tenth that of the physical surface roughness (Burman, 2003).

In light of the complex nature of this formulation, a number of empirical estimations of atmospheric convection have been developed. A particular method used by Solaimanian and Kennedy (1993) to predict the convection coefficient,  $k_{conv,atm}$ , for a pavement energy balance is

$$k_{conv,atm} = 698.24 \left[ 0.00144 T_m^{0.3} U_a^{0.7} + 0.00097 (T_s - T_a)^{0.3} \right] \quad (B.9)$$

where  $T_m$  is the average of the surface and air temperatures,  $U_a$  is the measured wind speed,  $T_s$  is the temperature of the surface in question, and  $T_a$  is the air temperature. The temperatures are in units of K, and the wind speed is in m/s. The above equation for the convection coefficient,  $k_{conv,atm}$ , can be substituted back into the original convection equation B.7 for the term  $(\rho * C_p)_a / r_a$ . A modification of the above equation was used by Hermansson (2001) in a pavement temperature model. A strength of Equation B.9 is that it includes both free and forced convection, as do many formulations for convective heat transfer from lakes and ponds.

The method used in our model was developed by Deardorff (1978), and was chosen because it is general enough to be applied to different land covers by modifying some coefficients. The Deardorff equation for ground-air convection, including a vegetation canopy, is:

$$h_{conv,atm} = \rho_a C_{p,a} (C_{Hg} u_{af} + C_{fc} \Delta T_v^{1/3}) (T_g - T_{af}) \quad (B.11)$$

where  $\rho_a$  is the density of air,  $C_{p,a}$  is the specific heat of air,  $C_{Hg}$  is the ground-canopy transfer coefficient,  $u_{af}$  is the characteristic wind velocity between ground and canopy,  $C_{nc}$  is the free (natural) convection transfer coefficient,  $\Delta T_v$  is the virtual temperature difference between the ground and air,  $T_g$  is the ground temperature, and  $T_{af}$  is a characteristic temperature of the air and vegetation.

To simplify this equation for the prediction of convection from runoff (water) to the atmosphere, the ground temperature is assumed to be that of the runoff. In the absence of a canopy,  $u_{af}$  becomes the measured wind velocity and  $T_{af}$  the measured air temperature. The ground-canopy coefficient,  $C_{Hg}$ , will be equal to the transfer coefficient for bare ground,  $C_{H0}$ , which has a value of 0.0057 for a relatively smooth surface.  $C_{fc}$  has a value of 0.0016 for a saturated surface. The virtual temperature difference between the ground and air is given by

$$\Delta T_v = T_{v,g} - T_{v,a}, \quad \text{where } T_v = \frac{T}{(1 - 0.61 \cdot q)}, \quad (B.12)$$

and  $q$  is the specific humidity at a given temperature. When runoff is occurring, the air is assumed to be saturated near the surface (due to the presence of water), and the specific humidity of the air can be calculated from the measured relative humidity and air temperature.

## APPENDIX C. ADVECTIVE HEAT FLUXES

In this section the remaining terms in the runoff energy balance (Eq. 19) are described. They are the heat transfer rates associated with the ‘advection’ of water by precipitation, infiltration, and runoff.

### Precipitation heat flux

The heat flux associated with the precipitation,  $h_{rain}$ , can be formulated for a cell ‘j’ using the intensity of rainfall and the difference in temperature between the rainfall and runoff:

$$h_{rain} = \rho_w C_{p,w} \cdot i \cdot (T_p - T_{ro,j}^{i-1}) \quad (C.1)$$

where  $i$  is the rainfall intensity,  $T_p$  is the temperature of the rainfall, and  $T_{ro,j}^{i-1}$  is the temperature of the runoff in the previous time step, which is used because it represents the temperature of the runoff at the beginning of a new time step. It is assumed that if a short enough time step is used this assumption will not result in a large error. Since rainfall temperature is rarely measured it is approximated by the dew point temperature. The sign convention used implies that a positive heat flux into the runoff will result if the rainfall temperature is greater than the runoff temperature.

### Infiltration heat flux

The heat flux associated with infiltration is zero in the current runoff model because infiltration into a paved surface is assumed to be zero. If there is infiltration on a permeable surface, and the formulation for the infiltration heat flux is similar to that of the precipitation heat flux, the infiltration heat flux will still be zero because the temperature difference between the runoff water and the infiltrating water is zero. Infiltration of runoff water will not change the temperature of the runoff water. It will only decrease its volume.

### Runoff (net lateral advection) heat flux

The first term on the right-hand side of Eq. (19) is the net runoff advection term:

$$\rho_w C_{p,w} \frac{\partial(q \cdot T)}{\partial x}$$

where  $T = T_{ro}$  is the runoff temperature and  $q$  is the per-width flow rate. Two assumptions can be made to simplify this term: 1) the flow rate for the runoff volume, or cell, is roughly constant over the whole cell, and 2) the temperature gradient ( $\partial T / \partial x$ ) is approximated by the temperature difference between the upstream cell and the cell of

interest, also known as an ‘upwinding’ scheme (Patankar, 1980). The advection term is then discretized as:

$$\rho_w C_{p,w} \frac{\partial(q \cdot T)}{\partial x} \approx \rho_w C_{p,w} \cdot \bar{q}_j \frac{\partial T}{\partial x} = \rho_w C_{p,w} \cdot q_j^i \frac{T_j^{i-1} - T_{j-1}^{i-1}}{\Delta x}, \quad (C.2)$$

which can easily be evaluated if the flow rate for the current time step ( $q^i$ ) and the runoff temperatures at the previous time step ( $T^{i-1}$ ) are used, since the runoff temperature for the current cell (cell ‘j’) will not be known. It is assumed that using a small enough time step will not result in too much error.

#### **APPENDIX D. DRY WEATHER HEAT BUDGET OF PAVEMENT AND SOIL: GROUND TEMPERATURE PROFILE BEFORE A RAINFALL EVENT**

A necessary input to the hydro-thermal runoff models is the temperature profile in the pavement and sub-grade at the onset of rainfall. It is therefore important to be able to run the simulation both before and after a rainfall event for the purpose of predicting ground temperatures for the next event. The heat budget at the ground surface during the time period between rainfall events can be obtained from an equation similar to equation (19) by neglecting all heat fluxes associated with precipitation, infiltration, and runoff. In the absence of rainfall the surface water mass balance is also irrelevant. The “dry weather” heat balance for the a pavement or soil surface is

$$h_{cond,g} = h_{rad} + h_{evap} + h_{conv,atm}, \quad (D.1)$$

where  $h_{rad}$  is the net total radiation,  $h_{conv,atm}$  is the convective heat transfer from the soil surface to the atmosphere, and  $h_{cond,g}$  is the net heat flux into the ground.  $h_{evap}$  is the evaporative heat flux, which is zero from a dry pavement surface, but may not be zero from a soil surface. It should be noted that for the case of a vegetated surface, the evaporation term would have to be modified to include the effects of transpiration by plants. Many equations exist for the prediction of combined evaporation and transpiration (evapotranspiration) from vegetation, but this issue will not be addressed here. The evaporation term disappears from the balance once all water on a paved surface has evaporated. Thus for most periods of dry weather, the heat conducted into the ground is simply the difference between the net absorbed total radiation and the sensible heat removed from the surface via convection. The equations for net radiation and atmospheric convection used in the “wet weather” energy balance can also be used for the “dry weather” energy balance. The sensible heat flux from the ground into the atmosphere can be inserted into the heat diffusion equation as:

$$h_{cond,g} = - \left( k_s \frac{\partial T}{\partial z} \right) \Big|_{z=0}. \quad (D.2)$$

The soil thermal diffusivity,  $k_s$ , is a function of the soil type, moisture content, and temperature.

The heat flux at the ground surface serves as the upper boundary condition for the heat diffusion equation (Eq. 37) in the soil, and the lower boundary condition will be a constant temperature or zero flux at some specified depth. With the boundary conditions defined, the heat diffusion equation can be solved to give the dry weather temperature profile in the pavement, sub-grade and soil below,  $T(z,t)$ .

### **Estimation of an initial sub-surface temperature profile for sensitivity study**

In the sensitivity study described in this report, the initial sub-surface temperature profile was the same for each simulation. The temperature profile was determined by fixing the soil temperature at some depth, and imposing a temperature at the surface, which in this case was the assumed initial surface temperature. A typical late afternoon temperature profile would be a roughly exponential increase in temperature from the constant temperature at depth to the specified surface temperature. This exponential profile was determined from an analytical solution of the heat diffusion equation for a constant surface temperature (Incropera and Dewitt, 2002):

$$\frac{T(z,t) - T_s}{T_0 - T_s} = \text{erf}\left(\frac{z}{2\sqrt{\alpha \cdot t}}\right) \quad (\text{D.3})$$

where  $\text{erf}$  is the Gaussian error function,  $T_s$  is the specified constant surface temperature,  $T_0$  is the initial temperature of the subsurface, and  $\alpha$  is the thermal diffusivity of the pavement or soil. This analytical solution assumes that the sub-surface is infinite in the horizontal direction, and that the sub-surface temperature at time  $t=0$  is only a function of depth, and not any horizontal distance.

In the sensitivity study outlined in this report, the lower boundary condition was a constant temperature of 26.6 °C at a depth of 60cm, which was the mean July temperature observed at this depth under an asphalt pavement at the Minnesota Department of Transportation's MNRoad research site. A surface temperature of 30 °C was imposed as an initial pavement temperature at the beginning of a late afternoon rainfall event in the middle of summer. With the above specifications a pavement/soil temperature profile was calculated for at an elapsed time of 8 hours (i.e.,  $t=8$  hours in Eq. D.3.) An initial pavement/soil temperature profile can be calculated for any combination of specified bottom boundary and upper boundary temperatures; initial temperature profiles for a bottom temperature of 26.6°C, and surface temperatures of 30°C, 40°C, and 50°C are shown in Figure 6 in the main text.

## **APPENDIX E. THERMAL PROPERTIES OF SOILS AND PAVEMENT**

Both the heat and mass balances rely on the estimation of a number of properties of pavements and soils. Thermal and hydrologic properties of paved surfaces and various types of soils can be found in a number of literature sources (Kersten, 1948; Rawls et al., 1989; Abu-Hamdeh et al., 2000; Luca and Mrawira, 2005). Thermal properties are summarized in Tables E.1 and E.2.

The pavement consists of a pavement layer and a sub-grade layer. The thermal properties of each remain constant with depth, and are a function of temperature only. In the special case of soil beneath a paved surface, infiltration and subsurface water flow can be assumed negligible. Thus the moisture content would be expected to be roughly constant throughout the soil column, making the soil properties also a function of temperature only.

The calculation of temperature profiles in the soil relies heavily upon determination of a thermal diffusivity for various types of soils. Soil properties can be a function of soil type, moisture content, and temperature. A significant amount of research has been done, but many results are highly empirical because of the generally complicated nature of soil structure and composition. In the general case of a permeable ground surface, a soil moisture model - however simplified - requires knowledge of the saturated hydraulic conductivity, wilting point, field capacity, and porosity or saturated moisture content

Table E.1. Thermal properties of pavements.

<b>Parameter</b>	<b>Value</b>	<b>Range</b>	<b>Units</b>	<b>Source</b>
<b>Concrete</b>				
Specific Heat (Cp)	880	n/a	J/kg*K	<i>Incropera and Dewitt (2002)</i>
Thermal Conductivity (k)	1.4	n/a	W/m*K	<i>Incropera and Dewitt (2002)</i>
Density ( $\rho$ )	2300	n/a	kg/m <sup>3</sup>	<i>Incropera and Dewitt (2002)</i>
<b>Asphalt</b>				
Thermal Diffusivity ( $\alpha$ )	5.40E-07	4.4 - 6.4E-7	m <sup>2</sup> /s	<i>Luca and Mrawira (2005)</i>
Specific Heat (Cp)	1225	1100 - 1350	J/kg*K	<i>Luca and Mrawira (2005)</i>
Thermal Conductivity (k)	1.6	1.4 - 1.8	W/m*K	<i>Luca and Mrawira (2005)</i>
Density ( $\rho$ )	2375	2300 - 2450	kg/m <sup>3</sup>	<i>Luca and Mrawira (2005)</i>

Table E.2. Thermal properties of soils.

<b>Parameter</b>	<b>Value</b>	<b>Range</b>	<b>Units</b>	<b>Source</b>
<b>Sand</b>				
Specific Heat (Cp)	1840*	n/a	J/kg*K	<i>Incropera and Dewitt (2002)</i>
Thermal Conductivity (k)	0.7	0.43 - 0.98	W/m*K	<i>Abu-Hamdeh et al. (2000)</i>
Density ( $\rho$ )	1400	1300 - 1500	kg/m <sup>3</sup>	<i>Abu-Hamdeh et al. (2000)</i>
<b>Sandy Loam</b>				
Specific Heat (Cp)	1840*	n/a	J/kg*K	<i>Incropera and Dewitt (2002)</i>
Thermal Conductivity (k)	0.45	0.35 - 0.55	W/m*K	<i>Abu-Hamdeh et al. (2000)</i>
Density ( $\rho$ )	1400	1300 - 1500	kg/m <sup>3</sup>	<i>Abu-Hamdeh et al. (2000)</i>
<b>Loam</b>				
Specific Heat (Cp)	1840*	n/a	J/kg*K	<i>Incropera and Dewitt (2002)</i>
Thermal Conductivity (k)	0.42	0.34 - 0.50	W/m*K	<i>Abu-Hamdeh et al. (2000)</i>
Density ( $\rho$ )	1400	1300 - 1500	kg/m <sup>3</sup>	<i>Abu-Hamdeh et al. (2000)</i>
<b>Clay Loam</b>				
Specific Heat (Cp)	1840*	n/a	J/kg*K	<i>Incropera and Dewitt (2002)</i>
Thermal Conductivity (k)	0.37	0.29 - 0.44	W/m*K	<i>Abu-Hamdeh et al. (2000)</i>
Density ( $\rho$ )	1400	1300 - 1500	kg/m <sup>3</sup>	<i>Abu-Hamdeh et al. (2000)</i>

\* value of  $C_p$  from *Incropera and Dewitt (2002)* for a 'generic soil'.